

Heavy-Ion Test Results of the Voltage Comparator RH1016MW

29 May 2013

Sana Rezgui¹, Rocky Koga², Steve Lalumondiere², Jeffrey George², Stephen Moss², Brian Hamilton¹, Robert Dobkin¹, and Rafi Albarian¹

¹Linear Technology, ²The Aerospace Corporation

Acknowledgements

The authors would like to thank the Application Signal Conditioning Group Tim Regan, Jim Mahoney, and Antonina Karpova, from Linear Technology for their help with the board design and assembly as well as Steve Bielat and Jeffrey George from The Aerospace Corporation for their assistance with the beam experiments. Special Thanks to the Aerospace Corporation team, mainly David Meshel, and Rocky Koga, for their expediting these experiments.

Executive Summary

This report details the heavy-ion test experiments performed on the RH1016M at the Lawrence Berkeley National Labs (LBNL). The RH1016 is an UltraFast™ 10ns comparator that interfaces directly to TTL/CMOS logic while operating from either +/-5V or single 5V supplies [1-2, 4-5]. Heavy-ions induced SEE (Single Event Effect) experiments included Single Event Transient (SET), Single Event Upset (SEU) and Single Event Latchup (SEL) tests up to an LET of 91 MeV.cm²/mg at elevated temperatures (to case temperatures of 100°C). Under heavy-ion irradiations, with various inverting input bias conditions (proportional to differential input voltage as the non-inverting input voltage is fixed), the RH1016M showed sensitivities only to SETs. Beam tests confirmed the SEL and SEU immunity of this part in all test conditions. The measured SET sensitive cross-section is about 5x10⁻⁴ cm²/circuit and represents about 2.5% of the total die's area. In addition, 99% of the SETs are smaller in amplitude than +/-3V and smaller in widths than 100ns. If such SETs can be tolerated in a design then this comparator can be used as is. The remaining 1% of SETs may attain +/-6V in amplitudes and represent only 5x10⁻⁶ cm²/comparator. Note that positive SETs wide upto 18us and of amplitudes less than 2V have been observed on the positive output voltage but those won't cause errors at the comparator output. However, the designer needs to account for maximum tolerated voltages. The beam data showed also clear dependence of the SET cross-sections on the comparator differential input voltage. When the comparator inverting-input voltage was very close to the hysteresis boundary voltages, the SET pulse-width (PW) was the widest, and the measured SET cross-sections were the highest. At higher LET near the limiting cross-section, the dependence on differential input bias became less significant, as most SETs became wide.

The SET cross-sections dependence on these biases could be simply due to the peripheral capacitances charge/discharge times, so what might seem as bias dependence is truly related to parasitic time constants. We believe that the initial SET-PW will depend on the circuit response and the flux but its propagation on its parasitic and the ion's diffusion. Careful selection of the circuit parasitic is crucial when operating the circuit in radiation beams, as they can change the time constants for signal propagation and widen the radiation-induced transients. This circuit can be used as is, as the widest measured SET-PW is less than 200ns at the comparator output at an LET of 58.78MeV.cm²/mg. However, for accurate selection of the SET filter or for the circuit peripheral parasitic, we would recommend that the designer simulates his design by injecting SETs at the circuit inputs/outputs, as wide as the DUT maximum response time, as well as varying the bias during these injections. This could be accomplished by the LTSpice tool offered by Linear Technology, as most of the Linear LT parts spice models are offered [3]. That should provide guidance to the designer but the result should be correlated with laser and beam tests as most of the RH and LT parts differ in their process and sometimes in their design as well. The wrong selection of these parasitic can make things worse and widen the SET from nanoseconds to microseconds, making it harder on the following circuit to not propagate them.

1. Overview

This report details the heavy-ion test experiments performed on the RH1016MW at the Lawrence Berkeley National Labs (LBNL). The RH1016 is an UltraFast™ 10ns comparator that interfaces directly to TTL/CMOS logic while operating from either +/-5V or single 5V supplies. Tight offset voltage specifications and high gain allow the RH1016 to be used in precision applications. Matched complementary outputs further extend the versatility of this comparator. A unique output stage provides active drive in both directions for maximum speed into TTL/CMOS logic or passive loads, yet does not exhibit the large current spikes found in conventional output stages. This allows the RH1016 to remain stable with the outputs in the active region which greatly reduces the problem of output “glitching” when the input signal is slow moving or is low level. The RH1016 has a LATCH pin which will retain input data at the outputs, when held high. Quiescent negative power supply current is only 3mA. This allows the negative supply pin to be driven from virtually any supply voltage with a simple resistive divider. Device performance is not affected by variations in negative supply voltage. The RH1016M voltage offset (VOS) does not exceed ±4mV across the full range of the spec'd die junction temperature (-55°C to 125°C).

The wafer lots are processed to Linear Technology's in house Class S flow to yield circuits usable in stringent military applications. The device is qualified and available in hermetically sealed package (10-Lead flatpack (W10)). More details are given about this voltage comparator in [1-2, 4-5]. This is a 7um technology using exclusively bipolar transistors. The part's block diagram is shown in Fig. 1. The W package designation is given in Fig. 2.

Absolute Maximum Ratings

(Note 1)

Positive Supply Voltage (Note 2)	7V
Negative Supply Voltage	-7V
Differential Input Voltage (Note 3)	+/-5V
+IN, -IN and LATCH ENABLE Current (Note 3)	+/-10mA
Output Current (Continuous) (Note 3)	+/-20mA
Operating Temperature Range	-55°C to 125°C
Storage Temperature Range	-65°C to 150°C
Lead Temperature (Soldering, 10 sec)	300°C

Note 1: Stresses beyond those listed under Absolute Maximum Ratings may cause permanent damage to the device. Exposure to any Absolute Maximum Rating condition for extended periods may affect device reliability and lifetime.

Note 2: Electrical specifications apply only up to 5.4V.

Note 3: This parameter is guaranteed to meet specified performance through design and characterization. It has not been tested

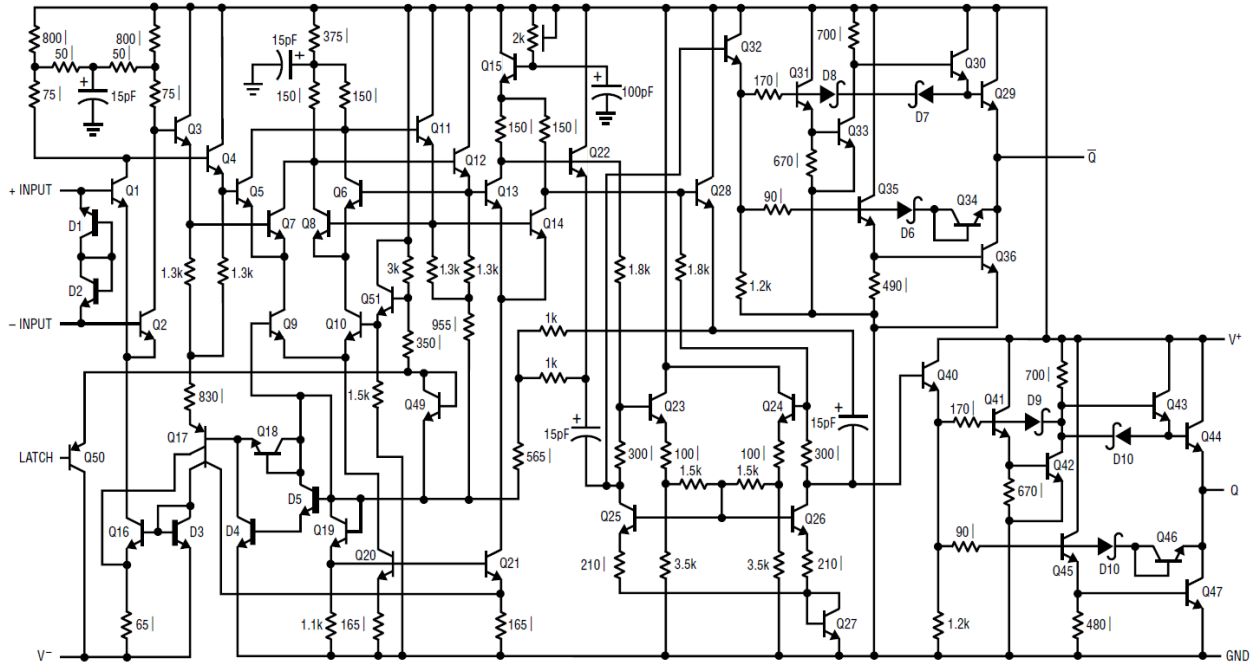


Fig. 1: Block Diagram of the RH1016M DIE

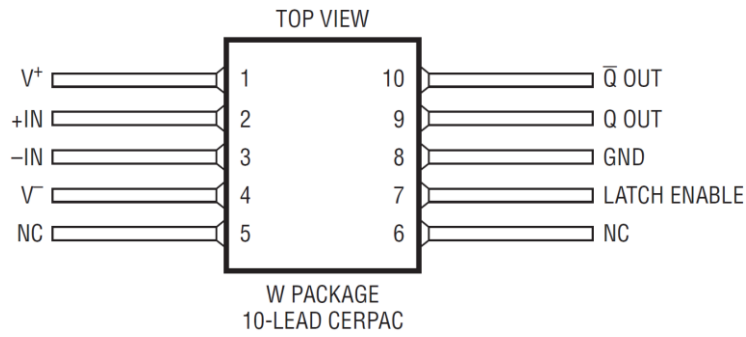


Fig. 2: RH1016M in W Package

Table 1 summarizes the parts' features and the electrical test equipment.

Table 1: Test and Part's Information

Generic Part Number	RH1016M
Package Marking	RH1016 Date Code
Manufacturer	Linear Technology
Fabrication Lot/Lot Date Code (LDC)	xx
Quantity tested	2
Dice Dimension	$56 \times 54 \text{ mils}^2 \approx 1.95 \text{ mm}^2 \approx 1/51 \text{ cm}^2$
Part Function	Voltage Comparator
Part Technology	BIPH400
Package Style	Hermetically sealed W-Package 10-Lead CERPAC
Test Equipment	Power supply, digital oscilloscope, multimeter, and computer
Temperature and Tests	SET, SEU and SEL @ Room Temp. and 100°C
Test Date, Test Site	Dec. 2012, LBNL

2. Test Setup

Custom SEE boards were built for heavy-ion tests by the Linear Technology team, along with the Boeing, The Aerospace Corporation, Ball Aerospace, SEAKR, ITT Exelis, and LMCO engineers. The RH1016MW parts were tested at LBNL on Dec. 2012 at two different temperatures (at room temperature as well as at 100°C). During the beam runs, we were monitoring the temperature of the adjacent sense transistor (2N3904) to the DUT but not the die temperature (junction temperature). Hence the test engineer needs to account for additional temperature difference between the dice and the sense transistor, which was not measured in vacuum. In-air, both of the case and the sense transistor temperatures were measured to be the same. The temperature difference between the junction of the die and the case is a function of the DUT power dissipation multiplied by the thermal resistance $R_{\text{theta-JC}}(\Theta_{\text{JC}})$. With no heating, the temperature of the adjacent temperature sense transistor (2N3904) to the DUT (or the DUT case) was measured on average at about 35°C. The junction temperature was not measured in vacuum; its calculation is provided in Eq.1. This value was correlated in-air with a thermocouple.

$$T_J = T_C + P_D * \Theta_{\text{JC}} \quad (1)$$

Where: T_J is the junction temperature, T_C the case temperature, P_D the power dissipated in the die and Θ_{JC} the thermal resistance between the die and the case. Note: A relatively small amount of power is dissipated in other components on the board. The sense transistor temperature (very similar to the case one) during each run is shown in Tables 2 and 3. That is not considered in this calculation.

The calculation of the dissipated power in the die is provided in Eq. 2:

$$P_D = P_{\text{in}} - P_{\text{out}} = |V_+ * I_+| + |V_- * I_-| - P_{\text{out}} \quad (2)$$

Where:

1. V_+ is the positive voltage supply
2. V_- is the negative voltage supply
3. I_+ is the positive current supply
4. I_- is the negative current supply
5. P_{in} : Input Power Dissipation
6. P_{out} : Output Power Dissipation

Assuming that $P_{\text{out}} = 0$ and in the case where:

$$T_c = 25^\circ\text{C}; V_+ = 5\text{V}; V_- = -5\text{V}; I_+ = 28\text{mA}; I_- = 3.1\text{mA}; \text{ and } \Theta_{\text{JC}} = 40^\circ\text{C/W [4],}$$

$$\underline{P_D = 43.5\text{mW and } T_J \approx 27^\circ\text{C}}$$

The SEE test board contains:

- The DUT with open-top
- The filtering caps for the voltage supplies (V- (-5V), V+ (+5V), VRef (+5V), VD (+5V))
- A filtering capacitance for the output (0.1uF used only for the filtering case)
- The hysteresis circuit (R6, and R12 resistors)
- The 2N3904 (Q1) bipolar transistor to sense the board temperature
- Q1 and Q2 to heat the board during the SEL tests. They are placed as close as possible to the DUT.

Fig. 3 shows the SEE test board schematics and Fig. 4, its picture.

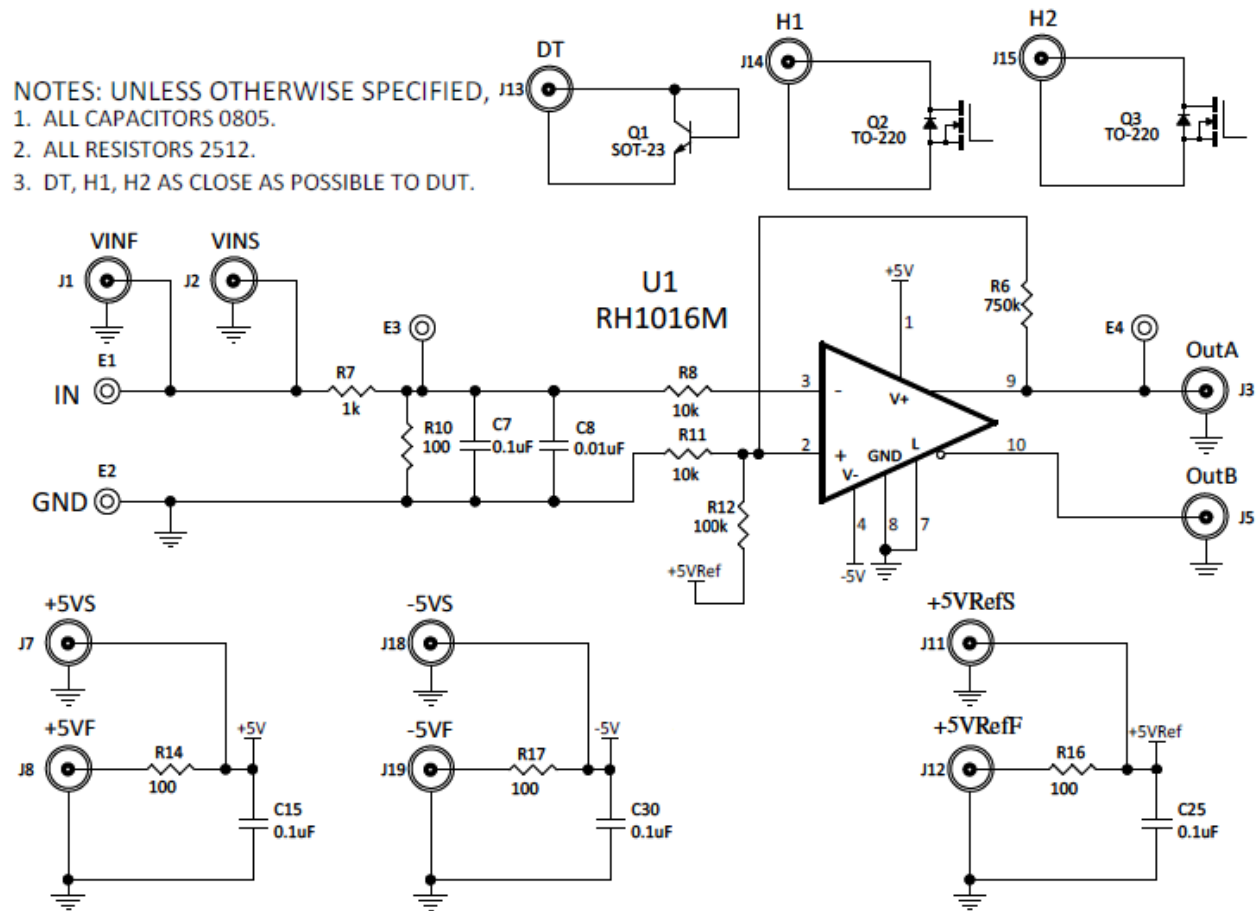


Fig. 3: Block Diagram of the RH1016MW SEE Board

To minimize the distortion of the measured SET-PW, the test setup was placed as close as possible to the vacuum chamber. It is connected with two 3 feet long BNC cables to two Agilent power supplies (PS) (N6705B) and to a LeCroy Oscilloscope (Wavepro 7300, 3 GHz) with extended monitor/cables to view the output signal (Vout). The first PS supplies the input voltages to the SEE test board and allows the automated logging and storage every 1 ms of the current input supplies (Iin), as well as the automation of power-cycles after the detection of a current spike on the input current that exceeds the current limit set by the user. The second PS is used for sensing the voltages of the input power supplies. This was done to

avoid any interference from the power supplies that might cause widening of the transients upon the occurrence of an SET. The output pin (Vout) was connected to the scope with 3 feet BNC cable (vacuum chamber feed-through) and a scope probe of 11pF. For better accuracy, the equivalent capacitive load of the BNC cable and the scope probe should be calculated and accounted for, as it might affect the SET pulse width and shape. In this case, the cables' capacitive load was about 120 pF.

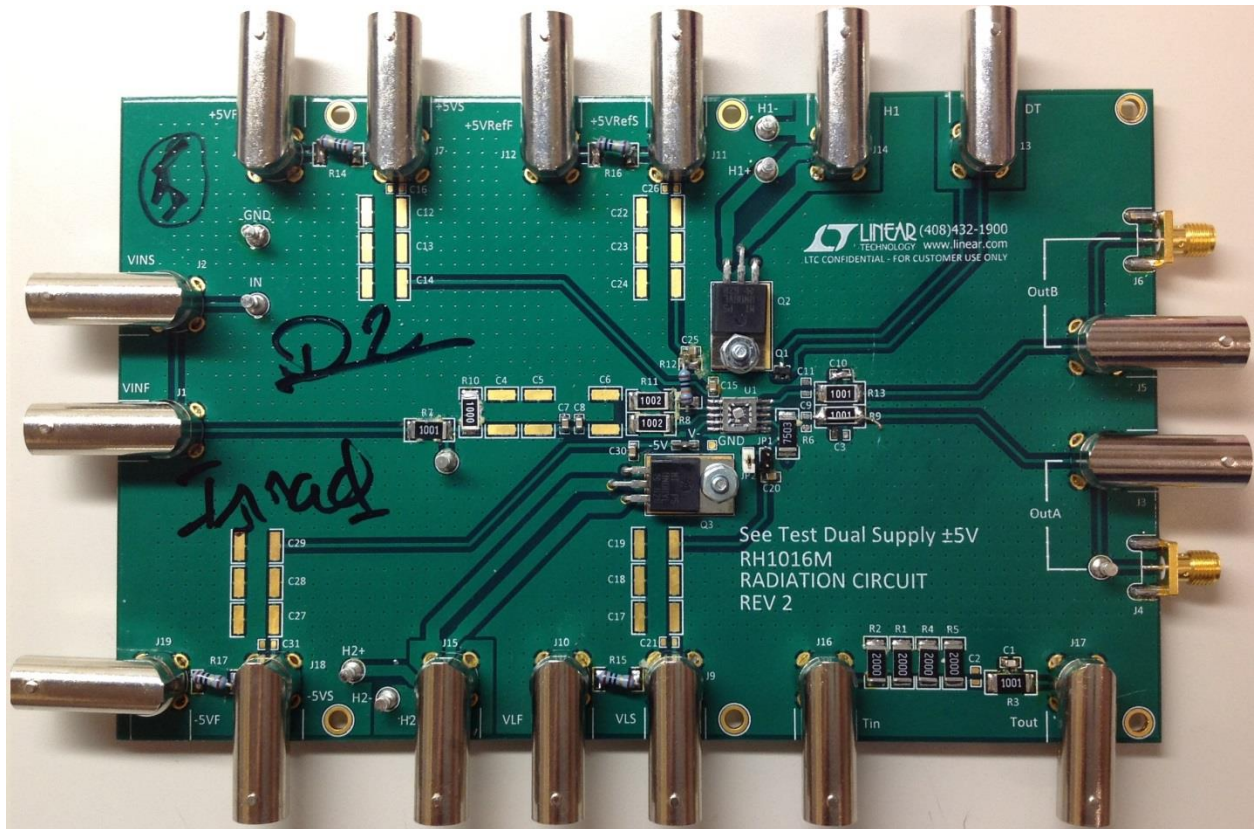


Fig. 4: Photograph of the SEE Test Board

3. Heavy-Ion Beam Test Conditions

The RH1016M part was tested under various input bias conditions ranging from 50 to 1000mV. The selected beam energy is 10MeV/nucleon, which correlates with beam ions delivered at a rate of 7.7 MHz (eq. to a period of 130 ns). During these 130 ns, the ions are generated only within very short pulses that last for 10 ns, as shown in Fig. 5. At every pulse of 10 ns, N number of particles per square centimeter, depending on the flux, will be irradiating the DUT. The calculation of N is provided in Eq. 3:

$$N = \text{Flux} * 130\text{ns} \quad (3)$$

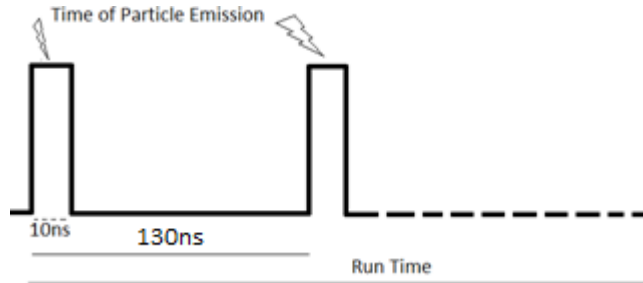


Fig. 5: Particle Emission during a Beam Run at Beam Energy of 10 MeV/nucleon; Emission Frequency = 7.7MHz

For instance, if the flux equals 10^4 particles/cm²/second, the probability (N) of having a particle emitted and striking within a defined square centimeter within a random 10ns active period and even during the entire period of 130 ns is 1.30×10^{-3} . Multiply that value by the die area to determine the probability of a particle striking the die; 1.30×10^{-3} particles/cm² * 1.95×10^{-2} cm² = 2.53×10^{-5} . We don't know exactly at what pulse this particle will be irradiating the DUT. The random nature of that emission will change the elapsed time between any two consecutive particles. The higher the beam's frequency or the flux; the higher is the likelihood to have more than one particle hitting the DUT in a very short time (within hundreds of nanoseconds). Indeed, the minimum time that is guaranteed by the facility to separate the occurrences of two particles can be as low as 130 ns but the probability of that happening is very low. To avoid overlapping of events, it is important then that the error-events last less than 130 ns or that the flux is much reduced.

Most importantly, in the case of these analog devices (power, signal conditioning, etc.), some of the DUT's transistors when hit by heavy-ions will cause wide SETs that might last for microseconds. To make sure that the error-rate calculation is accurate, the flux needs to be reduced until there is a consistency in the number of detected errors with the flux for a given ions' fluence. If that's not the case, the part is subject to multiple hits or SET widening from the peripheral parasitic. In these types of circuits, it is most likely to be the latter. The test engineer needs to account for the SET widening that the peripheral RC filters are causing. In other terms, if the original SET is widened at the DUT output, by the peripheral RC circuits or even the ones used to mitigate it, then the resulting event will dictate the maximum flux to be applied on the DUT. The run average and maximum fluxes during the heavy-ions tests are reported in Table 2.

4. Radiation Test Results

Heavy-ions SEE experiments included SET, SEU and SEL tests up to an LET of 91 MeV.cm²/mg at elevated temperatures (to case temperatures of 100°C). The RH1016M parts were irradiated under various bias conditions in 67 runs. Because of the cabling between the SEE test board and the scope, that adds a minimum capacitive load on the output signal of about 120pF, the input capacitances, the serial resistances on the comparator inputs and the feedback path (resistances and capacitances), the final measured SET-PW on the scope can be wider than the initial SET-PW originating from the DUT output. Ideally, the SET-PW on the DUT output should be about the comparator response time, which is less than 100ns at a 0.8V maximum step-size [2]. Once the hit input transistor has triggered to the ion's deposited charge, the part will need approximately the sum of the circuit response time (about 200ns) to rising and falling edges (Figs. 6 and 7). The circuit response to an SET will depend on the source resistance (10K in this case) and the output loading capacitance.

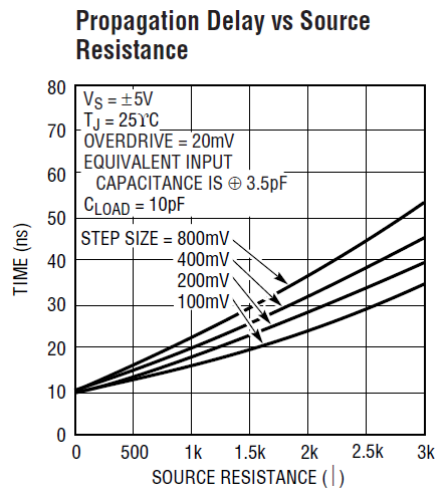


Fig. 6: DUT Responses Times to Rising and Falling Input Steps vs. Source Resistance

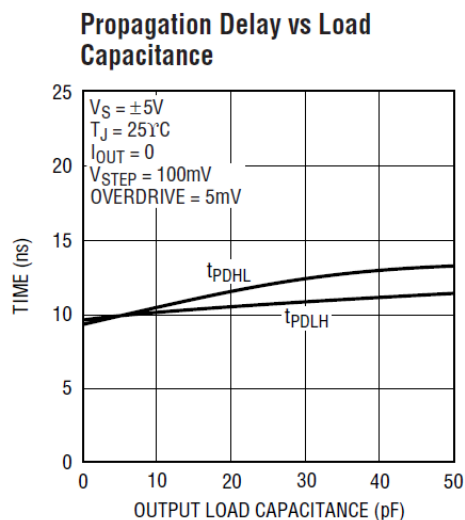


Fig. 7: DUT Responses Times to Rising and Falling Input Steps vs. Output Loading Capacitance

1) SET Detection Setup

For SET detection, the beam tests consisted of varying the input voltage from 50 to 1000 mV and triggering the scope on positive and negative SETs occurring on the comparator output signal. For SET detection, the scope was set to trigger on switching positive and negative SET pulse amplitude of +/- 200mV on both outputs (OutA and OutB). LeCroy scope allowed the implementation of such combination of four simultaneous logic test conditions (two on OutA and two on OutB). The raw heavy-ion test results are summarized in Table 2, showing SET sensitivities on both of the inverting and non-inverting comparator outputs. The data showed a few SET-types; some of them are displayed in Figs. 8 to 14. Most of the SET-types are of small widths, about 100ns, as shown in Figs. 8 to 13. In addition, as shown in Figs. 9 to 12, positive SETs as wide as 18 μ s were also observed on the comparator's output signals set initially high (A or B). These types of SET won't cause error but the designer needs to account for them in his design's maximum allowed voltages.

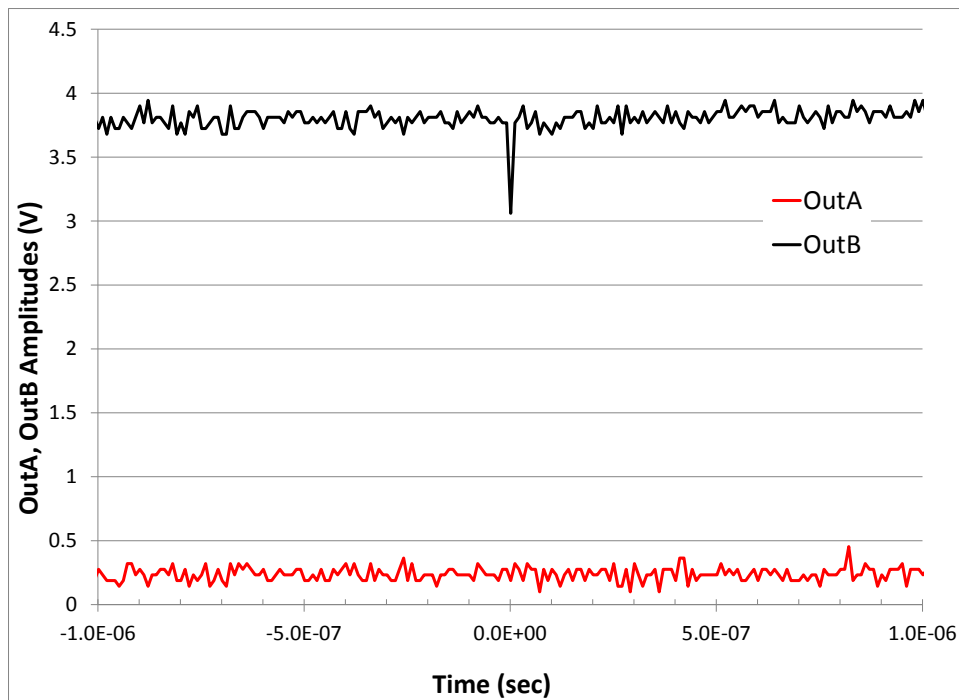


Fig. 8: Short Single SET on the DUT Output OutB; $V_{in}=0.6V$; Run#174, Waveform#4

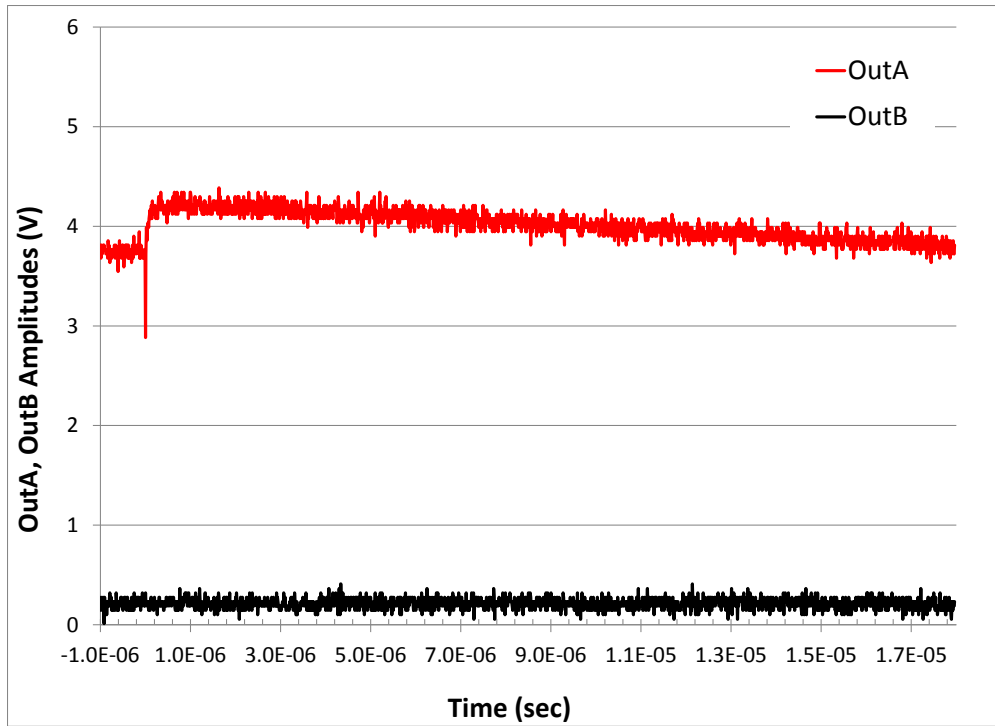


Fig. 9: Single SET on the DUT Output OutA; $V_{in}=0.4V$; Run#170, Waveform#7

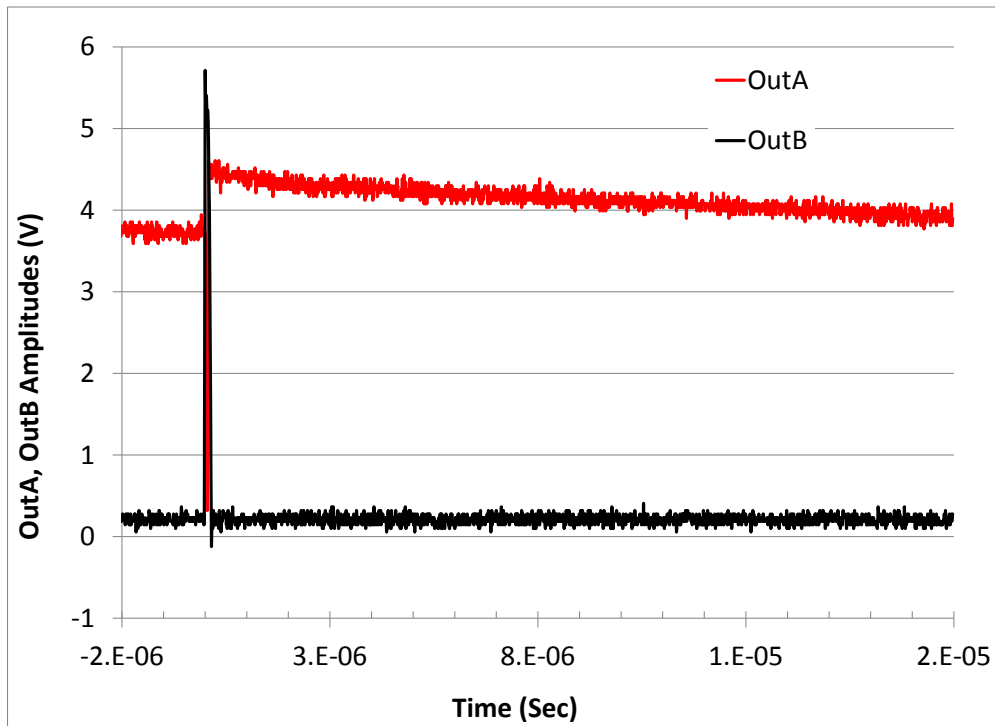


Fig. 10: Dual SETs on the DUT Outputs OutB and OutA; $V_{in}=0.4V$; Run#170, Waveform#1

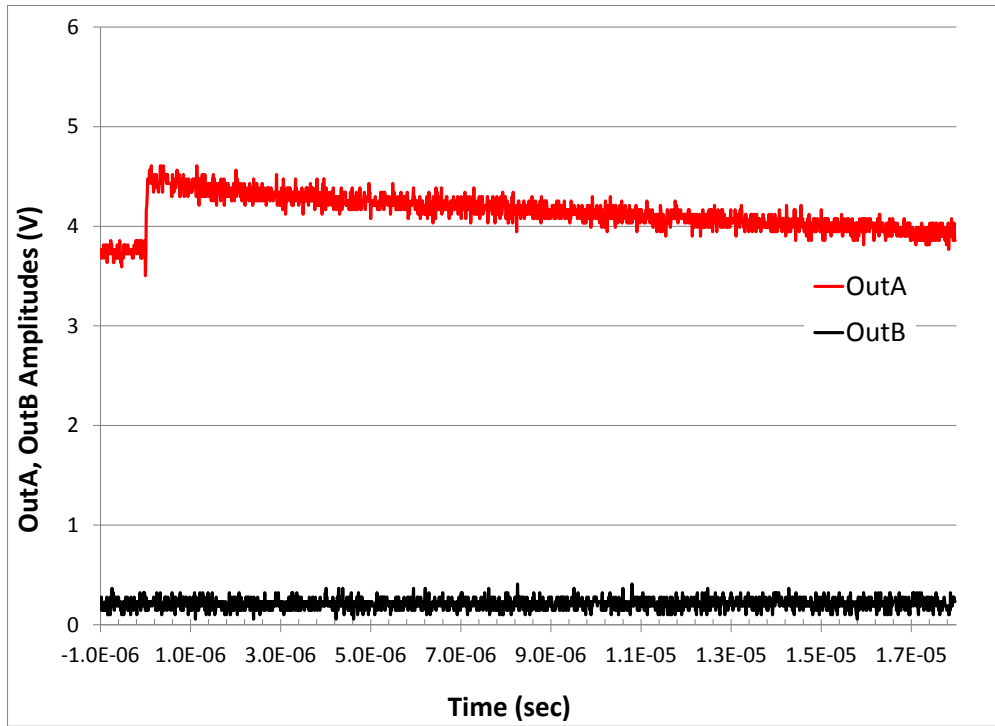


Fig. 11: Positive SET on DUT Output OutA; $V_{in}=0.4V$; Run#170, Waveform#4

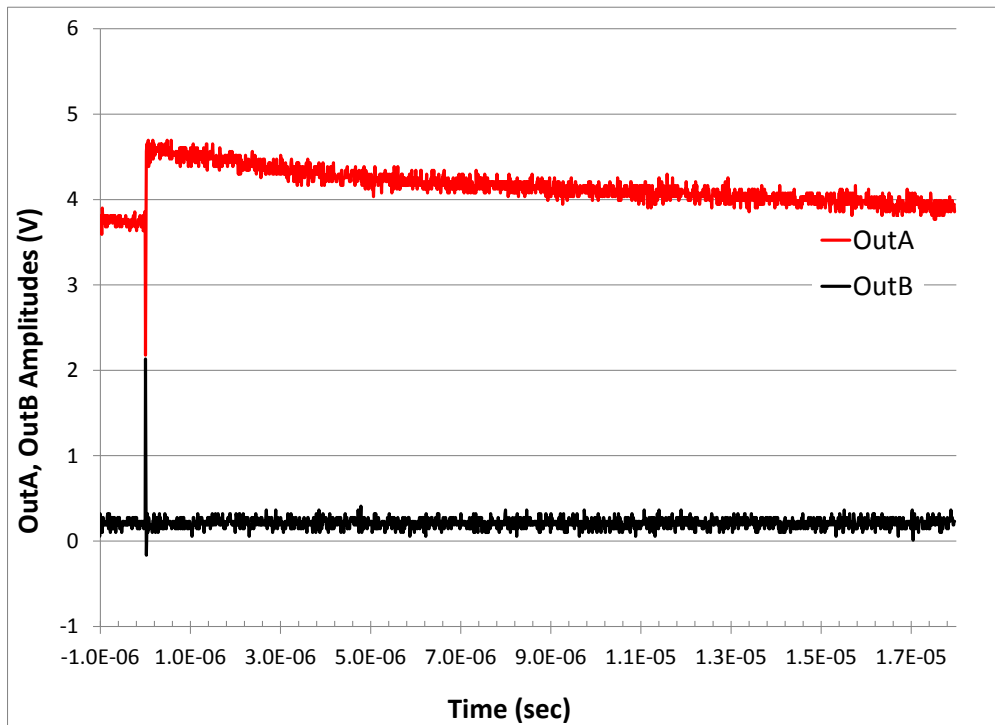


Fig. 12: Dual SET on DUT Outputs OutB and OutA; $V_{in}=0.4V$; Run#170, Waveform#5

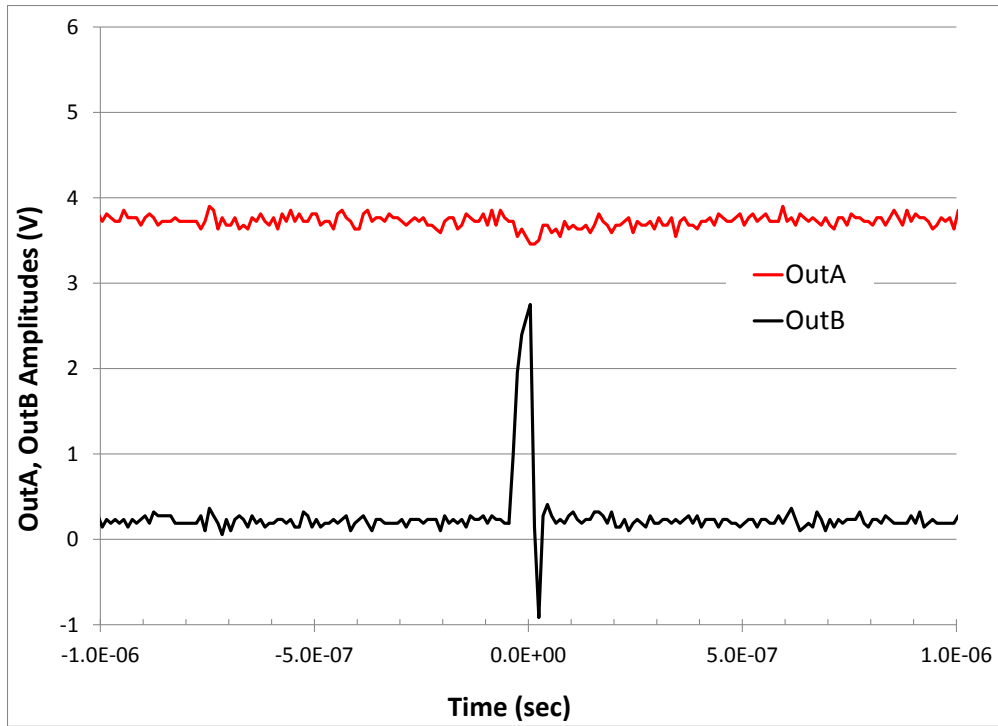


Fig.13: Single SET on DUT Output OutB; $V_{in}=0.6V$ - Run#174, Waveform#10

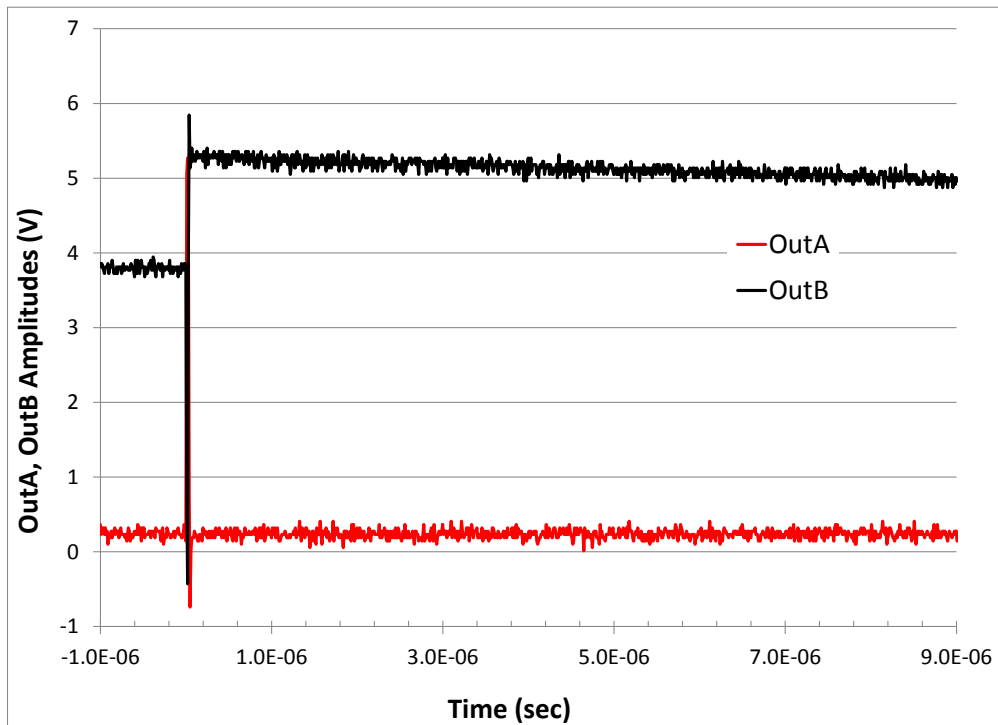


Fig. 14: Dual SET on the DUT Output OutA and OutB; $V_{in}=0.4V$; Run#170, Waveform#6

Since this part is only SET sensitive outside of the hysteresis area, only SET-data will be discussed in the remainder of this report.

2) SET Pulse Widths and Amplitudes

a) When OutA is initially High and OutB is initially Low with $V_{input} = (0.05V \text{ to } 0.4V)$

The SET pulse widths and amplitudes varied with the inverting-input-voltage (V_{in}). For V_{in} ranging between 0.05V and 0.4V, setting the non-inverting output OutA initially high and the inverting output OutB initially low, the data obtained under Xenon Ions ($LET=58.78 \text{ MeV}\cdot\text{cm}^2/\text{mg}$) show that:

1. 90% of the negative SET pulse amplitudes on OutA initially high are smaller than $\pm 2V$ (Fig. 15)
2. 90% of the positive SET pulse amplitudes on OutB initially Low are smaller than $\pm 3V$ (Fig. 15)
3. Although the SET pulse widths on OutA can go up to 18 μs (Fig. 16), only the negative SETs, which are smaller than 200ns (Fig. 17), may cause errors.
4. 99% of the negative SET-PWs on OutA are smaller than 100ns. Those are the only SETs that may induce errors on the comparator non-inverting output (Fig. 17).
5. 99% of the positive SET-PWs on OutB are smaller than 200ns. Those are the only SETs that may induce errors on the comparator inverting-output (Fig. 17), if OutB is used.

Fig. 18 shows the overall distribution of SET pulse amplitudes vs. SET pulse widths. Based on the given data (Fig. 15, and Fig17), this comparator can be used as if SET-PWs of 100ns can be tolerated at the comparator output OutA and of 200ns at the output OutB.

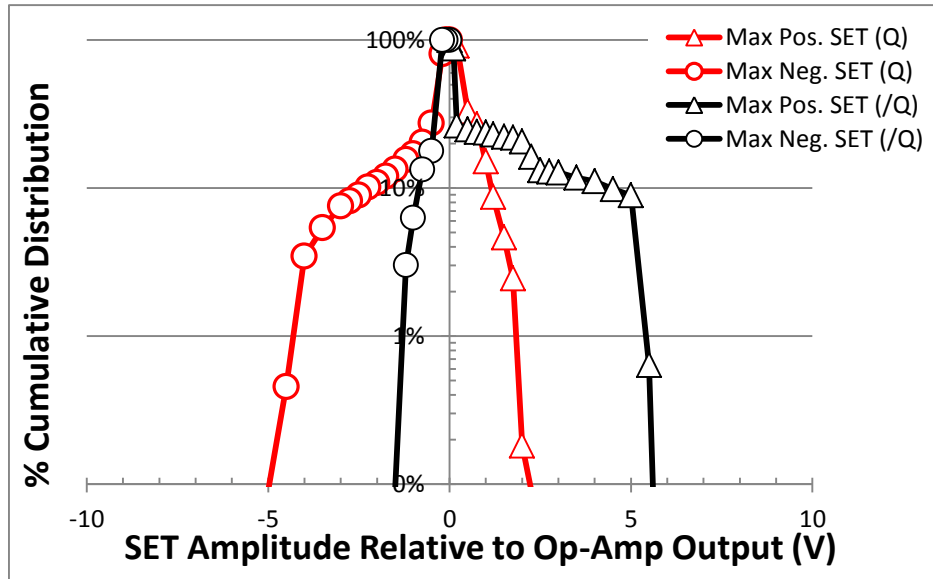


Fig. 15: % Cumulative Distribution vs. SET Positive and Negative Amplitudes at both comparator outputs (non-inverting (OutA) and inverting (OutB)). $V_{supply} = \pm 5V$; $V_{input} = (0.05V \text{ to } 0.4V)$; OutA Initially High, OutB Initially Low, Xenon Ions; $LET=58.78 \text{ MeV}\cdot\text{cm}^2/\text{mg}$ (Runs 163-170)

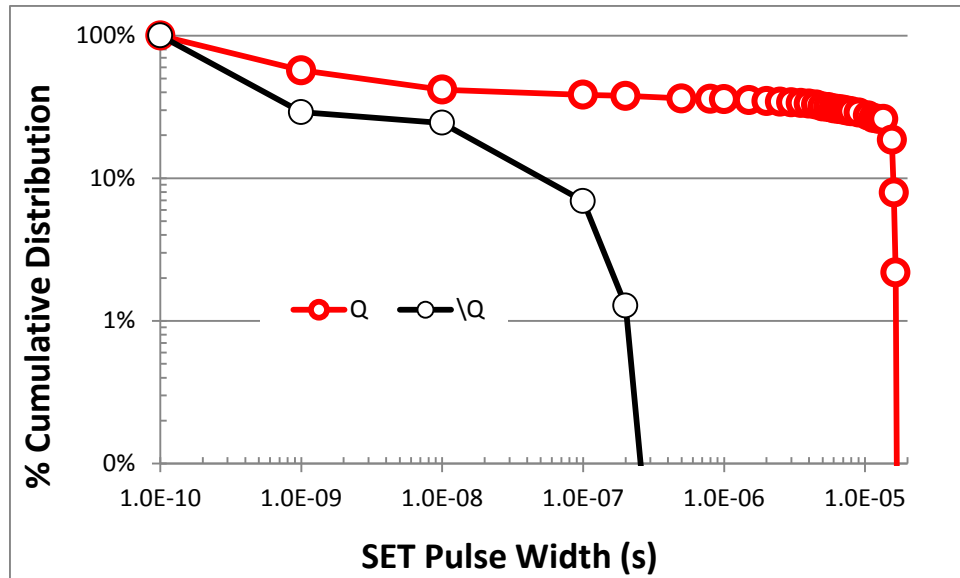


Fig. 16: % Cumulative Distribution vs. SET Pulse Widths at both comparator outputs (non-inverting (OutA) and inverting (OutB)). V supply= $\pm 5V$; V input= (0.05V to 0.4V); OutA Initially High, OutB Initially Low, Xenon Ions; LET=58.78 MeV.cm²/mg (Runs 163-170)

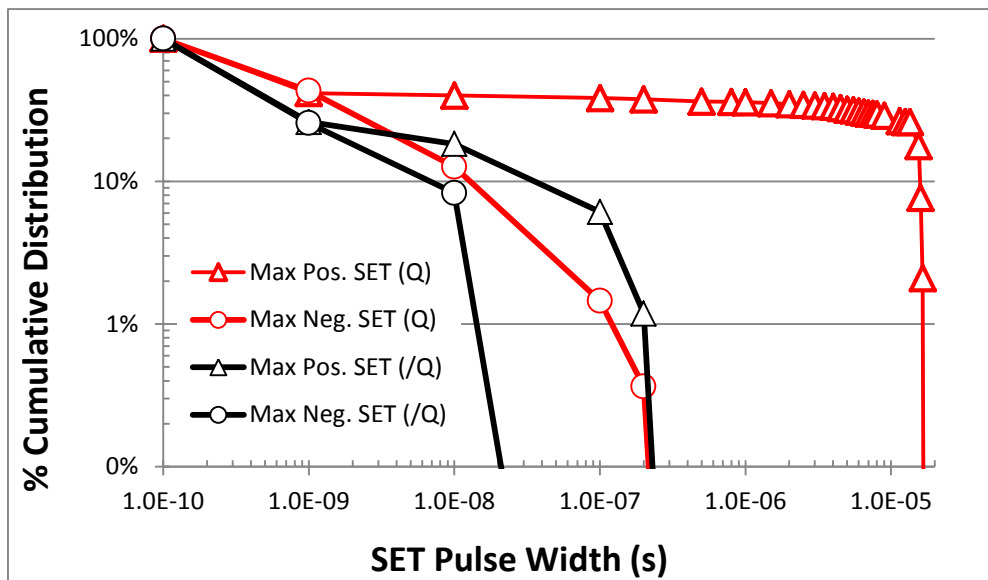


Fig. 17: % Cumulative Distribution vs. SET Positive and Negative Pulse Widths at both comparator outputs (non-inverting (OutA) and inverting (OutB)). V supply= $\pm 5V$; V input= (0.05V to 0.4V); OutA Initially High, OutB Initially Low, Xenon Ions; LET=58.78 MeV.cm²/mg (Runs 163-170)

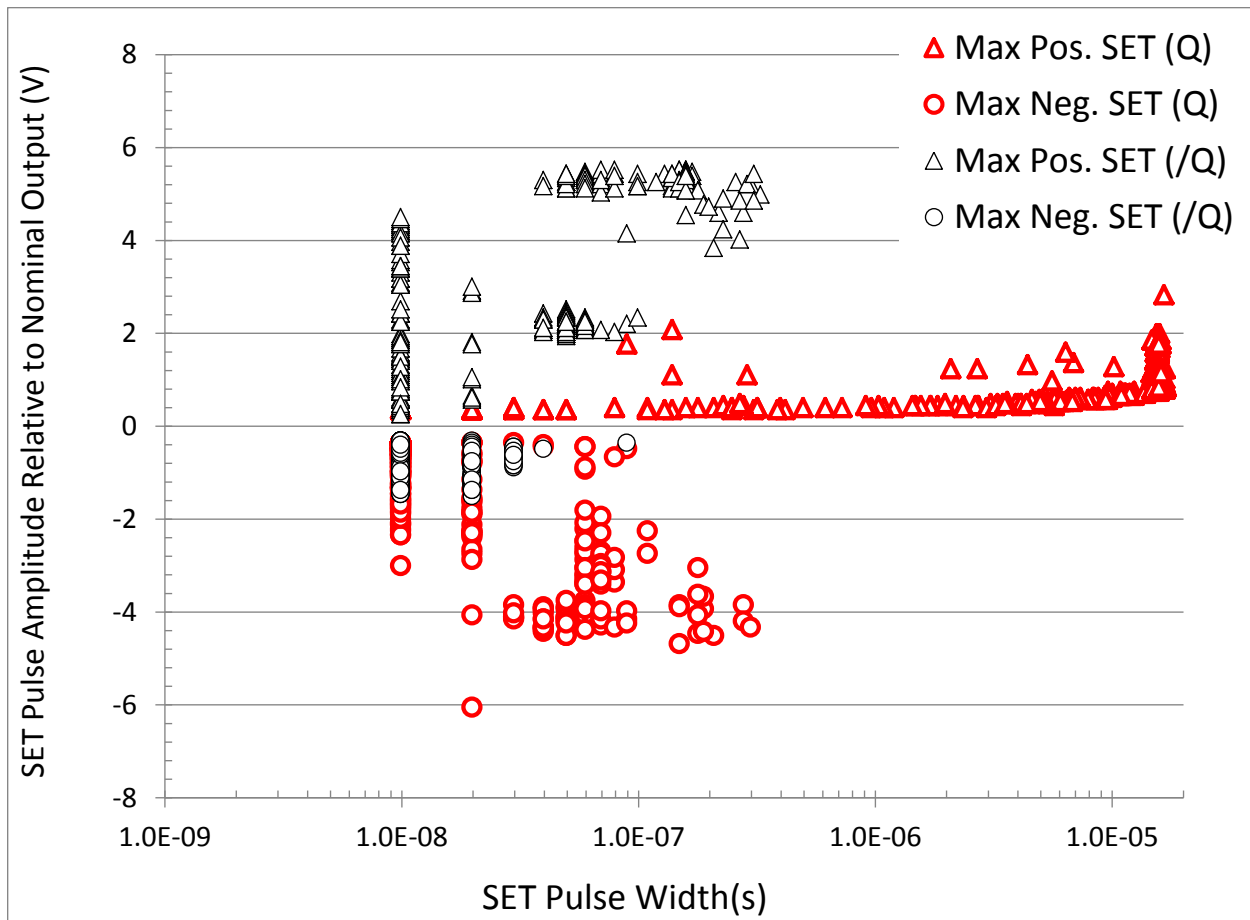


Fig. 18: Distributions of Negative and Positive SET Amplitudes vs. Positive and Negative SET Pulse Widths at both comparator outputs (non-inverting (OutA) and inverting (OutB)). V supply= ± 5 V; V input= (0.05V to 0.4V); OutA Initially High, OutB initially Low, Xenon Ions; LET=58.78 MeV.cm²/mg (Runs 163-170). Only negative SETs on OutA (Q) and positive SETs on OutB (/Q) may cause errors; they are smaller than 300ns.

b) When OutA is initially Low and OutB is initially High, with $V_{input}=(0.7 \text{ to } 1V)$

The SET pulse widths and amplitudes varied with the inverting-input-voltage (V_{in}). For V_{in} ranging between 0.7V and 1V, setting the non-inverting output OutA initially low and the inverting output OutB initially high, the data obtained under Xenon Ions ($LET=58.78 \text{ MeV.cm}^2/\text{mg}$) show that:

1. 90% of the positive SET pulse amplitudes on OutA initially low are smaller than $\pm 3V$ (Fig. 19)
2. 90% of the negative SET pulse amplitudes on OutB initially high are smaller than $\pm 2V$ (Fig. 19)
3. Although the SET pulse widths on OutB can go upto 18 us (Fig. 20), only the positive SETs on this output, which are smaller than 200ns (Fig. 21), may cause errors.
4. 99% of the positive SET-PWs on OutA are smaller than 100ns. Those are the only SETs that may induce errors on the comparator non-inverting output (Fig. 21).
5. 99% of the negative SET-PWs on OutB are smaller than 40ns. Those are the only SETs that may induce errors on the comparator inverting-output (Fig. 21), if OutB is used.

Fig. 22 shows the overall distribution of SET pulse amplitudes vs. SET pulse widths. Based on the given data (Fig. 19, and Fig. 21), this comparator can be used as is if SET-PWs of 100ns can be tolerated at the comparator output OutA and of 200ns at the output OutB.

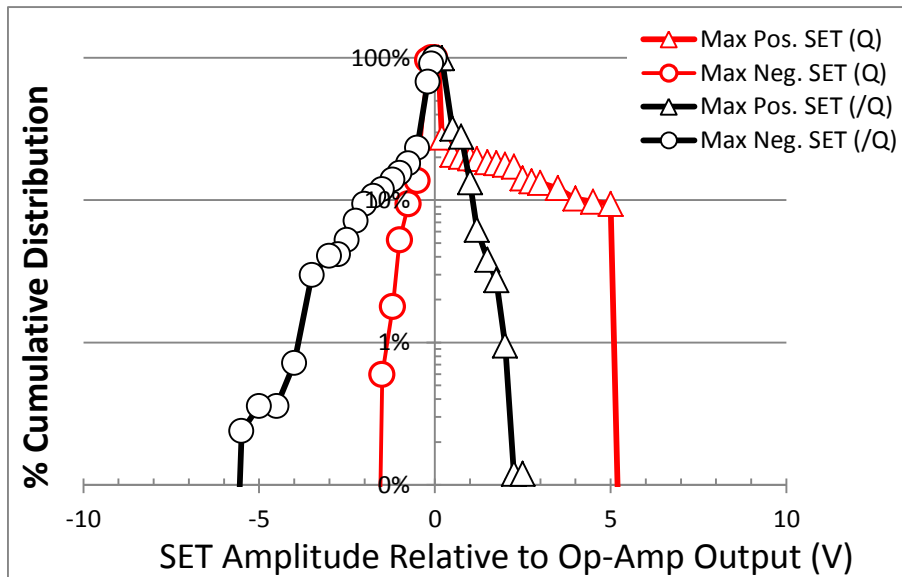


Fig. 20: % Cumulative Distribution vs. SET Positive and Negative Amplitudes at both comparator outputs (non-inverting (OutA) and inverting (OutB)). $V_{supply}=\pm 5V$; $V_{input}=(0.7 \text{ to } 1V)$; OutA Initially Low, OutB initially High, Xenon Ions; $LET=58.78 \text{ MeV.cm}^2/\text{mg}$ (Runs 176-182)

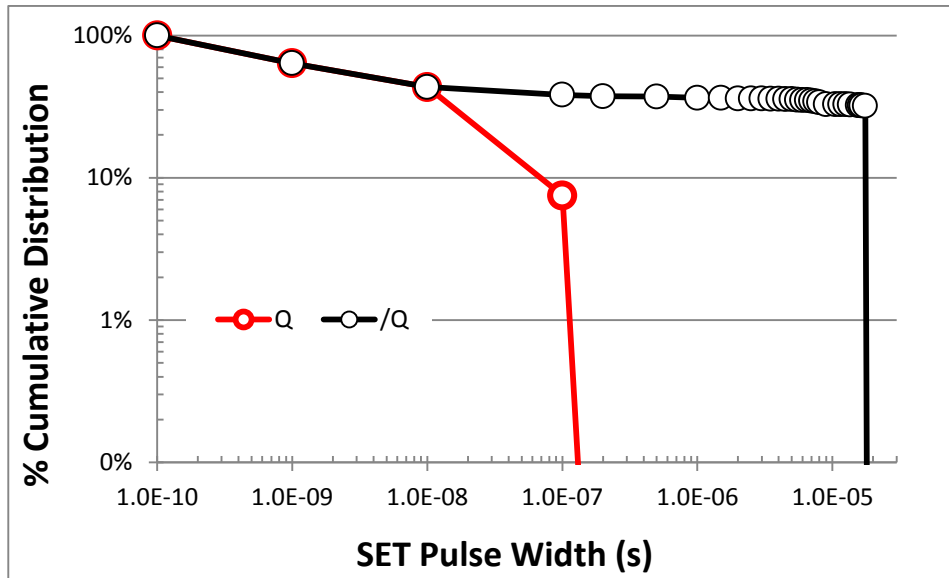


Fig. 21: % Cumulative Distribution vs. SET Pulse Widths at both comparator outputs (non-inverting (OutA) and inverting (OutB)). V supply= $\pm 5V$; V input= (0.7 to 1V); OutA Initially Low, OutB initially High, Xenon Ions; LET=58.78 MeV.cm²/mg (Runs 176-182)

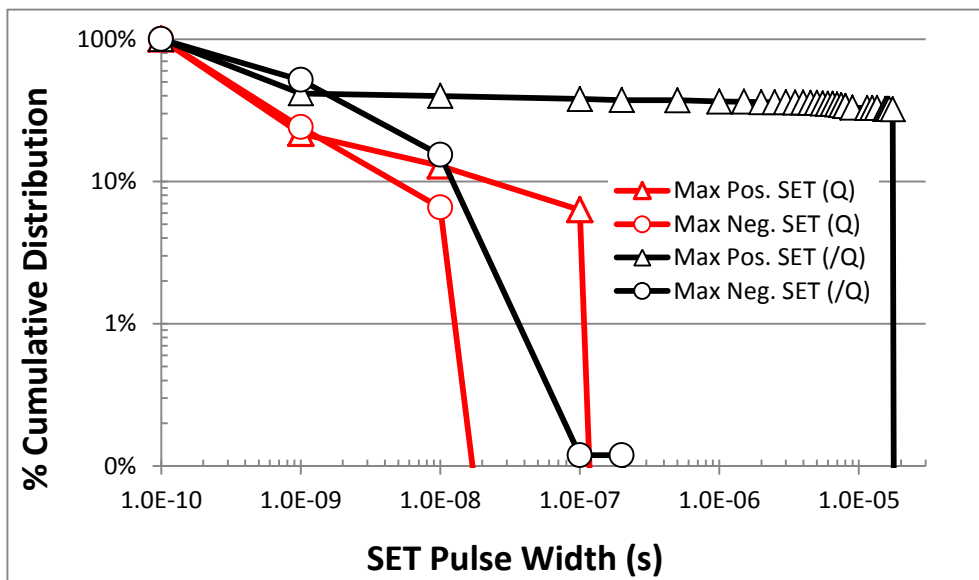


Fig. 22: % Cumulative Distribution vs. SET Positive and Negative Pulse Widths at both comparator outputs (non-inverting (OutA) and inverting (OutB)). V supply= $\pm 5V$; V input= (0.7 to 1V); OutA Initially Low, OutB initially High, Xenon Ions; LET=58.78 MeV.cm²/mg (Runs 176-182)

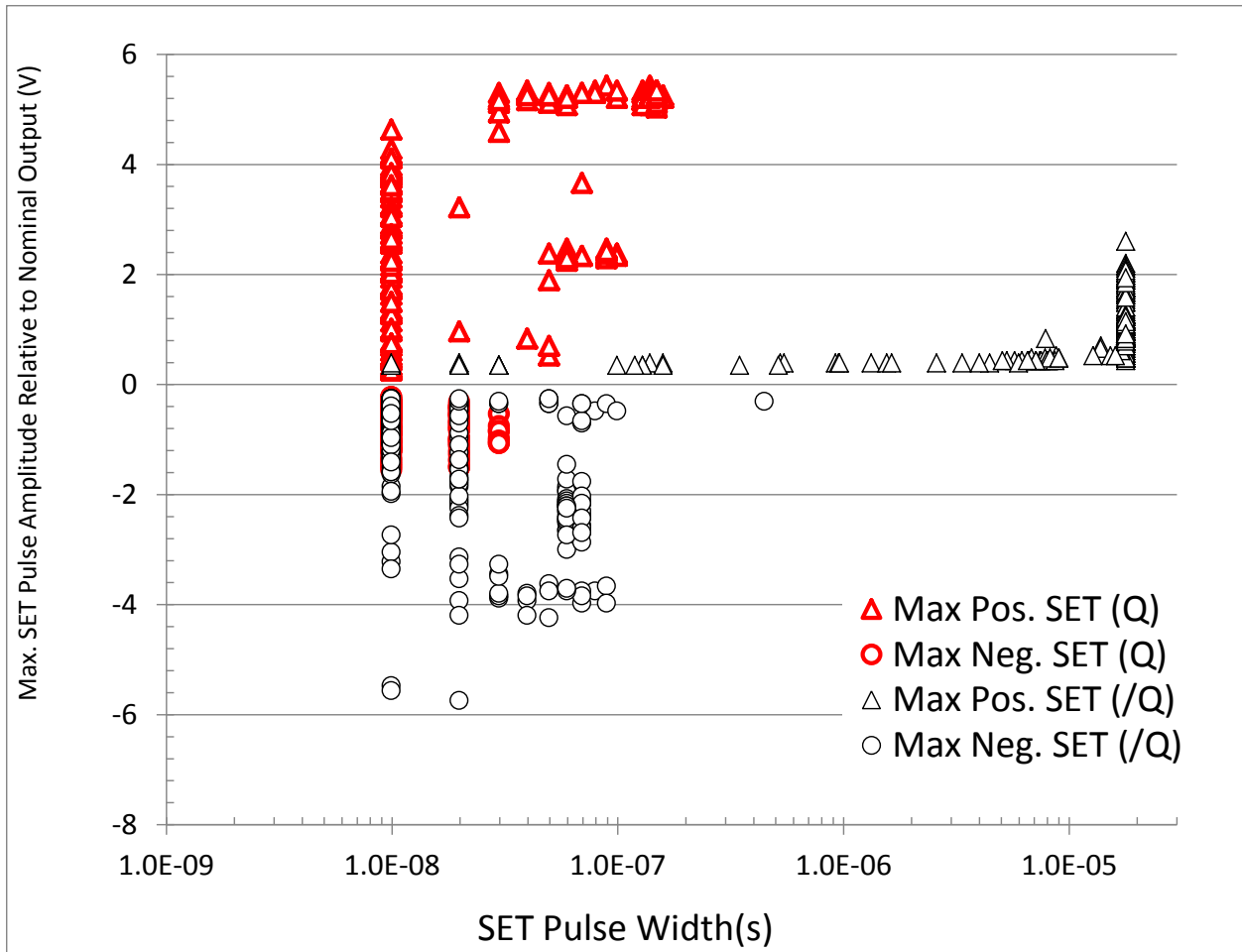


Fig. 23: Distributions of Negative and Positive SET Amplitudes vs. Positive and Negative SET Pulse Widths at both comparator outputs (non-inverting (OutA) and inverting (OutB)). V supply= $\pm 5V$; V input= (0.7 to 1V); OutA Initially Low, OutB initially High, Xenon Ions; LET=58.78 MeV.cm²/mg (Runs 176-182). Only positive SETs on OutA (Q) and negative SETs on OutB (/Q) may cause errors; they are smaller than 200ns.

3) SET Cross-Sections

Under heavy-ions irradiations, with various differential input bias conditions, the RH1016MW showed small sensitivities to SETs. Figs. 24 to 26 summarize the SET cross-sections at various biases. The measured SET sensitive cross-section is about $5 \times 10^{-4} \text{cm}^2/\text{circuit}$ and represents about 2.5% of the total die's area (1.95mm^2). When the comparator inverting input bias is close to the hysteresis boundary voltages, the SET pulse-width (PW) is the widest, and the measured SET cross-sections are the highest. The inverting input bias (at test point E6, Fig. 5) is proportional to the differential input bias as the non-inverting input bias is fixed. Hence, the lower the comparator input differential bias is, the higher the SET pulse amplitude and width as well as the cross-section are. Generally, the smaller is the comparator differential input bias, or the closer we are to the hysteresis region, the higher are the part's susceptibility to trigger and the higher are the resulting SET cross-sections. At higher LET near the limiting cross-section, the dependence on differential input bias becomes less significant, as most SETs become wide.

Furthermore, the SET cross-section is at its highest at the hysteresis area and SETs in these regions may induce SEUs, if the inverting input voltage is set between (0.45V-0.55V). It is important not to run the comparator in the hysteresis area to avoid SEUs, as it is the case for all comparators. Also, to avoid high SET cross-sections at LETs that are lower or equal than $30.86 \text{MeV.cm}^2/\text{mg}$, it is recommended to not operate the inverting input bias from (0.45V-0.65V), as if the hysteresis area was widened from (0.45V-0.55V) to (0.45V-0.65V) as clearly shown in Figs. 24 to 26. Outside of this hysteresis area and with these low SET cross-sections ($3 \times 10^{-5} \text{cm}^2/\text{circuit}$) at $30 \text{MeV.cm}^2/\text{mg}$, this part can be used as is in most space applications.

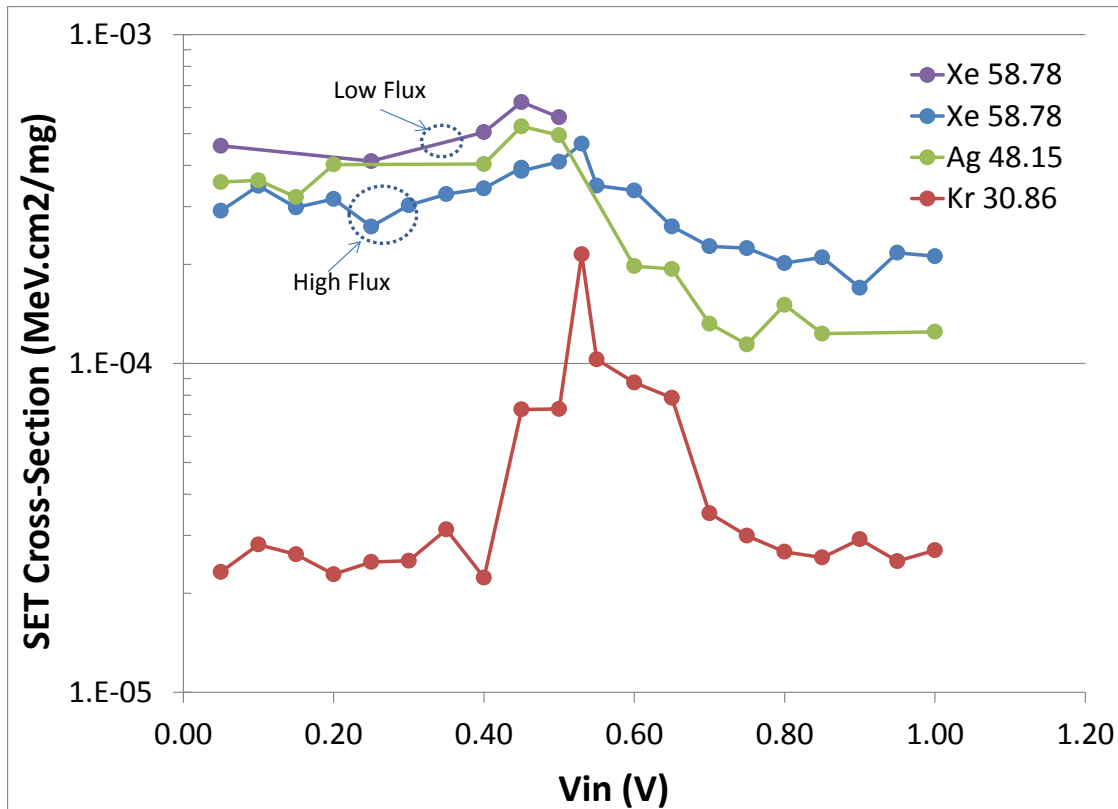


Fig. 24: Measured SET Cross-Sections vs. Inverting Input Bias (at test point E6, Fig. 3) and LET
 High Flux: $3.31 \text{E}3\text{-}5.5 \text{E}3 \text{ p/cm}^2/\text{sec}$; Low Flux: $5.23 \text{E}2 \text{ to } 5.7 \text{E}2 \text{ p/cm}^2/\text{sec}$

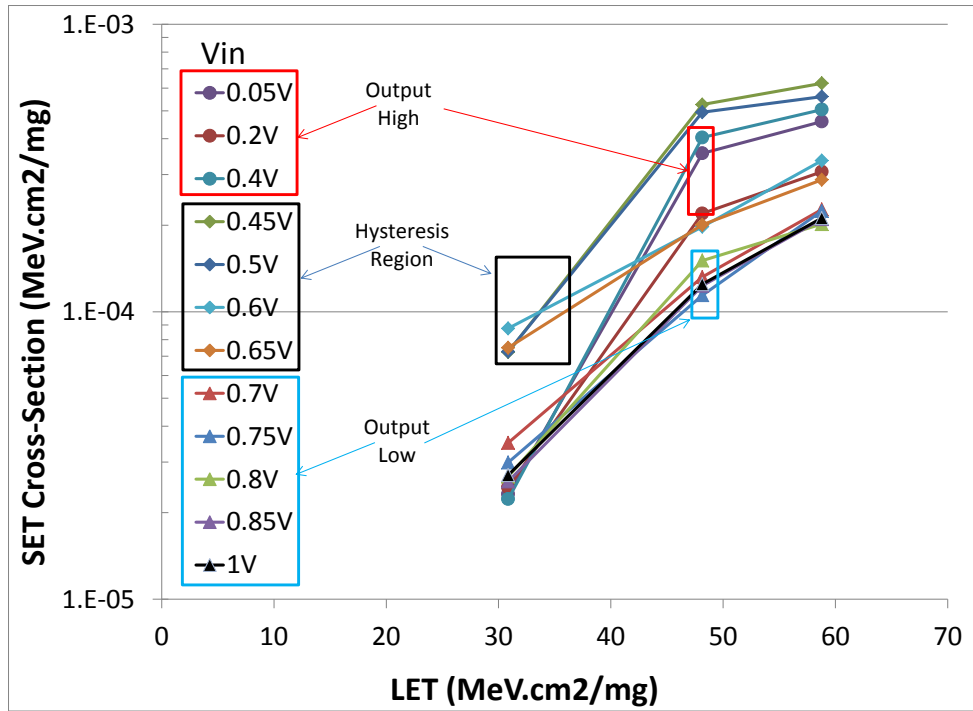


Fig. 25: Measured SET Cross-Sections vs. LET and Inverting Input Bias. This graph shows clearly the SET cross-sections dependence on the inverting input bias. In this case, the inverting input bias (at test point E6, Fig. 3) is proportional to the differential input bias as the non-inverting input bias is fixed. Hence, the lower the comparator input differential bias is, the higher the SET cross-section is.

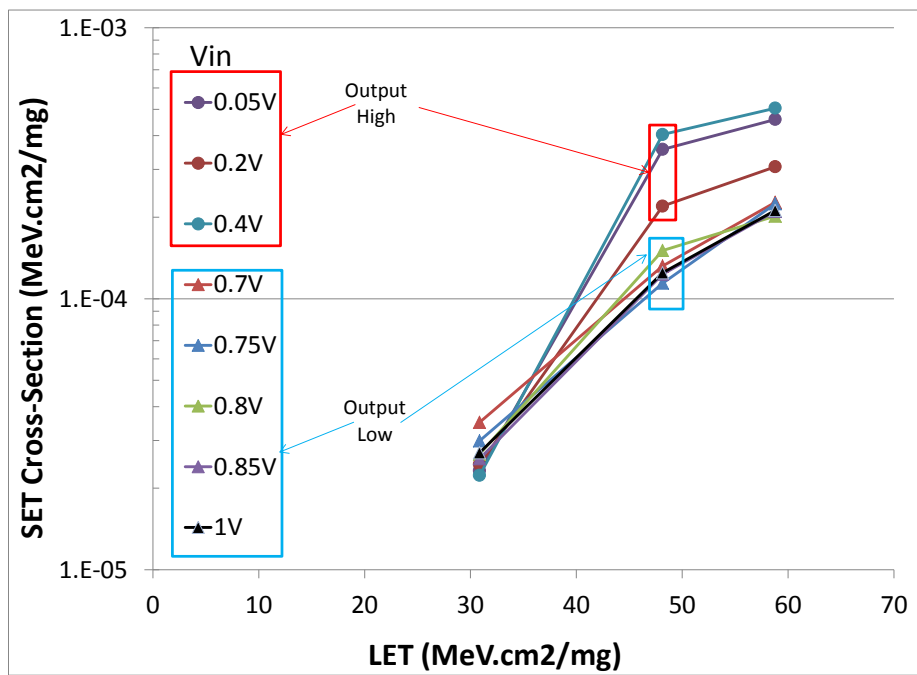


Fig. 26: Simplified figure of Fig. 25, avoiding the hysteresis area

4) *SEL Immunity With/Without Filtering (w/o capacitance at the Output Signal)*

With 0.1 μ F at the comparator's output and at high temperature (100°C) at the DUT case, the test results (green circles in Fig. 27) showed immunity to SELs up to an LET of 91 MeV.cm²/mg.

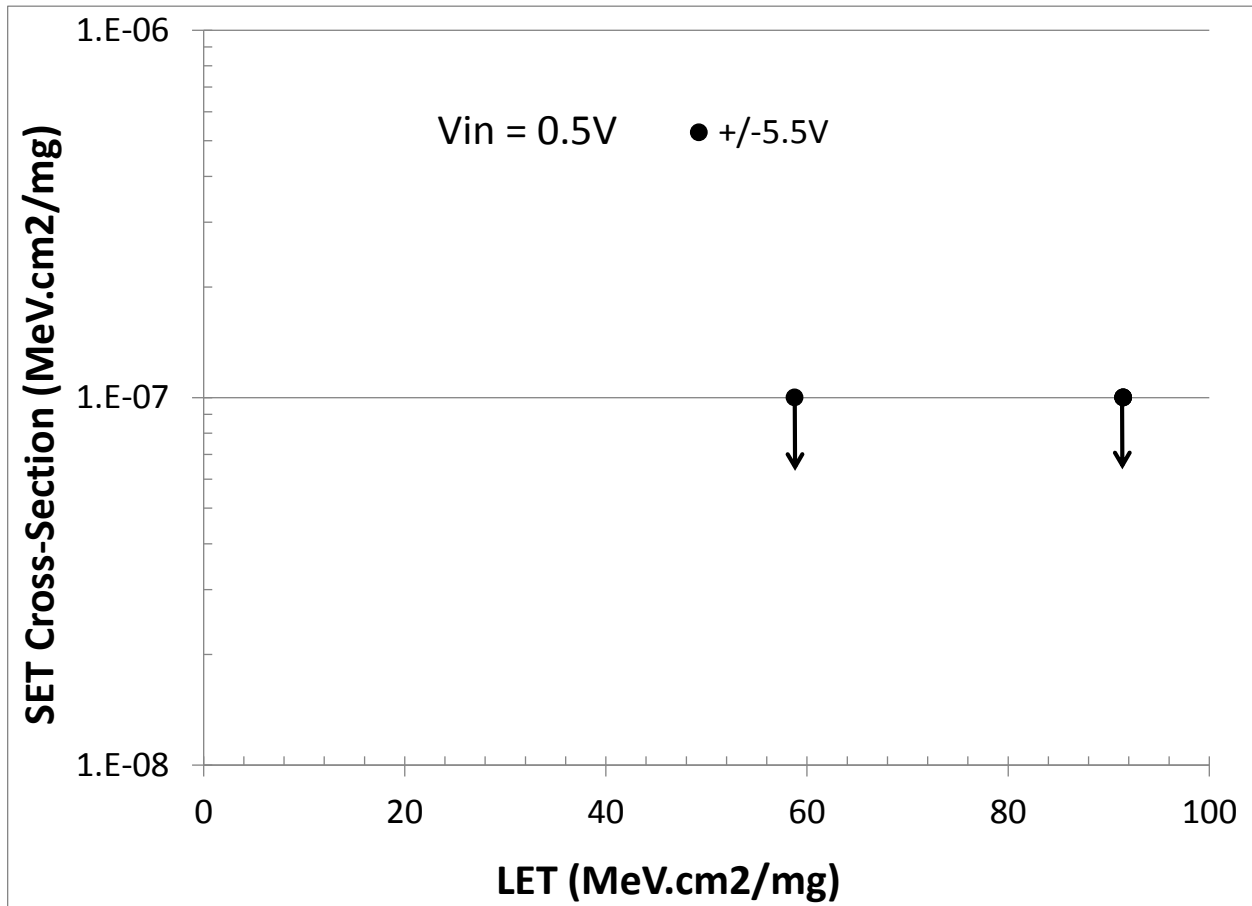


Fig. 27: Measured SEL Cross-Sections vs. LET, showing the comparator immunity to SELs

Arrows pointing down are indication of no observed SETs up to that fluence at tested LET

Table 2: Raw Data for the Heavy-Ion Beam Runs

Run #	DUT	Tb (Vacuum)	PS	Vin	Vin (E3)	Vout (Q)	Vout (/Q)	Ion	Eff. Fluence	Average Flux	Maximum Flux	LET	Tilt Angle	Eff. LET	TID (Run)	TID (Cum.)	SET	SEU	SEL	SETXS
		C	V	V	V	V	V		p/cm2	p/sec/cm2	p/sec/cm2	MeV.cm2/mg	degrees	MeV.cm2/mg	rads(Si)	rads(Si)				cm2/circuit
163	1	Room	+/-5	0.55	0.05	3.7	0	Xe	4.81E+05	5.48E+03	5.84E+03	58.78	0	58.78	4.52E+02	4.52E+02	140	0	0	2.91E-04
164	//	//	//	1.05	0.10	3.7	0	Xe	3.00E+05	4.05E+03	5.76E+03	58.78	0	58.78	2.82E+02	7.35E+02	104	0	0	3.47E-04
165	//	//	//	1.55	0.15	3.7	0	Xe	4.33E+05	3.41E+03	3.66E+03	58.78	0	58.78	4.07E+02	1.14E+03	129	0	0	2.98E-04
166	//	//	//	2.05	0.20	3.7	0	Xe	4.30E+05	3.36E+03	3.69E+03	58.78	0	58.78	4.04E+02	1.55E+03	136	0	0	3.16E-04
167	//	//	//	2.55	0.25	3.7	0	Xe	4.76E+05	3.44E+03	3.79E+03	58.78	0	58.78	4.48E+02	1.99E+03	124	0	0	2.61E-04
168	//	//	//	3.05	0.30	3.7	0	Xe	3.94E+05	3.44E+03	3.74E+03	58.78	0	58.78	3.71E+02	2.36E+03	118	0	0	2.99E-04
169	//	//	//	3.55	0.35	3.7	0	Xe	4.80E+05	3.46E+03	3.77E+03	58.78	0	58.78	4.51E+02	2.82E+03	157	0	0	3.27E-04
170	//	//	//	4.05	0.40	3.7	0	Xe	5.46E+05	3.45E+03	3.77E+03	58.78	0	58.78	5.14E+02	3.33E+03	186	0	0	3.41E-04
171	//	//	//	4.55	0.45	3.7	0	Xe	3.03E+05	3.31E+03	3.66E+03	58.78	0	58.78	2.85E+02	3.61E+03	118	0	0	3.89E-04
172	//	//	//	4.55	0.45	3.7	0	Xe	3.31E+05	3.35E+03	3.59E+03	58.78	0	58.78	3.11E+02	3.93E+03	127	0	0	3.84E-04
173	//	//	//	5.05	0.50	3.7	0	Xe	4.65E+05	3.41E+03	3.74E+03	58.78	0	58.78	4.37E+02	4.36E+03	193	y	0	4.15E-04
184	//	//	//	5.35	0.53	3.7	0	Xe	6.16E+05	3.38E+03	3.67E+03	58.78	0	58.78	5.79E+02	4.94E+03	122	y	0	1.98E-04
183	//	//	//	5.55	0.55	3.7	0	Xe	4.07E+05	3.55E+03	3.87E+03	58.78	0	58.78	3.83E+02	5.32E+03	125	y	0	3.07E-04
174	//	//	//	6.05	0.60	0	3.7	Xe	5.17E+05	3.61E+03	3.94E+03	58.78	0	58.78	4.86E+02	5.81E+03	208	0	0	4.02E-04
175	//	//	//	6.55	0.65	0	3.7	Xe	5.02E+05	3.60E+03	3.89E+03	58.78	0	58.78	4.72E+02	6.28E+03	107	0	0	2.13E-04
176	//	//	//	7.05	0.70	0	3.7	Xe	5.37E+05	3.58E+03	4.03E+03	58.78	0	58.78	5.05E+02	6.79E+03	118	0	0	2.20E-04
177	//	//	//	7.55	0.75	0	3.7	Xe	7.97E+05	4.37E+03	5.21E+03	58.78	0	58.78	7.50E+02	7.54E+03	112	0	0	1.41E-04
178	//	//	//	8.05	0.80	0	3.7	Xe	6.25E+05	4.69E+03	5.36E+03	58.78	0	58.78	5.88E+02	8.13E+03	109	0	0	1.74E-04
179	//	//	//	8.55	0.85	0	3.7	Xe	5.31E+05	4.28E+03	4.88E+03	58.78	0	58.78	4.99E+02	8.63E+03	168	0	0	3.16E-04
180	//	//	//	9.05	0.90	0	3.7	Xe	5.12E+05	4.04E+03	4.41E+03	58.78	0	58.78	4.82E+02	9.11E+03	107	0	0	2.09E-04
181	//	//	//	9.55	0.95	0	3.7	Xe	3.60E+05	4.14E+03	4.64E+03	58.78	0	58.78	3.39E+02	9.45E+03	115	0	0	3.19E-04
182	//	//	//	10.05	1.00	0	3.7	Xe	2.62E+05	4.20E+03	4.60E+03	58.78	0	58.78	2.46E+02	9.69E+03	108	0	0	4.12E-04
185	//	//	//	0.55	0.05	3.7	0	Kr	6.19E+06	1.47E+04	1.70E+04	30.86	0	30.86	3.06E+03	1.27E+04	144	0	0	2.33E-05
186	//	//	//	1.05	0.10	3.7	0	Kr	4.79E+06	1.63E+04	1.76E+04	30.86	0	30.86	2.37E+03	1.51E+04	135	0	0	2.82E-05
187	//	//	//	1.55	0.15	3.7	0	Kr	5.60E+06	1.67E+04	1.76E+04	30.86	0	30.86	2.77E+03	1.79E+04	147	0	0	2.63E-05
188	//	//	//	2.05	0.20	3.7	0	Kr	6.00E+06	1.67E+04	1.78E+04	30.86	0	30.86	2.96E+03	2.08E+04	137	0	0	2.28E-05

189	//	//	//	2.55	0.25	3.7	0	Kr	4.25E+06	1.66E+04	1.76E+04	30.86	0	30.86	2.10E+03	2.29E+04	107	0	0	2.52E-05
190	//	//	//	3.05	0.30	3.7	0	Kr	4.53E+06	1.62E+04	1.72E+04	30.86	0	30.86	2.24E+03	2.52E+04	113	0	0	2.49E-05
191	//	//	//	3.55	0.35	3.7	0	Kr	4.84E+06	1.65E+04	1.73E+04	30.86	0	30.86	2.39E+03	2.76E+04	150	0	0	3.10E-05
192	//	//	//	4.05	0.40	3.7	0	Kr	5.16E+06	1.68E+04	1.76E+04	30.86	0	30.86	2.55E+03	3.01E+04	116	0	0	2.25E-05
193	//	//	//	4.55	0.45	3.7	0	Kr	2.91E+06	1.66E+04	1.75E+04	30.86	0	30.86	1.44E+03	3.16E+04	210	0	0	7.22E-05
194	//	//	//	5.05	0.50	3.7	0	Kr	1.45E+06	5.61E+03	1.75E+04	30.86	0	30.86	7.16E+02	3.23E+04	109	y	0	7.52E-05
195	//	//	//	5.35	0.53	3.7	0	Kr	4.75E+05	3.17E+03	5.20E+03	30.86	0	30.86	2.35E+02	4.98E+04	103	y	0	2.17E-04
196	//	//	//	5.55	0.55	0	3.7	Kr	1.44E+06	3.80E+03	5.38E+03	30.86	0	30.86	7.11E+02	3.32E+04	144	y	0	1.00E-04
197	//	//	//	6.05	0.60	0	3.7	Kr	1.17E+06	4.96E+03	5.41E+03	30.86	0	30.86	5.78E+02	3.38E+04	105	0	0	8.97E-05
198	//	//	//	6.55	0.65	0	3.7	Kr	1.39E+06	4.91E+03	5.31E+03	30.86	0	30.86	6.86E+02	3.45E+04	110	0	0	7.91E-05
199	//	//	//	7.05	0.70	0	3.7	Kr	3.20E+06	8.36E+03	1.63E+04	30.86	0	30.86	1.58E+03	3.61E+04	112	0	0	3.50E-05
200	//	//	//	7.55	0.75	0	3.7	Kr	3.41E+06	8.57E+03	9.12E+03	30.86	0	30.86	1.68E+03	3.77E+04	102	0	0	2.99E-05
201	//	//	//	8.05	0.80	0	3.7	Kr	5.50E+06	1.33E+04	1.62E+04	30.86	0	30.86	2.72E+03	4.05E+04	147	0	0	2.67E-05
202	//	//	//	8.55	0.85	0	3.7	Kr	3.97E+06	1.50E+04	1.60E+04	30.86	0	30.86	1.96E+03	4.24E+04	102	0	0	2.57E-05
203	//	//	//	9.05	0.90	0	3.7	Kr	3.70E+06	1.50E+04	1.60E+04	30.86	0	30.86	1.83E+03	4.42E+04	108	0	0	2.92E-05
204	//	//	//	9.55	0.95	0	3.7	Kr	7.27E+06	1.51E+04	1.63E+04	30.86	0	30.86	3.59E+03	4.78E+04	182	0	0	2.50E-05
205	//	//	//	10.05	1.00	0	3.7	Kr	3.96E+06	1.54E+04	1.62E+04	30.86	0	30.86	1.96E+03	4.98E+04	107	0	0	2.70E-05
206	//	//	//	0.55	0.05	3.7	0	Ag	2.81E+05	2.06E+03	7.41E+03	48.15	0	48.15	2.16E+02	5.00E+04	100	0	0	3.56E-04
207	//	//	//	1.05	0.10	3.7	0	Ag	5.30E+05	1.36E+03	1.58E+03	48.15	0	48.15	4.08E+02	5.04E+04	191	0	0	3.60E-04
208	//	//	//	1.55	0.15	3.7	0	Ag	3.88E+05	2.10E+03	2.60E+03	48.15	0	48.15	2.99E+02	5.07E+04	125	0	0	3.22E-04
209	//	//	//	2.05	0.20	3.7	0	Ag	5.69E+05	2.38E+03	2.64E+03	48.15	0	48.15	4.38E+02	5.11E+04	229	0	0	4.02E-04
210	//	//	//	4.05	0.40	3.7	0	Ag	3.74E+05	1.56E+03	2.58E+03	48.15	0	48.15	2.88E+02	5.14E+04	151	0	0	4.04E-04
211	//	//	//	4.55	0.45	3.7	0	Ag	1.96E+05	5.87E+02	1.57E+03	48.15	0	48.15	1.51E+02	5.16E+04	103	0	0	5.26E-04
212	//	//	//	5.05	0.50	3.7	0	Ag	4.31E+05	5.48E+02	6.99E+02	48.15	0	48.15	3.32E+02	5.19E+04	213	y	0	4.94E-04
213	//	//	//	6.05	0.60	0	3.7	Ag	5.77E+05	1.03E+03	1.35E+03	48.15	0	48.15	4.45E+02	5.50E+04	114	0	0	1.98E-04
214	//	//	//	6.55	0.65	0	3.7	Ag	5.73E+05	1.24E+03	1.44E+03	48.15	0	48.15	4.41E+02	5.28E+04	111	0	0	1.94E-04
215	//	//	//	7.05	0.70	0	3.7	Ag	7.57E+05	1.92E+03	2.62E+03	48.15	0	48.15	5.83E+02	5.34E+04	100	0	0	1.32E-04
216	//	//	//	7.55	0.75	0	3.7	Ag	5.78E+05	2.47E+03	2.69E+03	48.15	0	48.15	4.45E+02	5.38E+04	66	0	0	1.14E-04
217	//	//	//	8.05	0.80	0	3.7	Ag	4.91E+05	2.54E+03	2.84E+03	48.15	0	48.15	3.78E+02	5.42E+04	74	0	0	1.51E-04
218	//	//	//	8.55	0.85	0	3.7	Ag	5.44E+05	2.57E+03	2.85E+03	48.15	0	48.15	4.19E+02	5.46E+04	67	0	0	1.23E-04

219	//	//	//	10.05	1.00	0	3.7	Ag	4.25E+05	2.58E+03	2.92E+03	48.15	0	48.15	3.27E+02	5.50E+04	53	0	0	1.25E-04
221	//	//	//	0.55	0.05	3.7	0	Xe	1.31E+05	5.23E+02	6.82E+02	58.78	0	58.78	1.23E+02	5.51E+04	50	0	0	3.82E-04
220	//	//	//	2.55	0.25	3.7	0	Xe	1.09E+05	5.61E+02	6.66E+02	58.78	0	58.78	1.03E+02	5.53E+04	54	0	0	4.95E-04
222	//	//	//	4.05	0.40	3.7	0	Xe	1.05E+05	5.59E+02	6.84E+02	58.78	0	58.78	9.88E+01	5.53E+04	53	0	0	5.05E-04
223	//	//	//	4.55	0.45	3.7	0	Xe	7.38E+04	5.64E+02	7.09E+02	58.78	0	58.78	6.94E+01	5.54E+04	46	0	0	6.23E-04
224	//	//	//	5.05	0.50	3.7	0	Xe	7.14E+04	5.70E+02	7.13E+02	58.78	0	58.78	6.72E+01	5.54E+04	40	y	0	5.60E-04
225	2	100	+/- 5.5	5.05	0.50	3.7	0	Xe	1.87E+03	6.06E+02	6.43E+02	58.78	0	58.78	1.76E+00	5.54E+04				invalid
226	//	//	//	5.05	0.50	3.7	0	Xe	2.99E+03	5.77E+02	6.59E+02	58.78	0	58.78	2.81E+00	5.54E+04	975	y	0	3.26E-01
227	//	//	//	5.05	0.50	3.7	0	Xe	1.01E+07	1.60E+05	1.65E+05	58.78	50	91.45	1.48E+04	7.02E+04	1369	y	0	1.36E-04
229	//	//	//	5.05	0.50	3.7	0	Xe	1.01E+07	1.60E+05	1.65E+05	58.78	50	91.45	1.48E+04	8.50E+04	1333	y	0	1.32E-04

*Tb is the temperature sensed by the transistor on the board (as shown in Fig. 5)

3ft BNC cable (120pF)	Energy Cocktail 10MeV/nucleon
-----------------------	-------------------------------

References:

- [1] RH1016M Product Webpage: <http://www.linear.com/product/RH1016M>
- [2] LT1016 Datasheet: <http://www.linear.com/product/LT1016>
- [3] LTSpice: <http://www.linear.com/designtools/software/#LTspice>
- [4] RH1016M Spec.: http://cds.linear.com/docs/en/spec-notice/RH1016M_05-08-5222_SPEC_REV.0.pdf
- [5] RH1016M Spec.: <http://cds.linear.com/docs/en/spec-notice/RH1016M%20%20DIE%20CAN%20SAM%2005-08-5242%20DICE%20SPEC%20REV%20%20A.pdf>

Appendix A.: SET Distributions in Pulse Widths and Amplitudes per Bias Conditions vs. LET

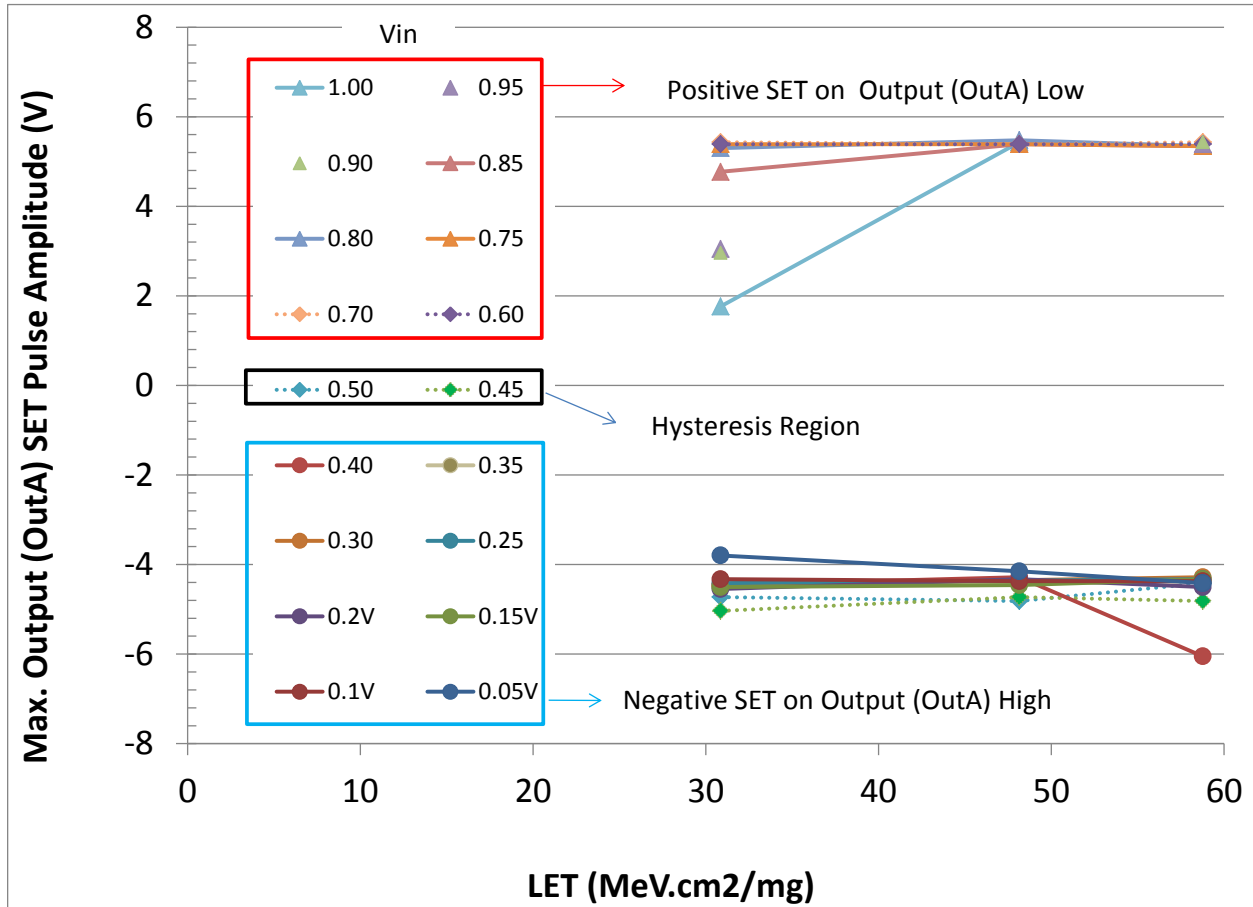


Fig. A-1: Measured Max. SET Pulse Amplitudes at Output (OutA) vs LET and Voltage of the inverting input (Vin). These types of SET may induce errors at the output of the comparator. They are however the smallest in width among all other SETs and represent less than 1% of the total number of SETs.

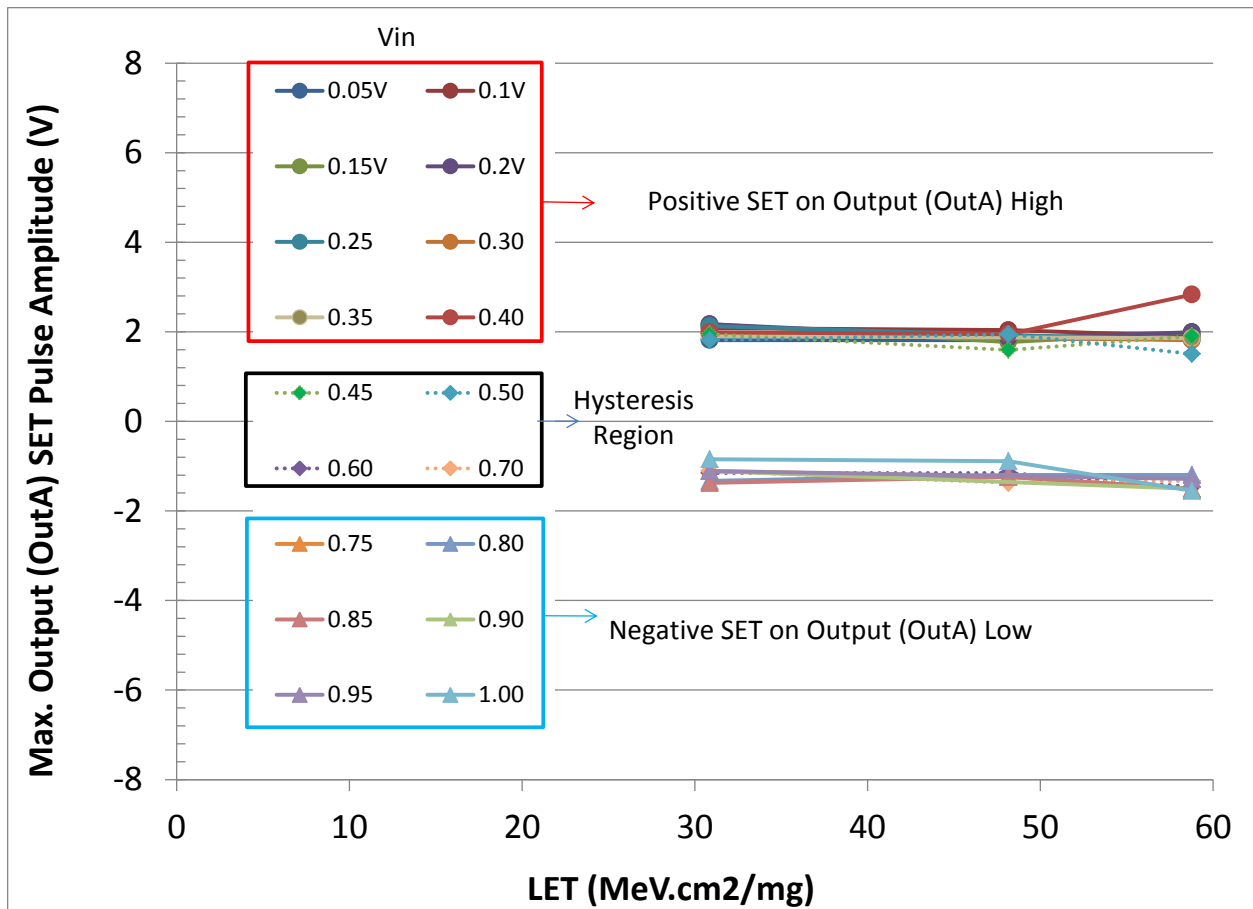


Fig. A-2: Measured Max. SET Pulse Amplitudes at Output (OutA) vs LET and Input Voltage of the Inverting-Input (Vin). These types of SET won't induce errors at the output of the comparator but the designer needs to take in account their amplitudes in his design.

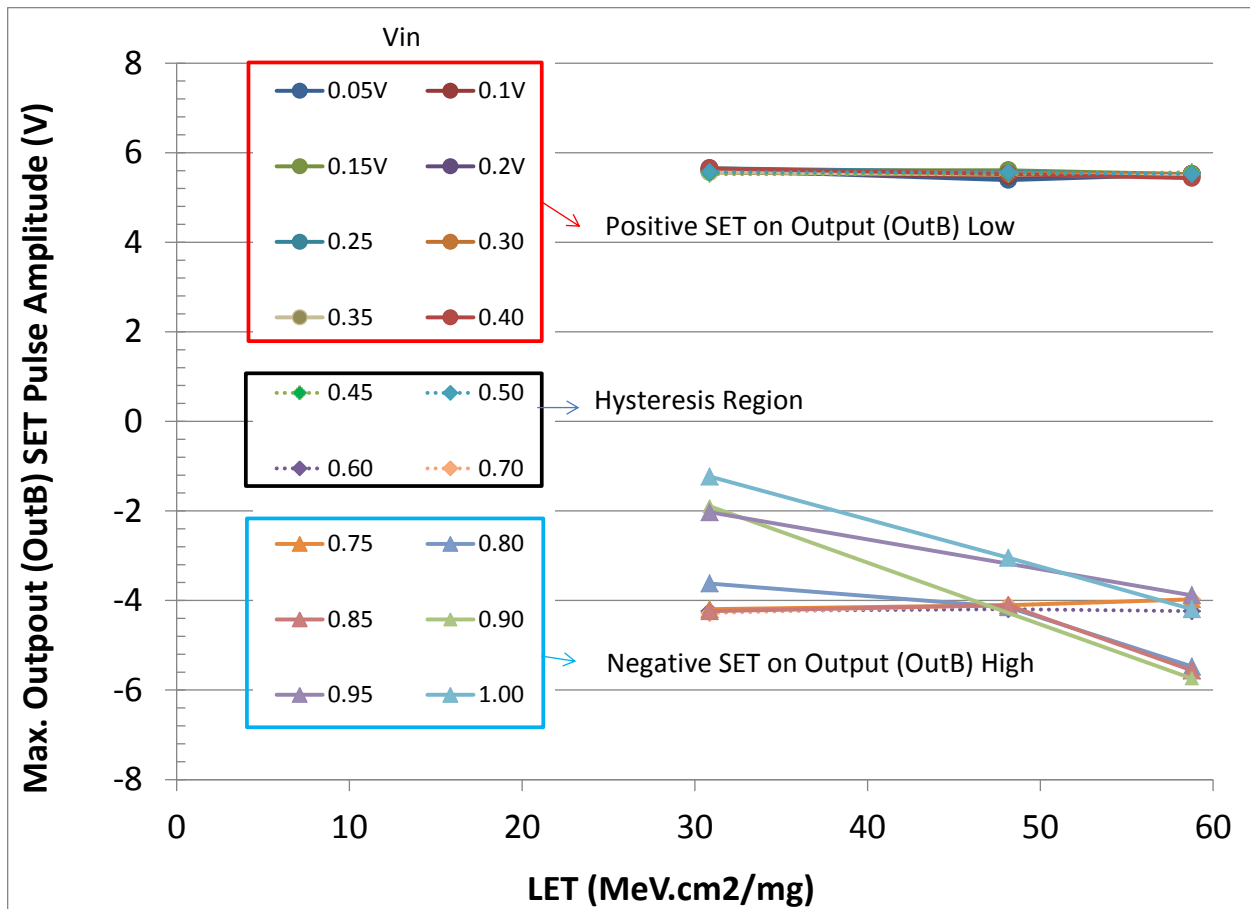


Fig. A-3: Measured Max. SET Pulse Amplitudes at Output (OutB) vs LET and Input Voltage of the Inverting-Input (Vin). These types of SET may induce errors at the output of the comparator, if the designer is using OutB. They are however the smallest in width among all other SETs and represent less than 1% of the total number of SETs.

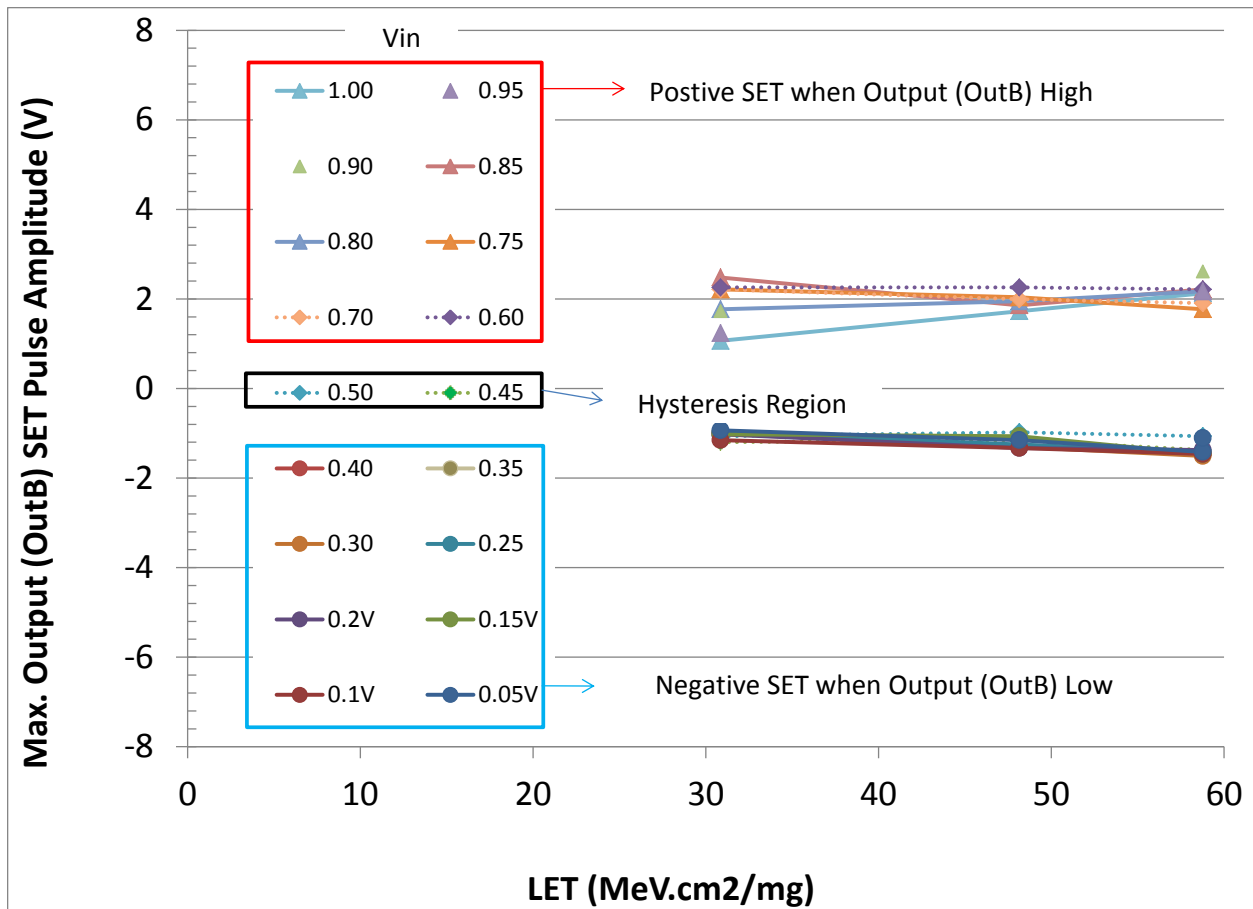


Fig. A-4: Measured Max. SET Pulse Amplitudes at Output (OutB) vs LET and Input Voltage of the Inverting-Input (Vin). These types of SET won't induce errors at the output of the comparator but the designer needs to take in account their amplitudes in his design, if using OutB.

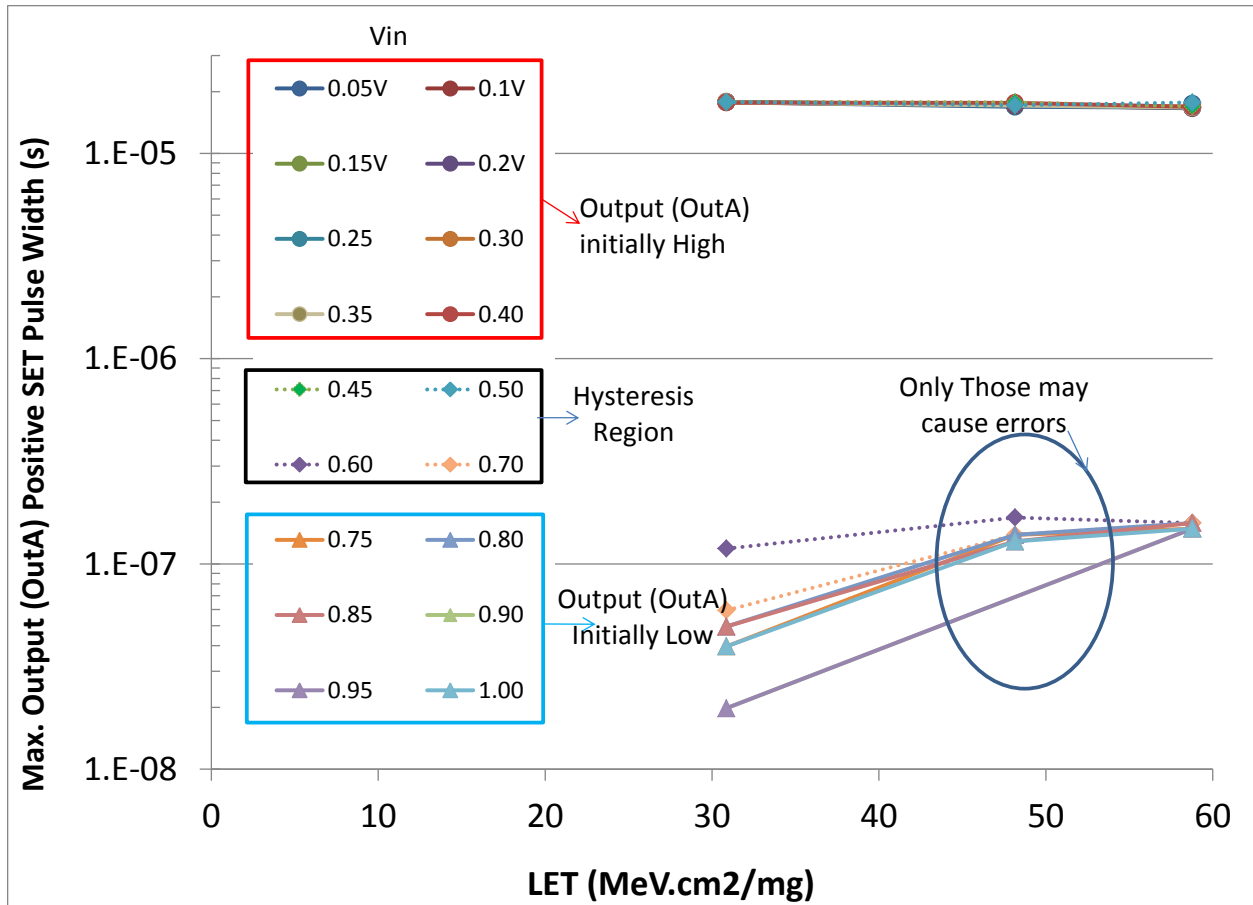


Fig. A-5: Measured Max. Positive SET Pulse Widths at Output (OutA) vs LET and Input Voltage of the Inverting-Input (Vin). Only SETs when Output is Low will cause errors and they are smaller than 200ns at LET=58.78MeV.cm2/mg. If such SET-PW can be accepted, then the part can be used as is.

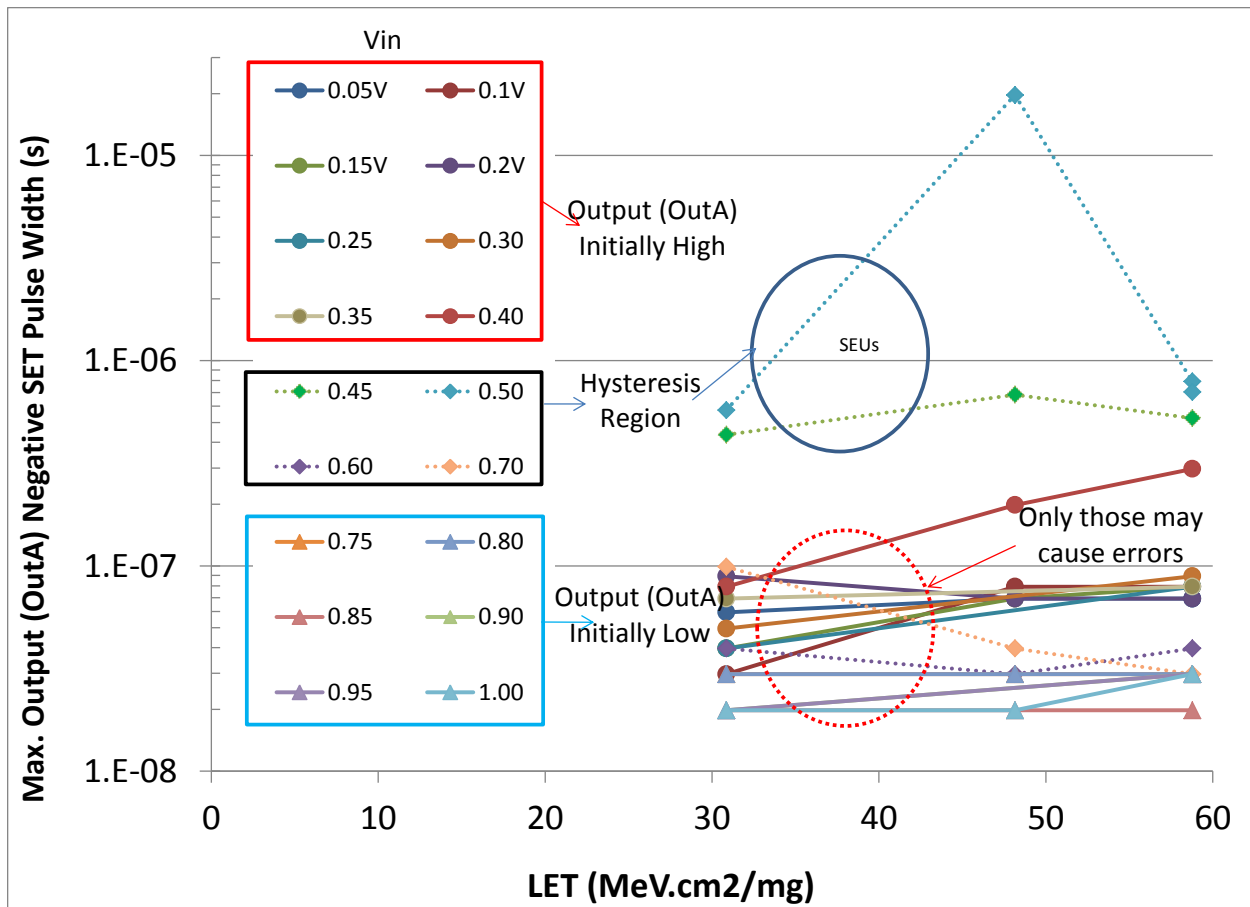


Fig. A-6: Measured Max. Negative SET Pulse Amplitudes at Output (OutA) vs LET and Input Voltage of the Inverting-Input (Vin). Only SETs when Output is High initially will cause errors and they are smaller than 300ns at LET=58.78MeV.cm2/mg. If such SET-PW can be accepted, then the part can be used as is.

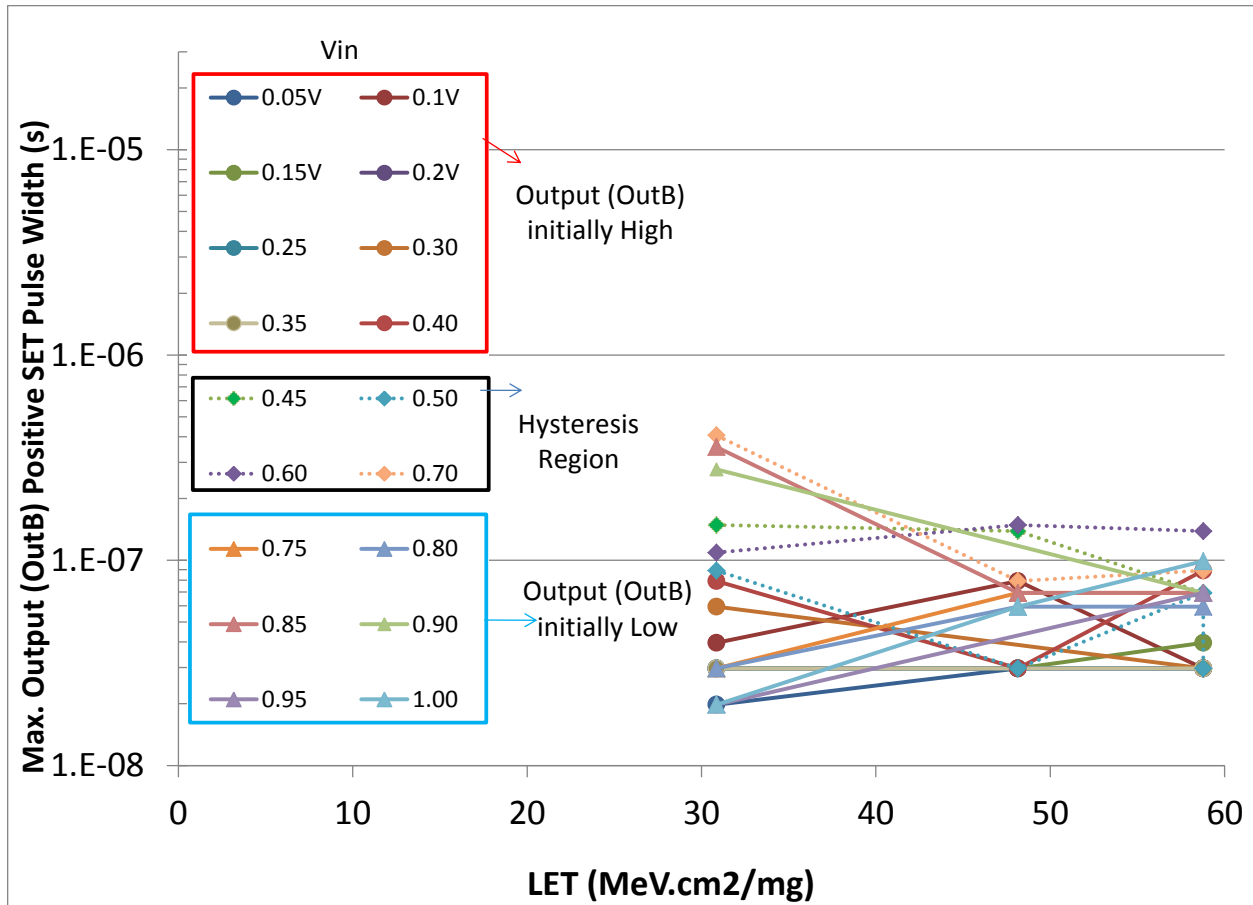


Fig. A-7: Measured Max. Negative SET Pulse Amplitudes at Output (OutA) vs LET and Input Voltage of the Inverting-Input (V_{in}). Only SETs when OutputB is Low initially will cause errors. If OutB is not used then these type of SETs are of no concern.

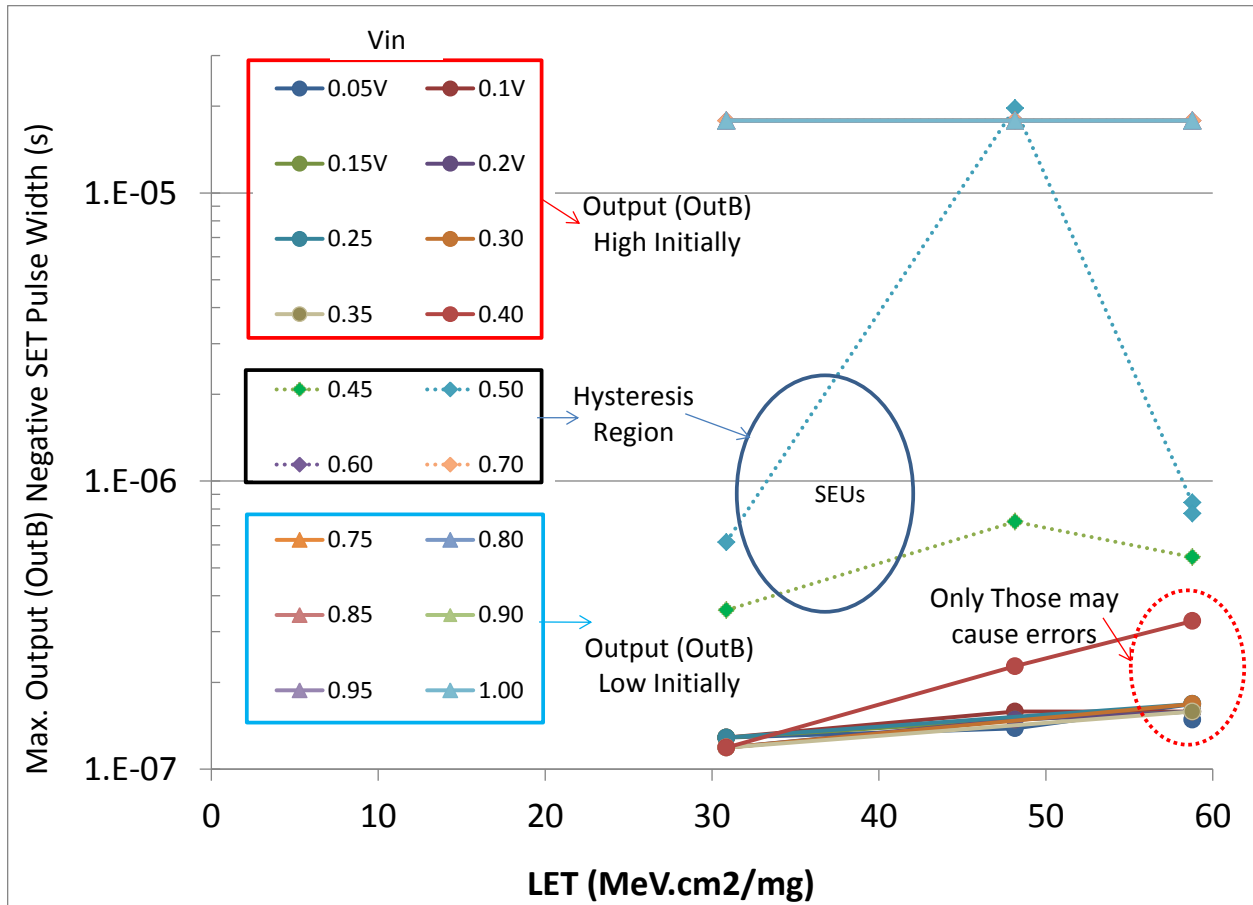
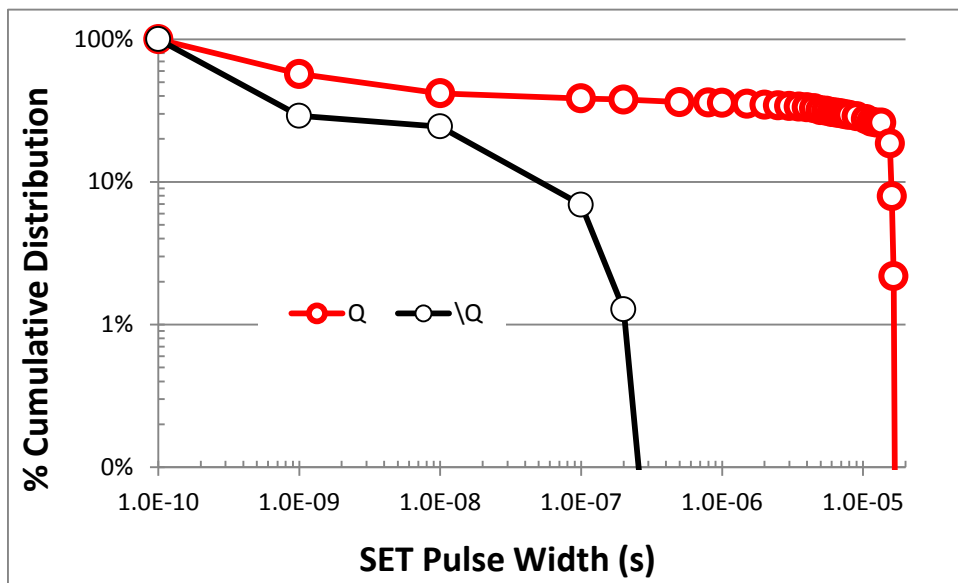
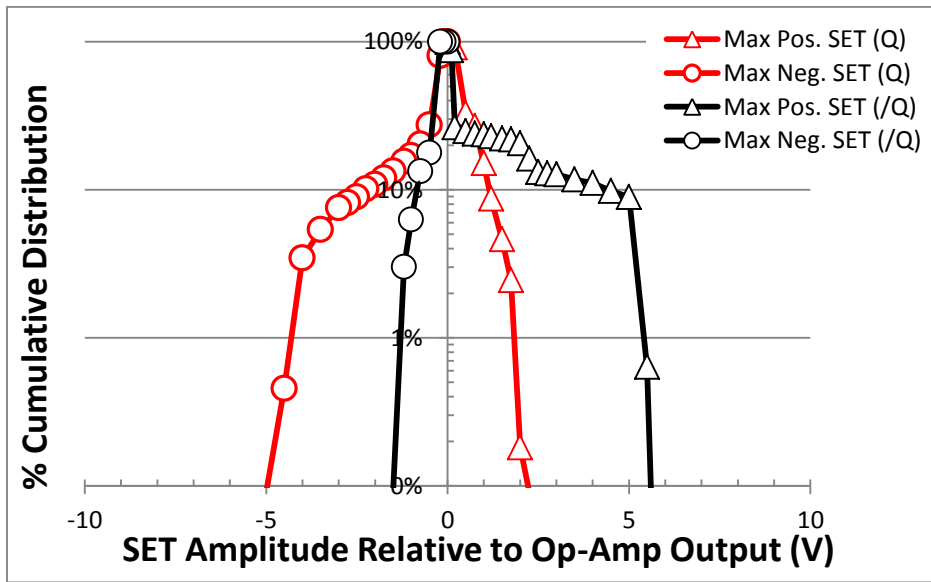


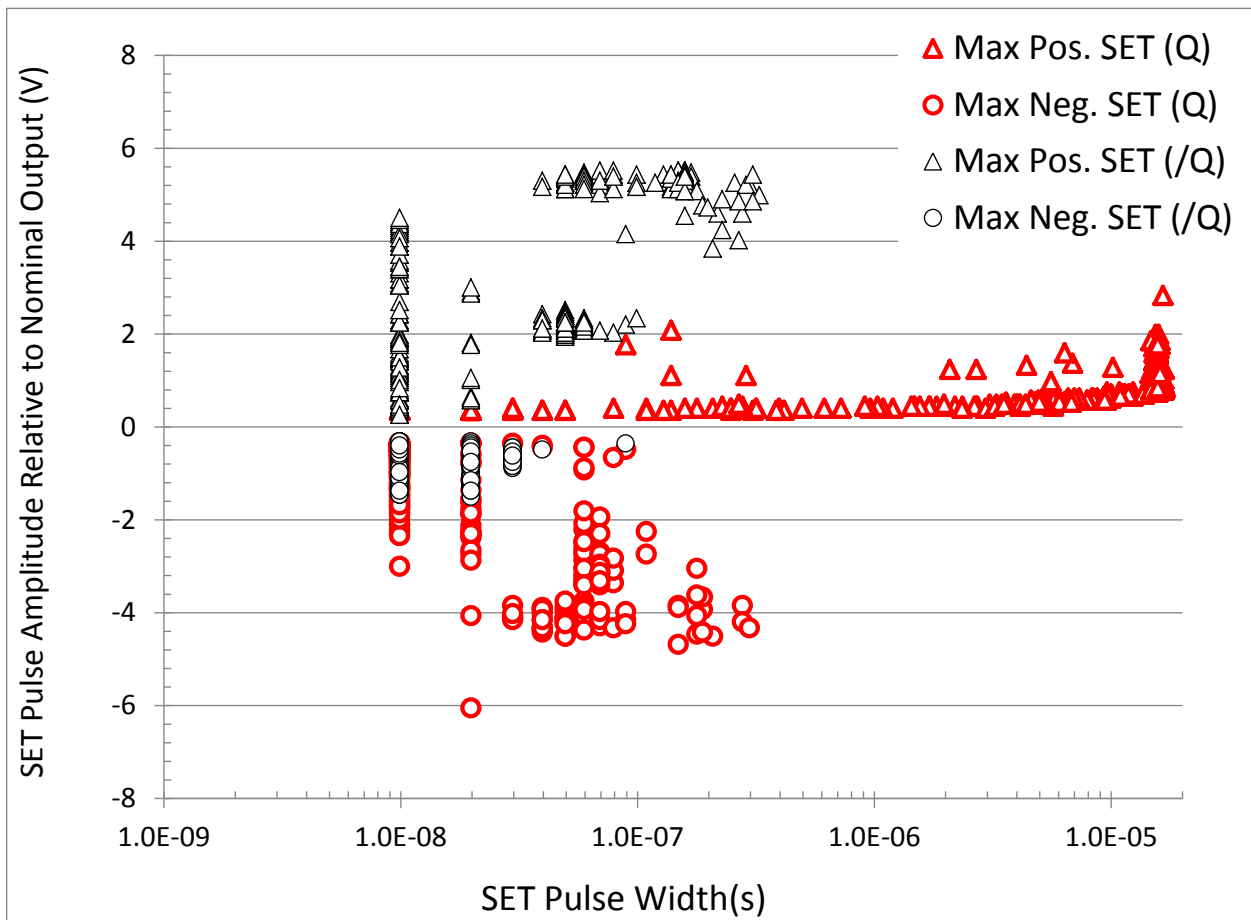
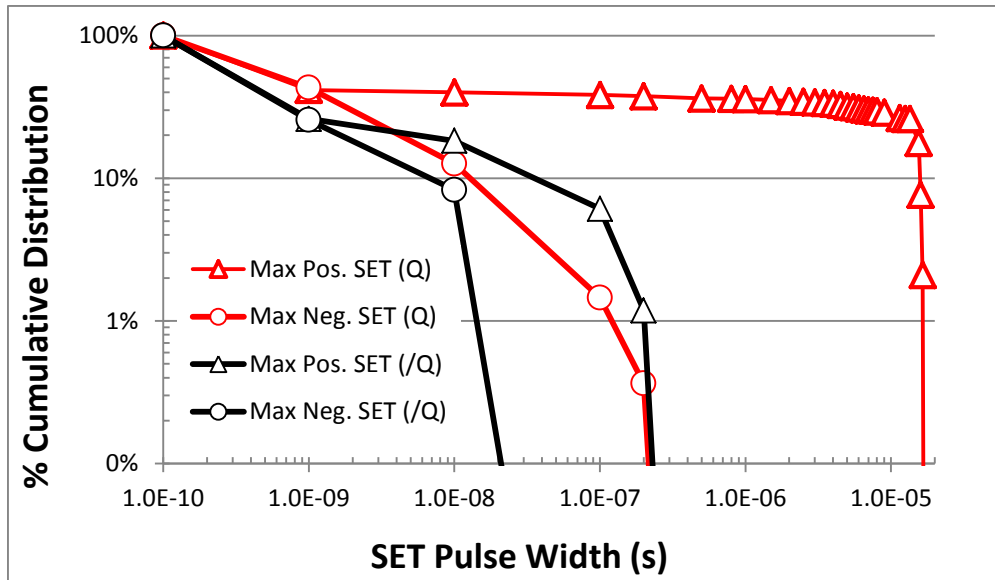
Fig. A-8: Measured Max. Negative SET Pulse Amplitudes at Output (OutA) vs LET and Input Voltage of the Inverting-Input (Vin). Only SETs when Output is High initially will cause errors. If OutB is not used then these type of SETs are of no concern.

Appendix B: SET Distributions in Pulse Widths and Amplitudes per Bias Conditions

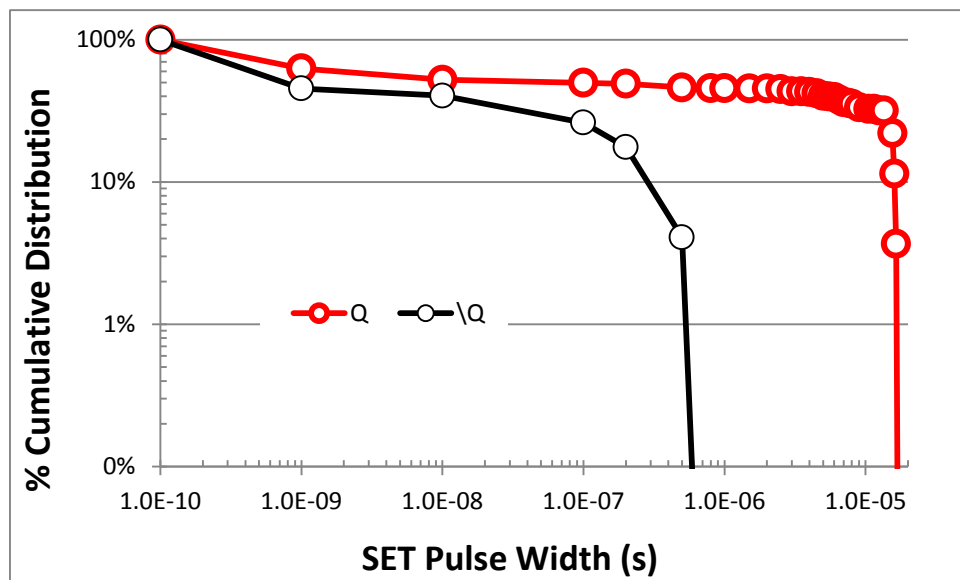
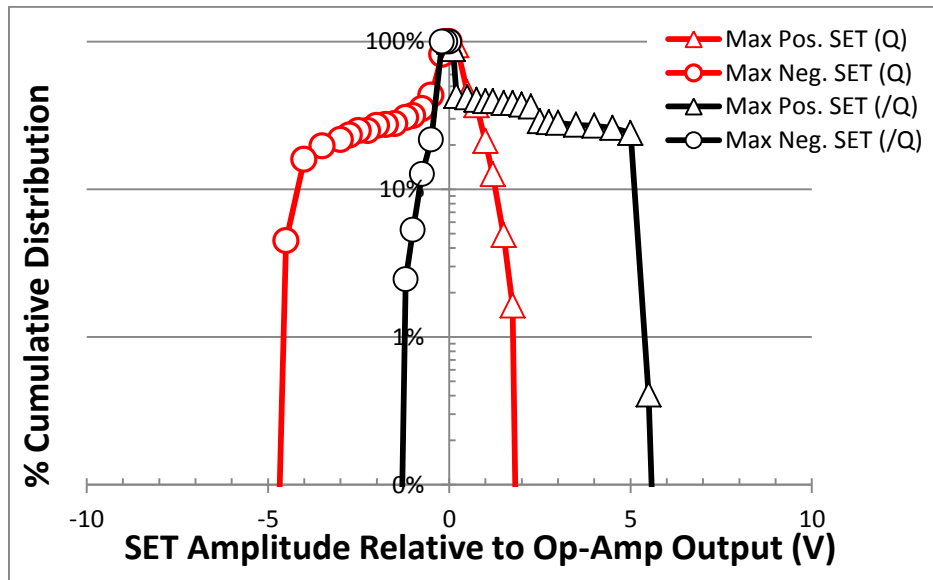
1. V supply= \pm 5V; V input=(0.05V to 0.4V); Xenon Ions; LET=58.78 MeV.cm²/mg (Runs 163-170)
2. V supply= \pm 5V; V input=(0.45 to 0.5V); Xenon Ions; LET=58.78 MeV.cm²/mg (Runs 171-173)
3. V supply= \pm 5V; V input=(0.6 to 0.65V); Xenon Ions; LET=58.78 MeV.cm²/mg (Runs 174-175)
4. V supply= \pm 5V; V input=(0.7 to 1V); Xenon Ions; LET=58.78 MeV.cm²/mg (Runs 176-182)
5. V supply= \pm 5V; V input=(0.05V to 0.4V); Krypton Ions; LET=30.86 MeV.cm²/mg (Runs 185-192)
6. V supply= \pm 5V; V input=(0.45V to 0.55V); Krypton Ions; LET=30.86 MeV.cm²/mg (Runs 193-196)
7. V supply= \pm 5V; V input=(0.6 to 0.65V); Krypton Ions; LET=30.86 MeV.cm²/mg (Runs 197-198)
8. V supply= \pm 5V; V input=(0.7 to 1V); Krypton Ions; LET=48.15 MeV.cm²/mg (Runs 199-205)
9. V supply= \pm 5V; V input=(0.05 to 0.4V); Silver Ions; LET=48.15 MeV.cm²/mg (Runs 206-210)
10. V supply= \pm 5V; V input=(0.45 to 0.5V); Silver Ions; LET=48.15 MeV.cm²/mg (Runs 211-212)
11. V supply= \pm 5V; V input=(0.6 to 0.65V); Silver Ions; LET=48.15 MeV.cm²/mg (Runs 213-214)
12. V supply= \pm 5V; V input=(0.7 to 1V); Silver Ions; LET=48.15 MeV.cm²/mg (Runs 215-219)
13. V supply= \pm 5V; V input=(0.05 to 0.4V); Xenon Ions; LET=58.78 MeV.cm²/mg (Runs 220-222)

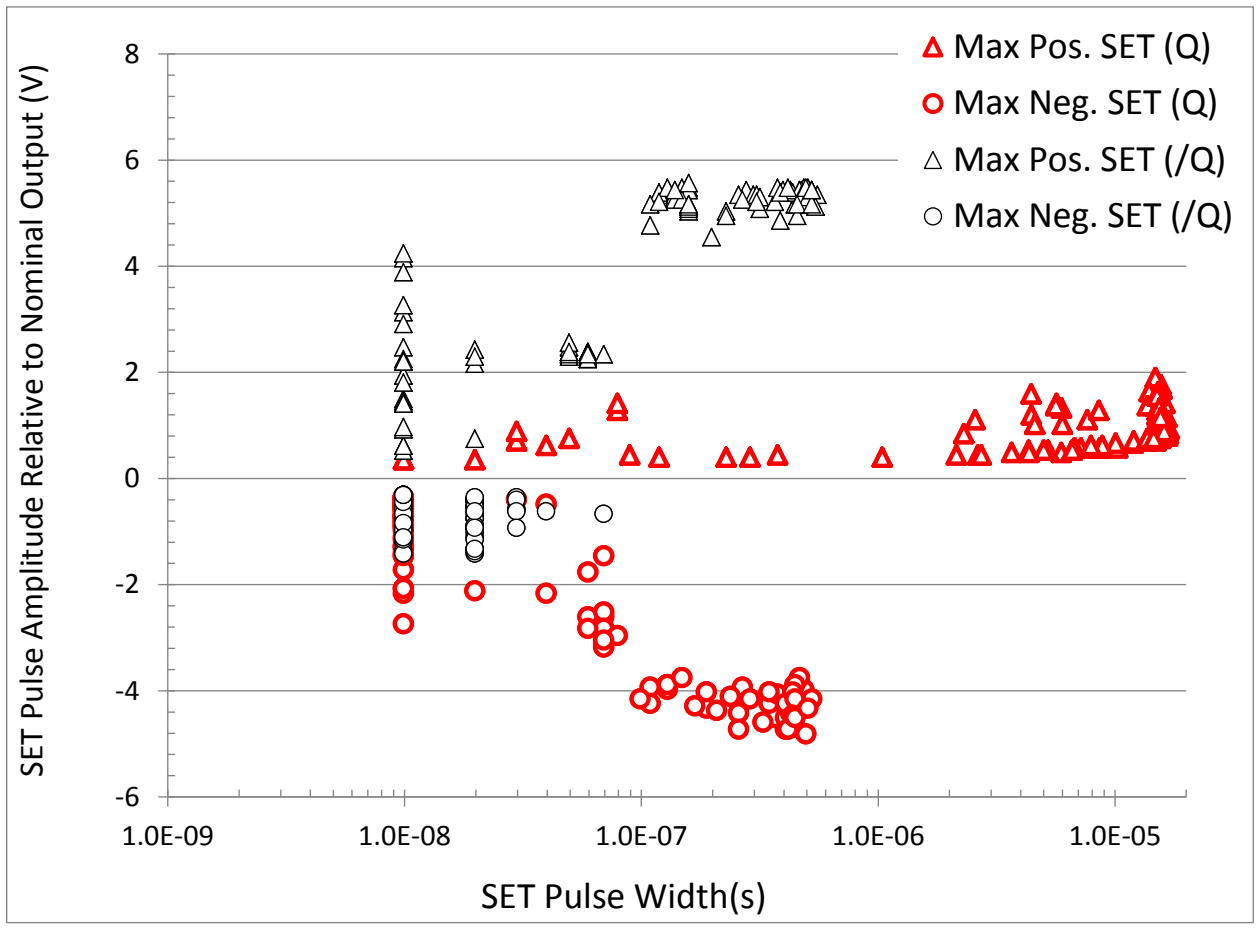
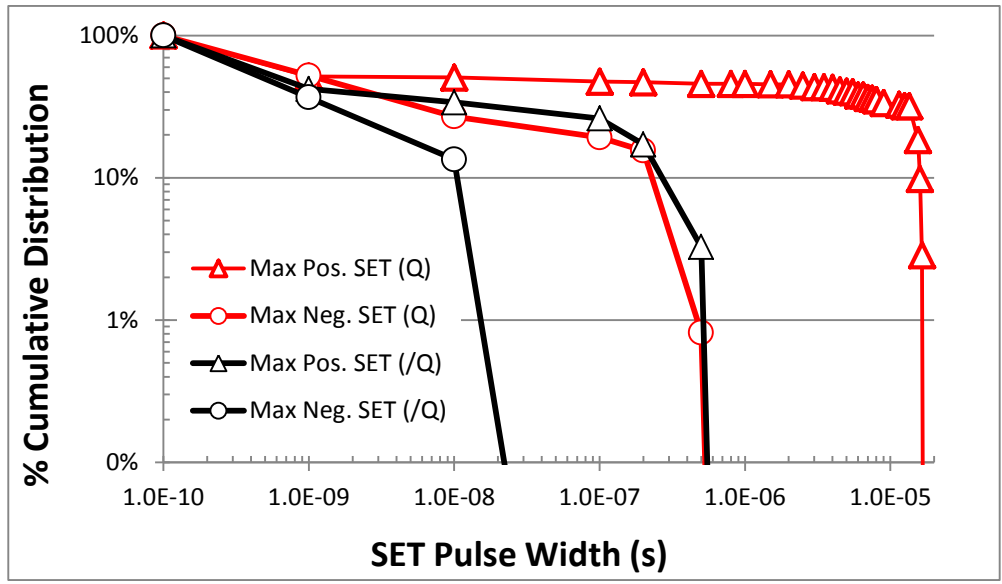
1. V supply=+/-5V; V input= (0.05V to 0.4V); Xenon Ions; LET=58.78 MeV.cm²/mg (Runs 163-170)



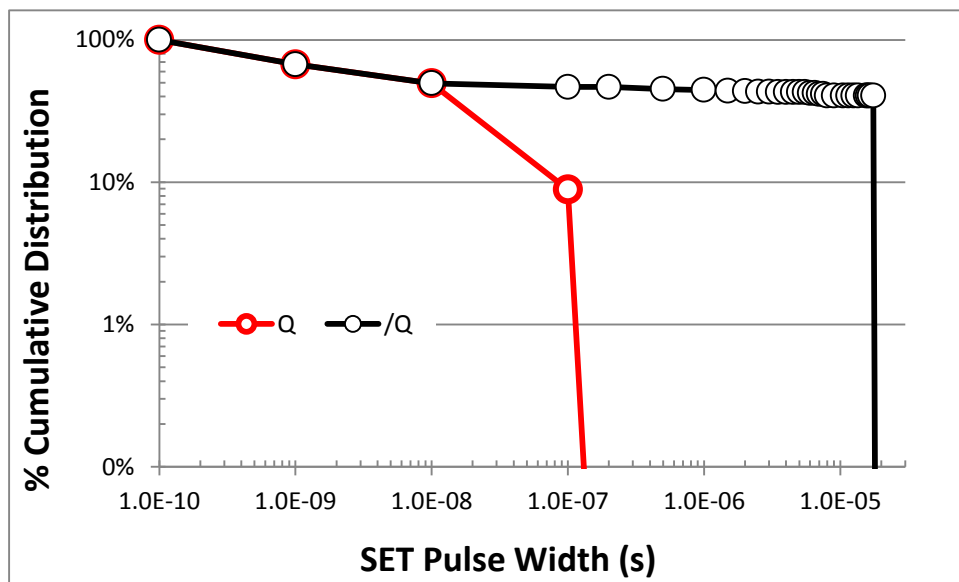
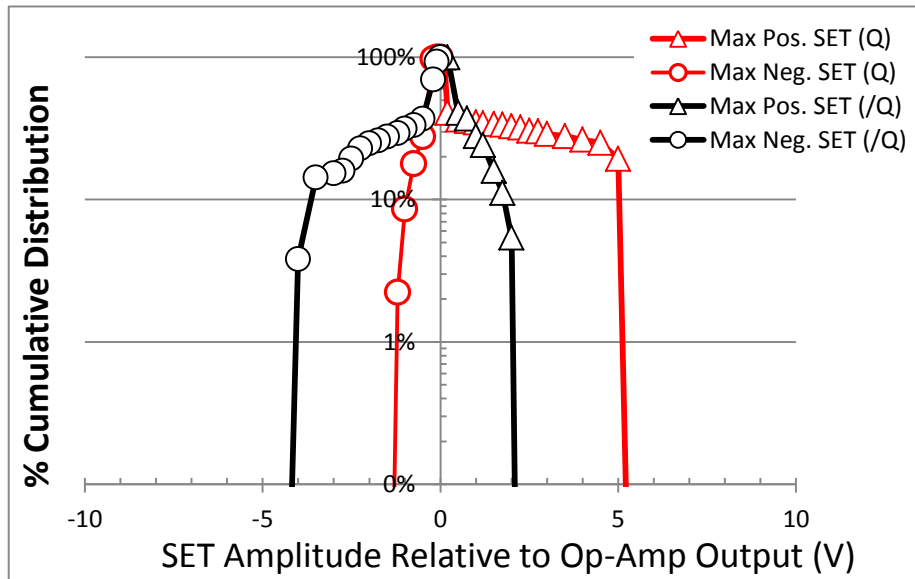


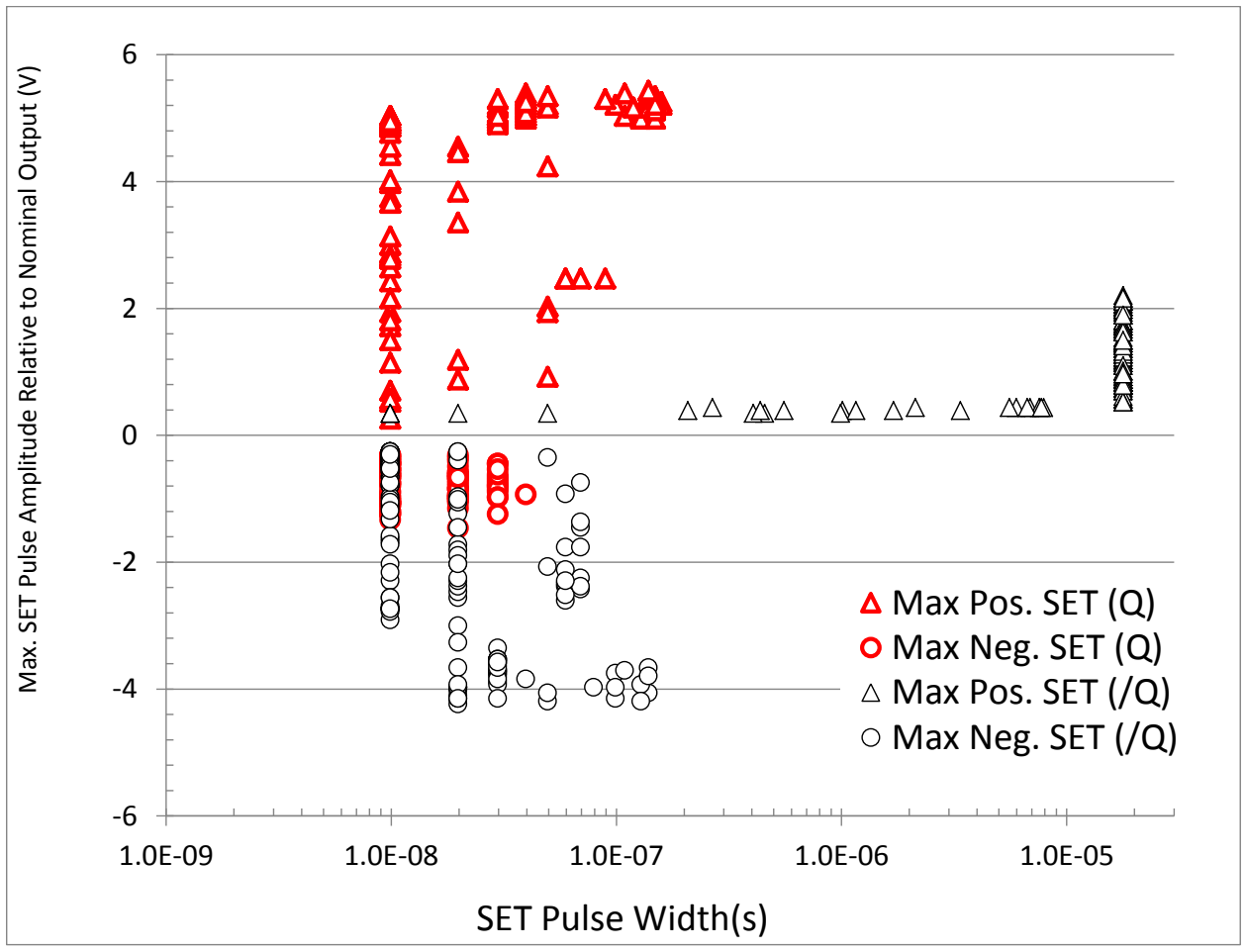
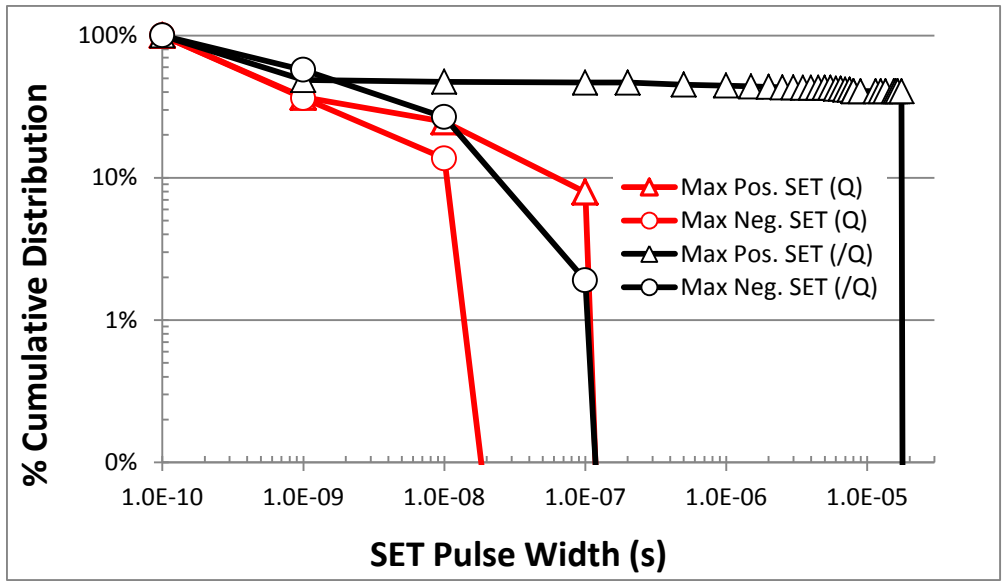
2. V supply= $\pm 5V$; V input=(0.45 to 0.5V); Xenon Ions; LET=58.78 MeV.cm²/mg (Runs 171-173)



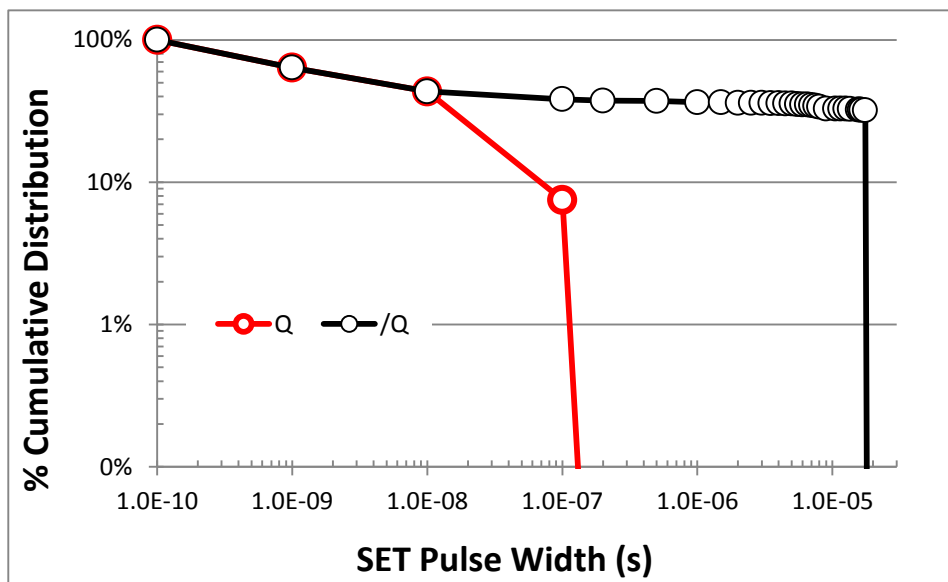
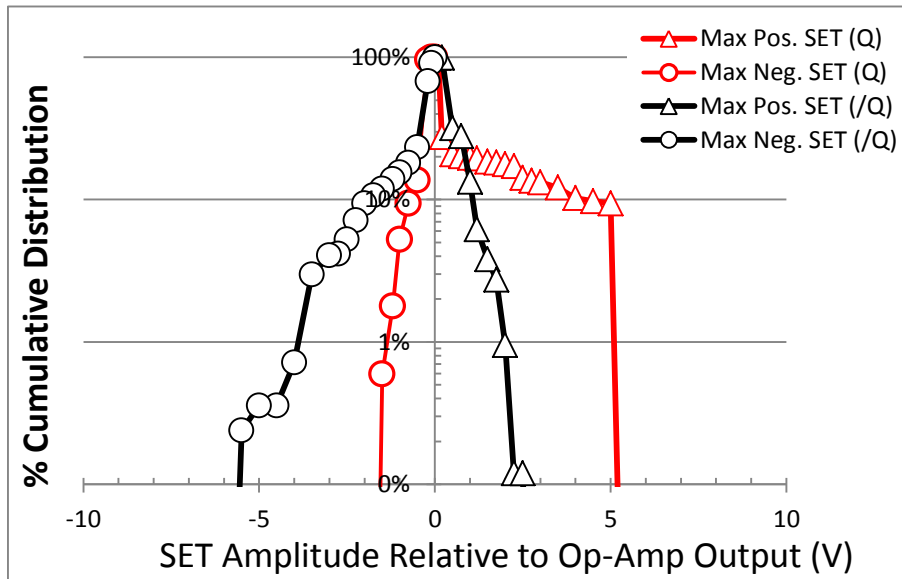


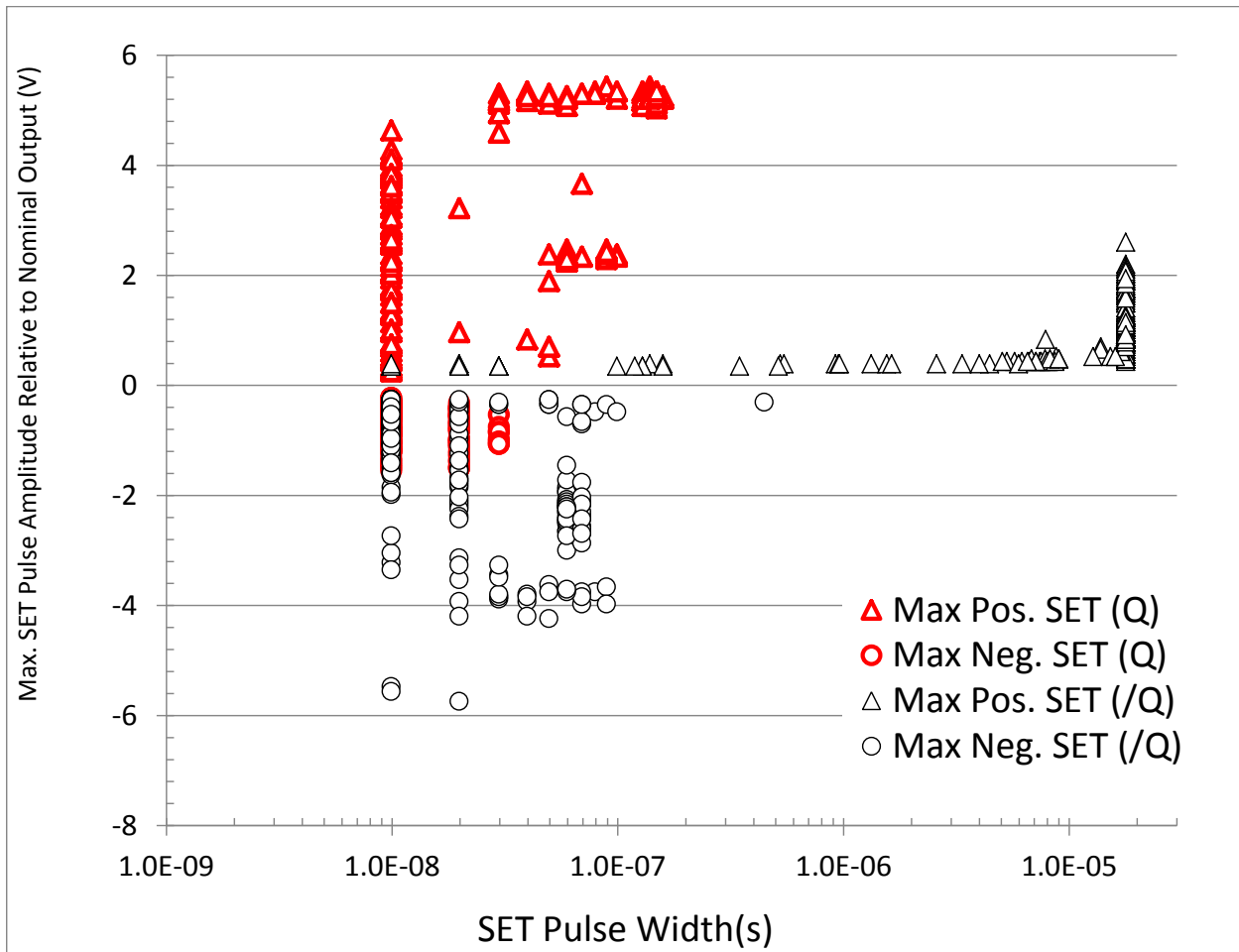
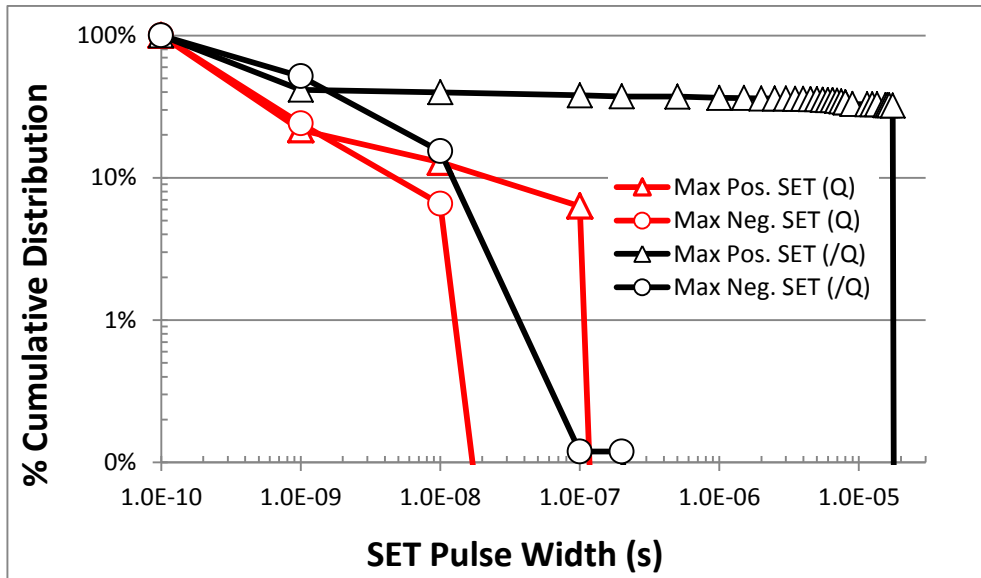
3. V supply= $\pm 5V$; V input=(0.6 to 0.65V); Xenon Ions; LET=58.78 MeV.cm²/mg (Runs 174-175)



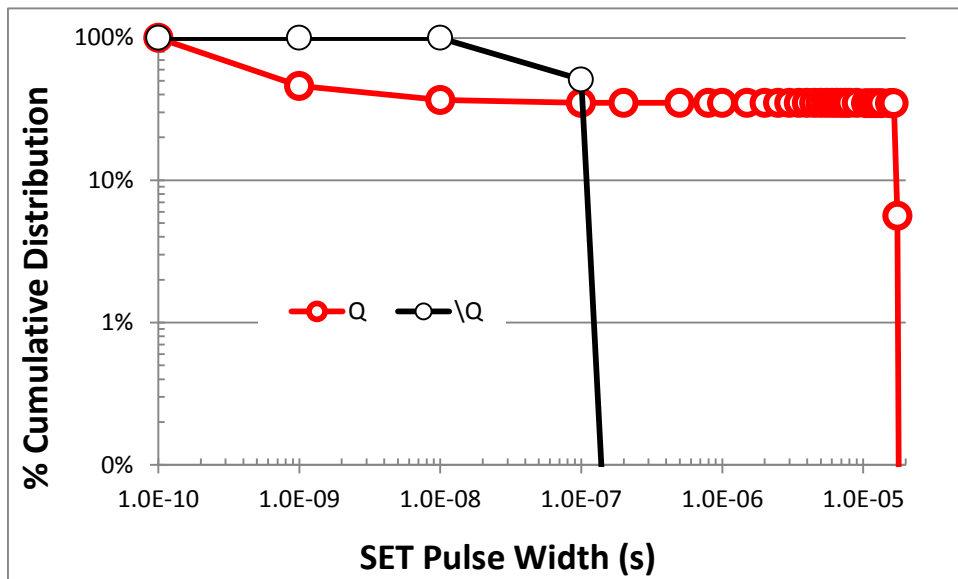
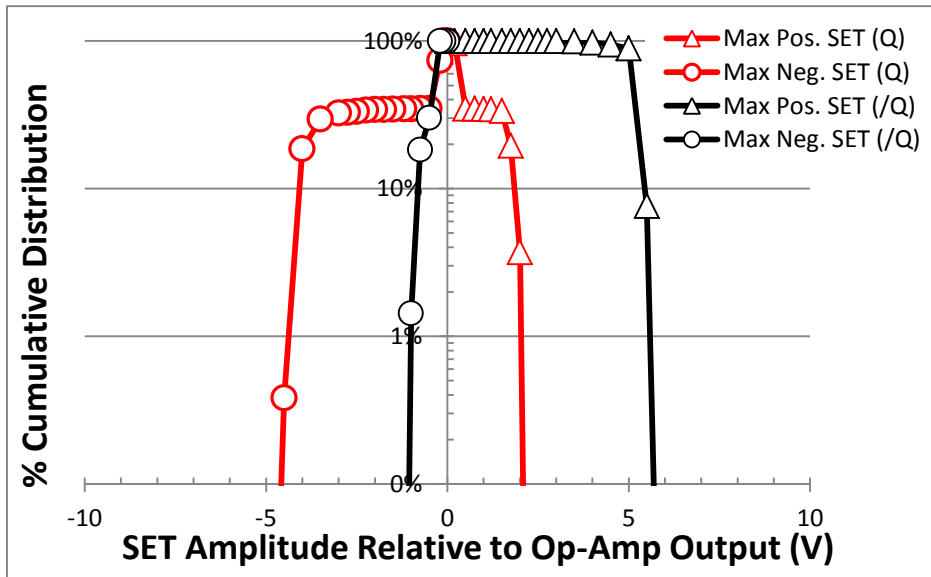


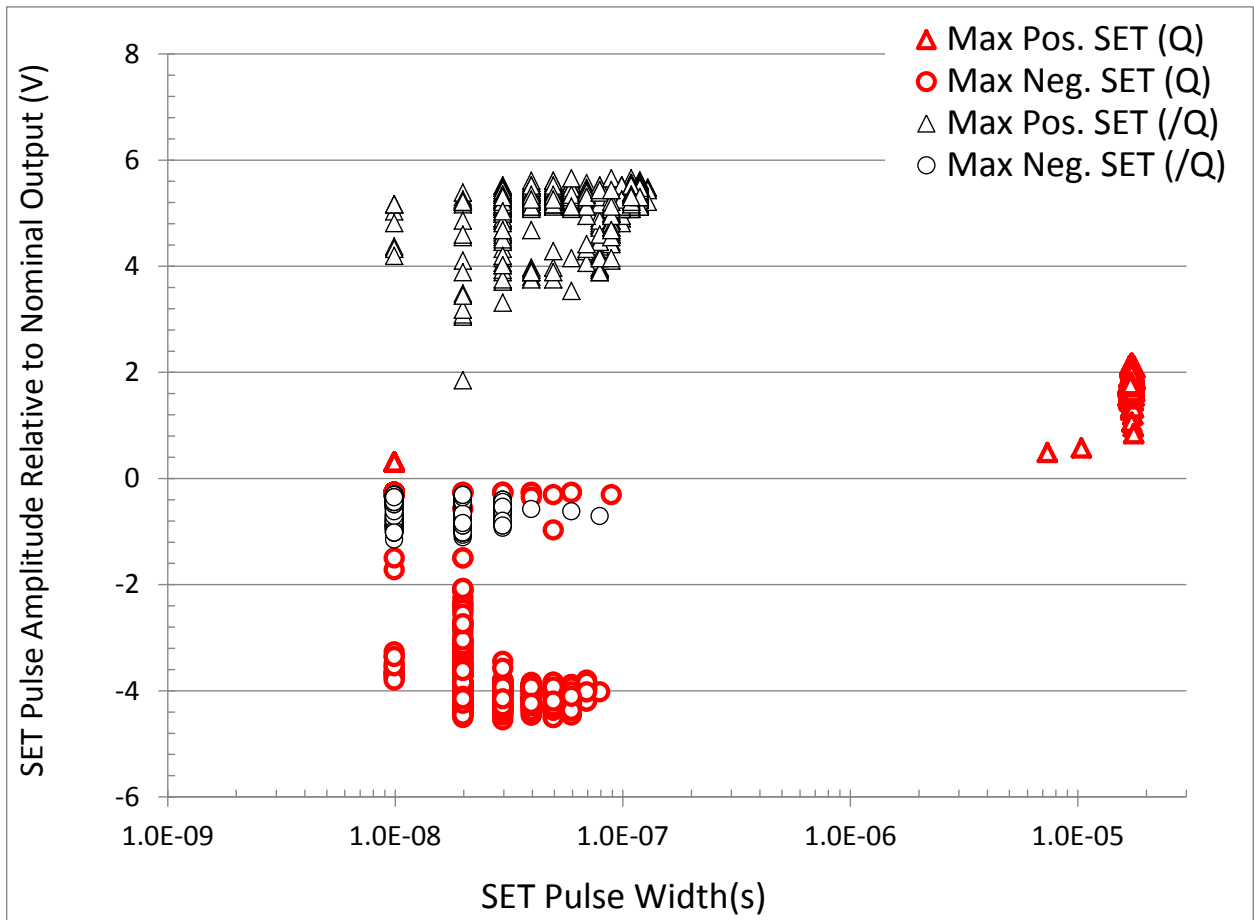
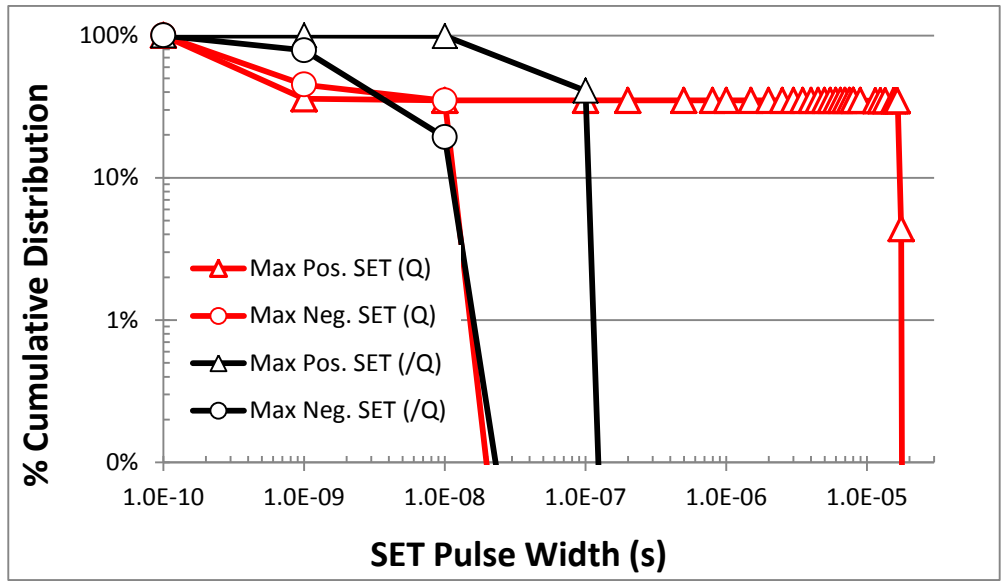
4. V supply= $\pm 5V$; V input=(0.7 to 1V); Xenon Ions; LET=58.78 MeV.cm²/mg (Runs 176-182)



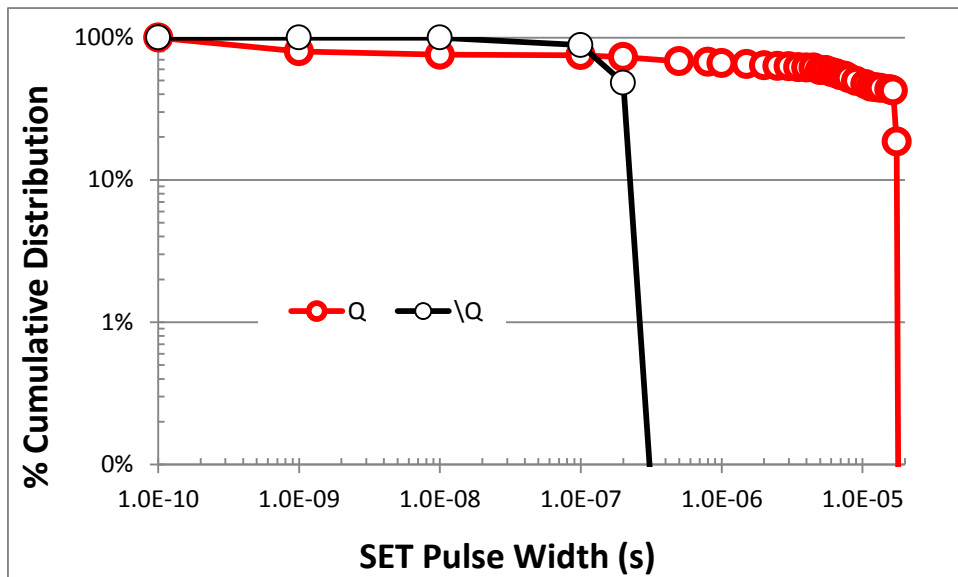
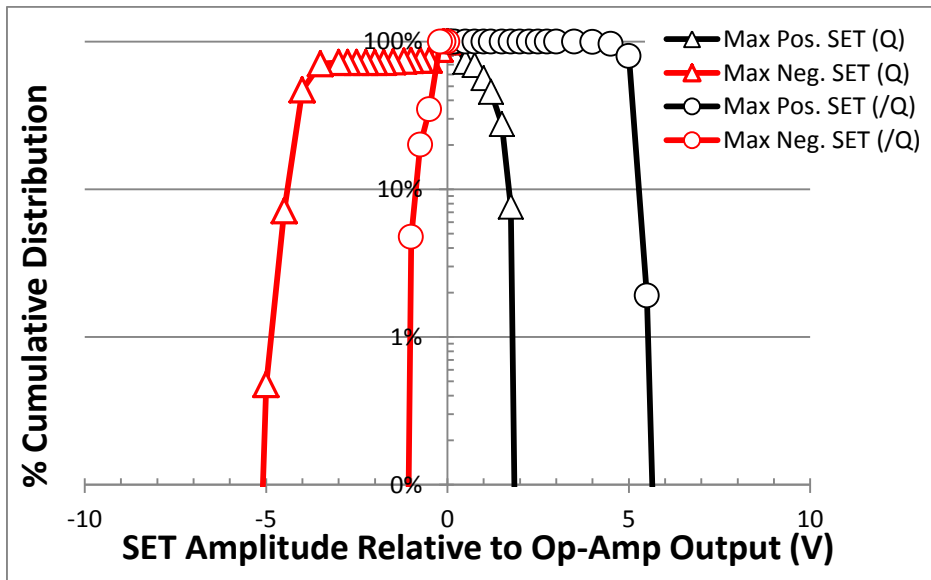


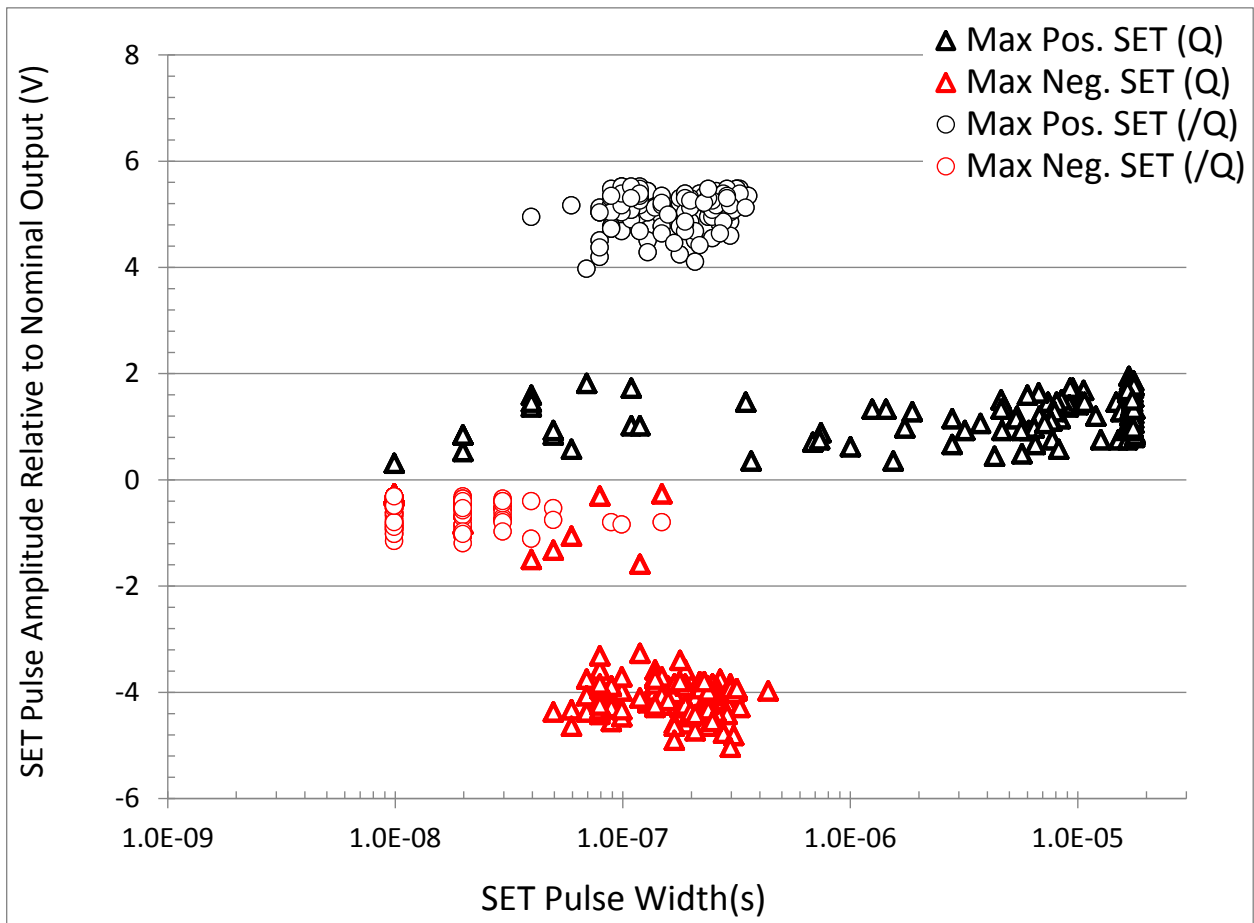
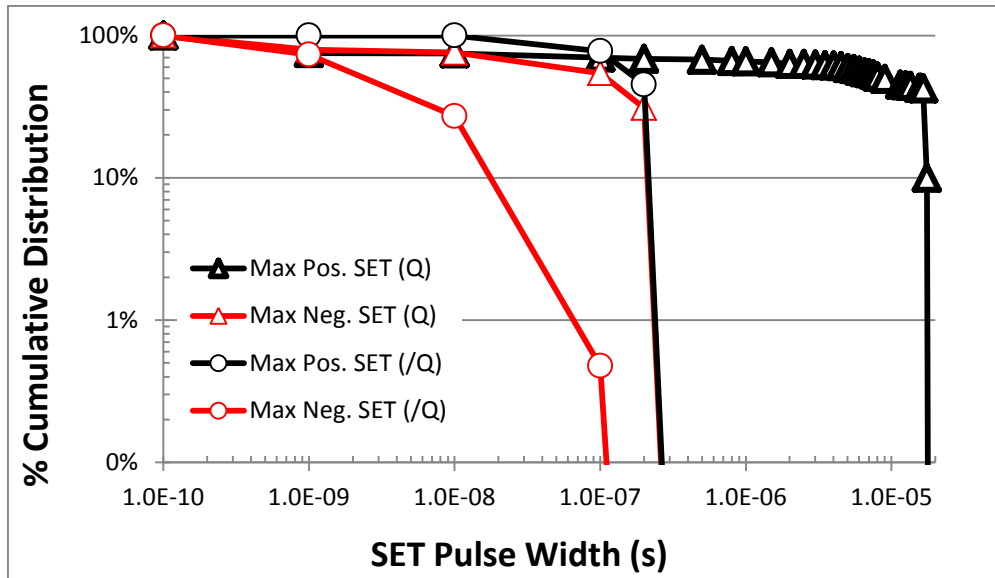
5. V supply= $\pm 5V$; V input=(0.05V to 0.4V); Krypton Ions; LET=30.86 MeV.cm²/mg (Runs 185-192)



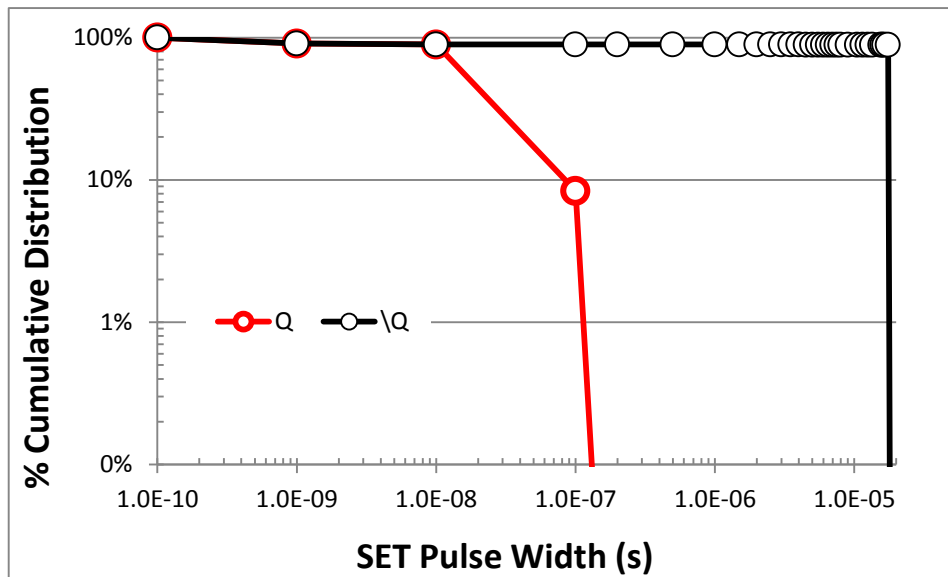
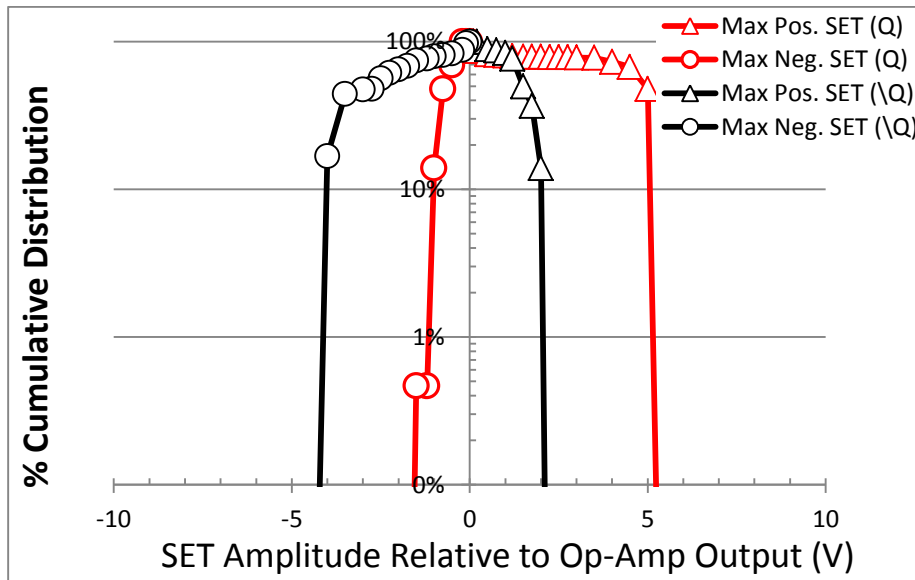


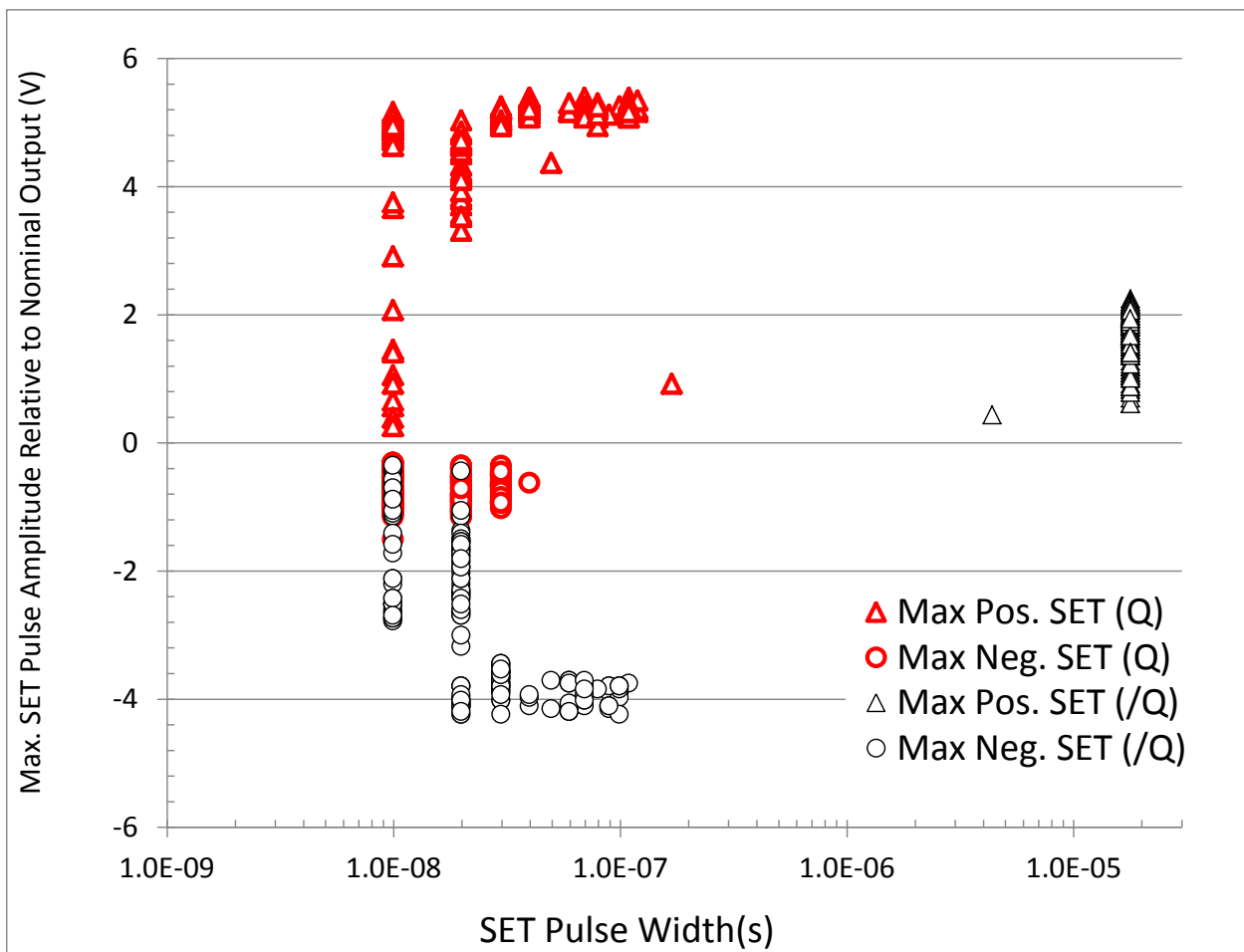
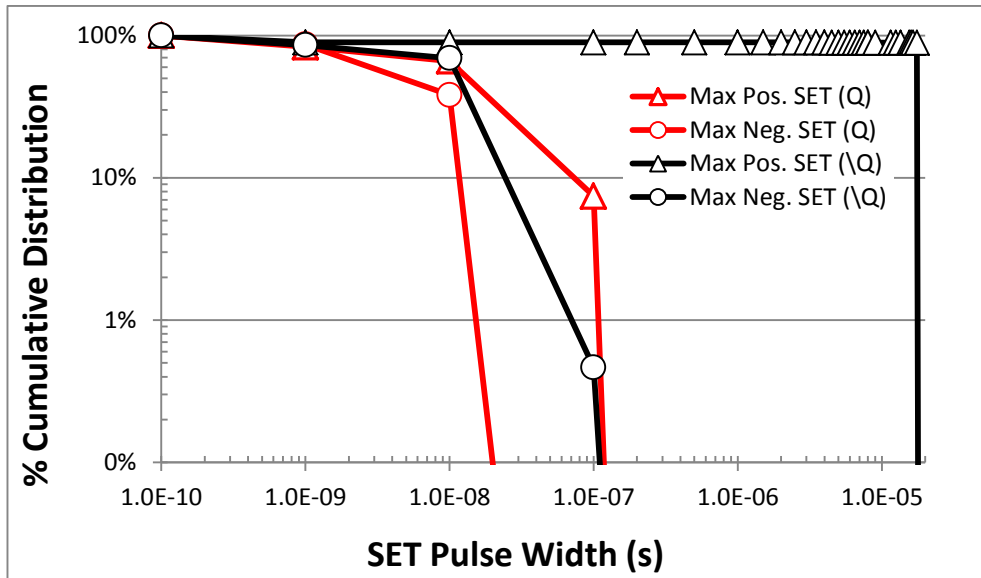
6. V supply= $\pm 5V$; V input=(0.45V to 0.55V); Krypton Ions; LET=30.86 MeV.cm²/mg (Runs 193-196)



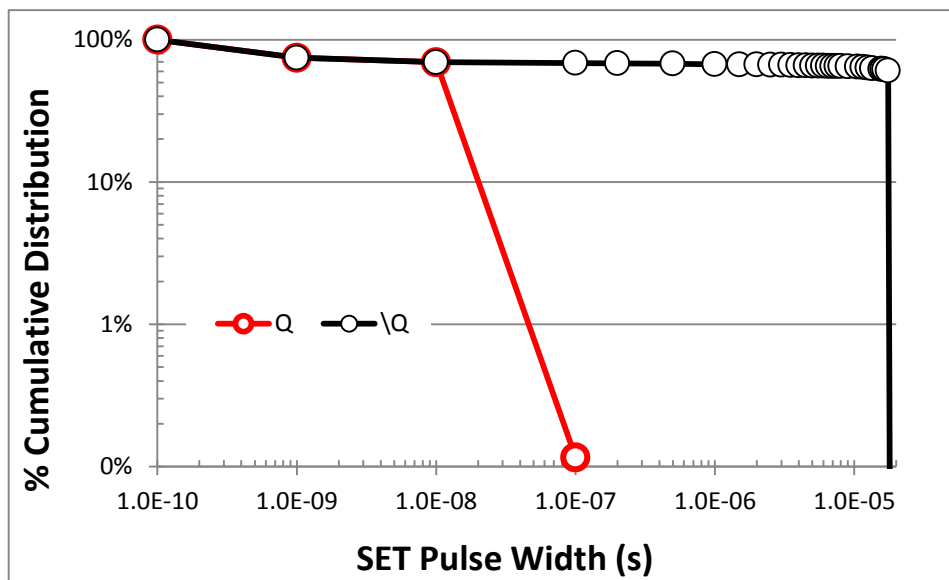
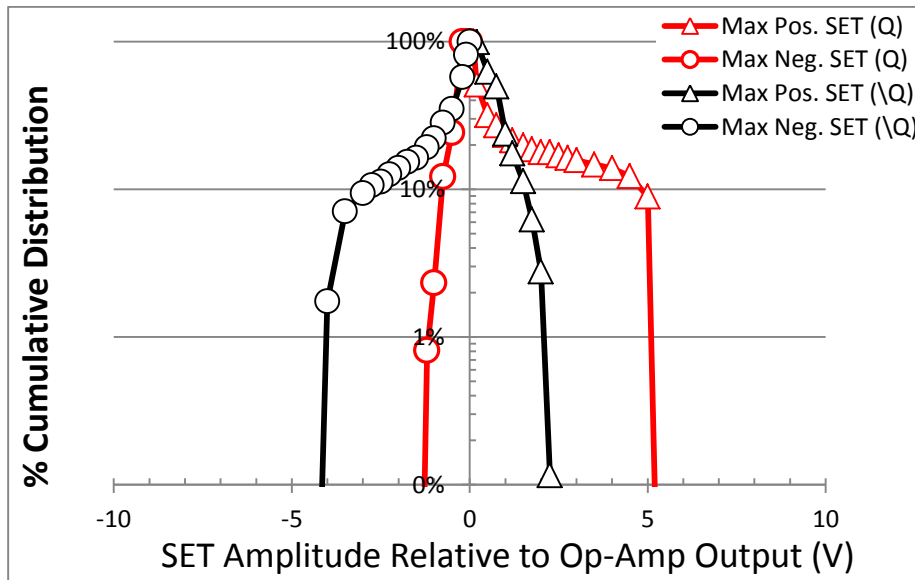


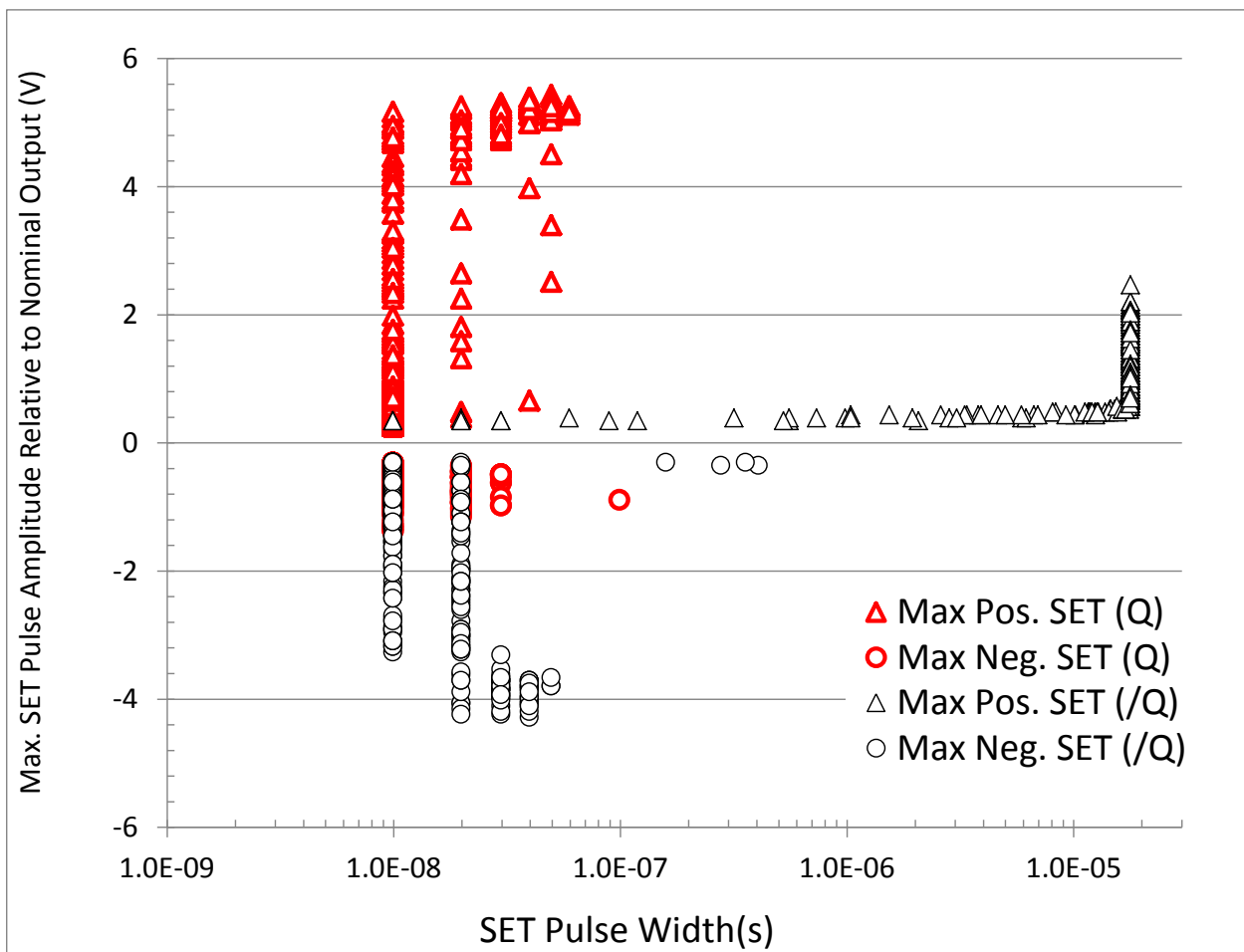
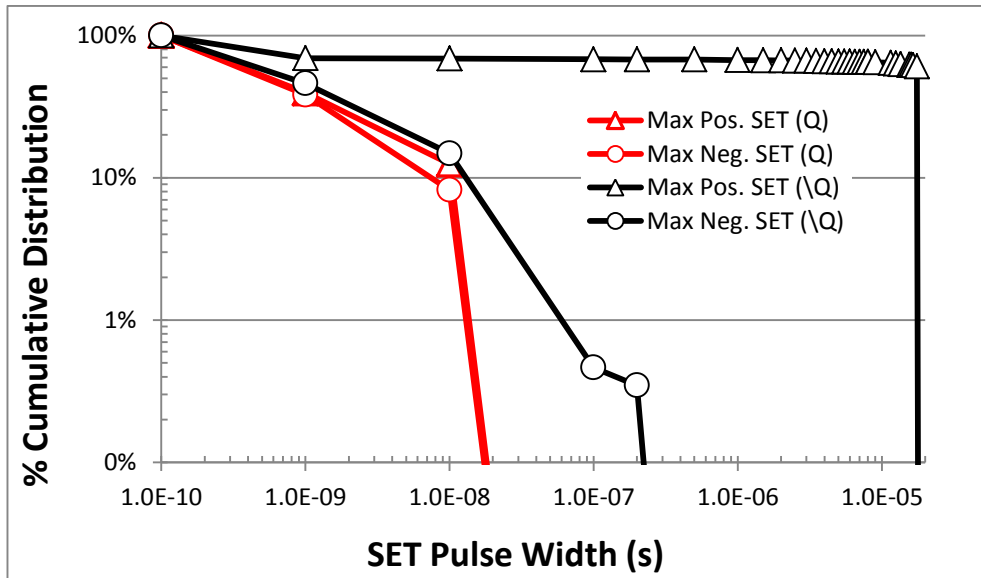
7. V supply= $\pm 5V$; V input=(0.6 to 0.65V); Krypton Ions; LET=30.86 MeV.cm²/mg (Runs 197-198)



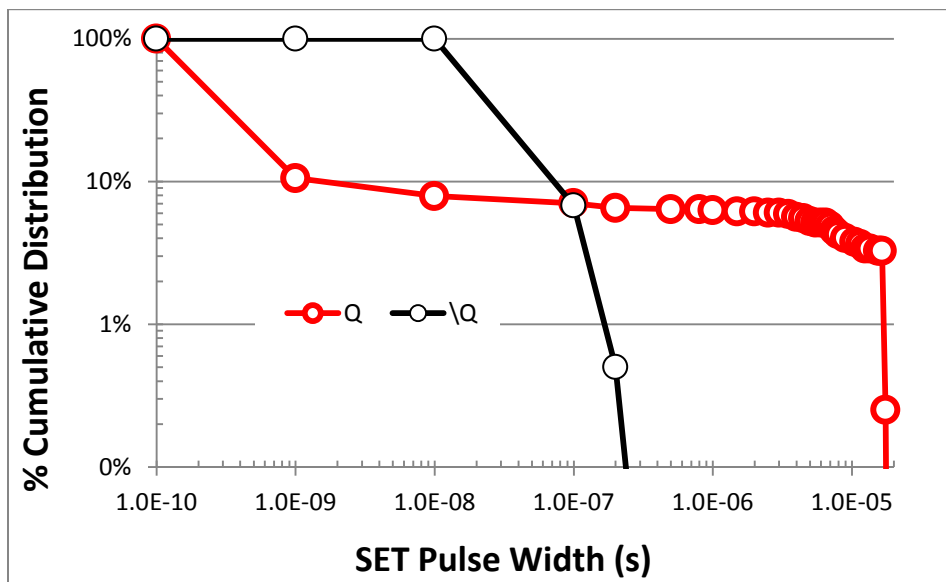
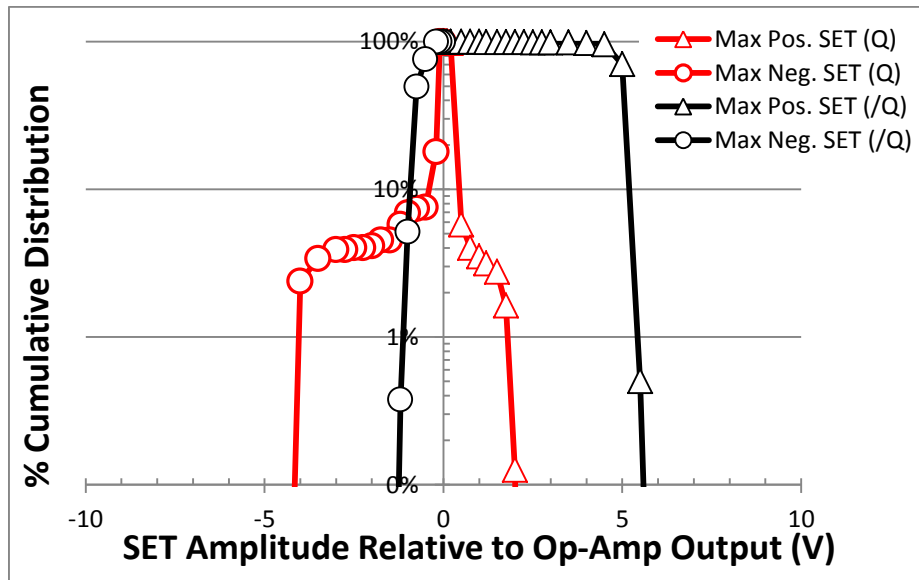


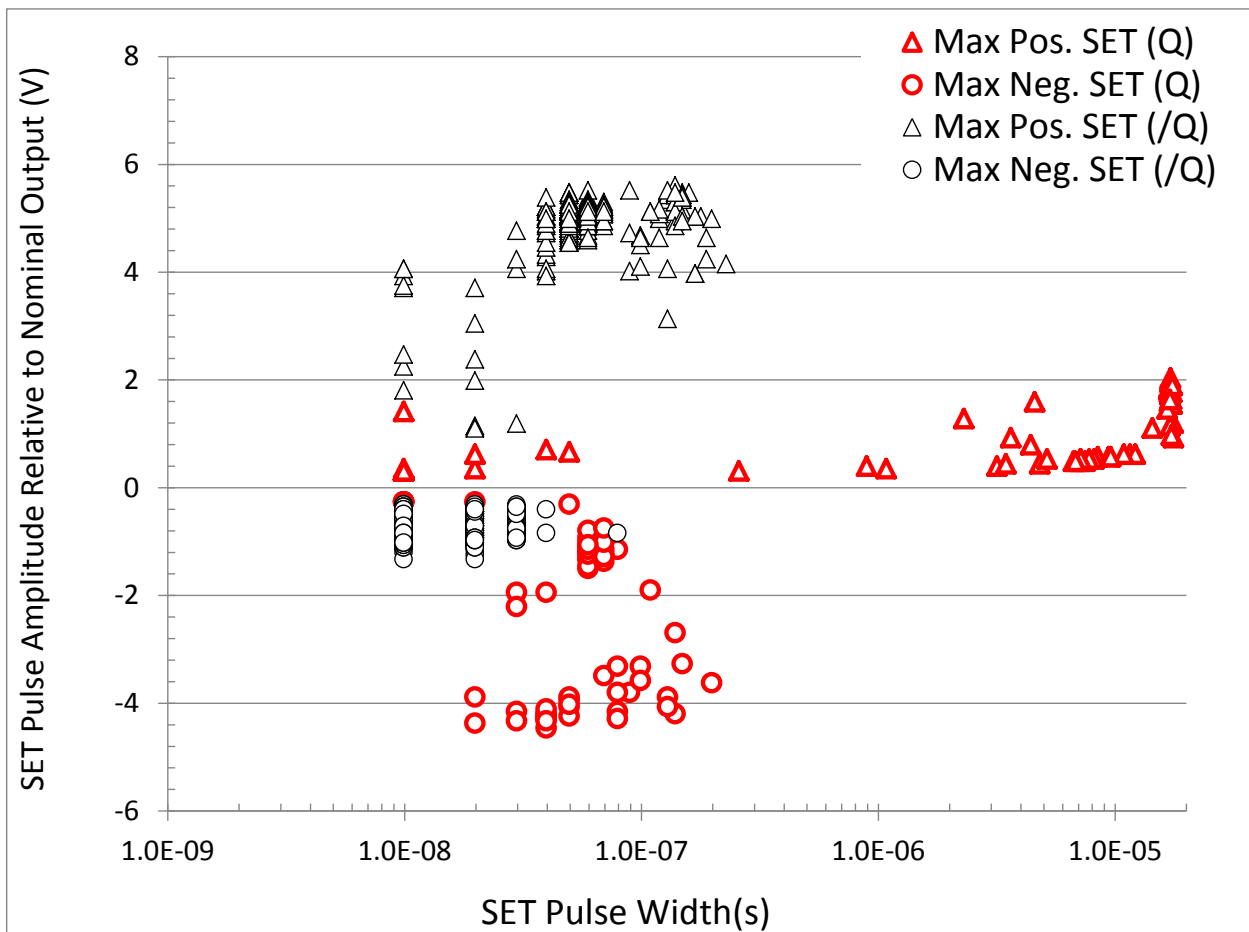
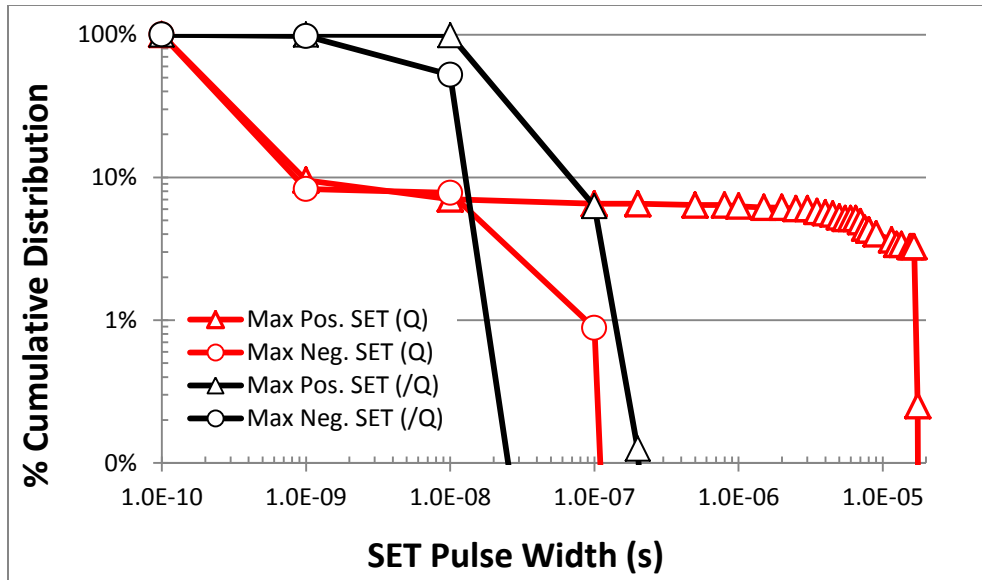
8. V supply= $\pm 5V$; V input=(0.7 to 1V); Krypton Ions; LET=48.15 MeV.cm²/mg (Runs 199-205)



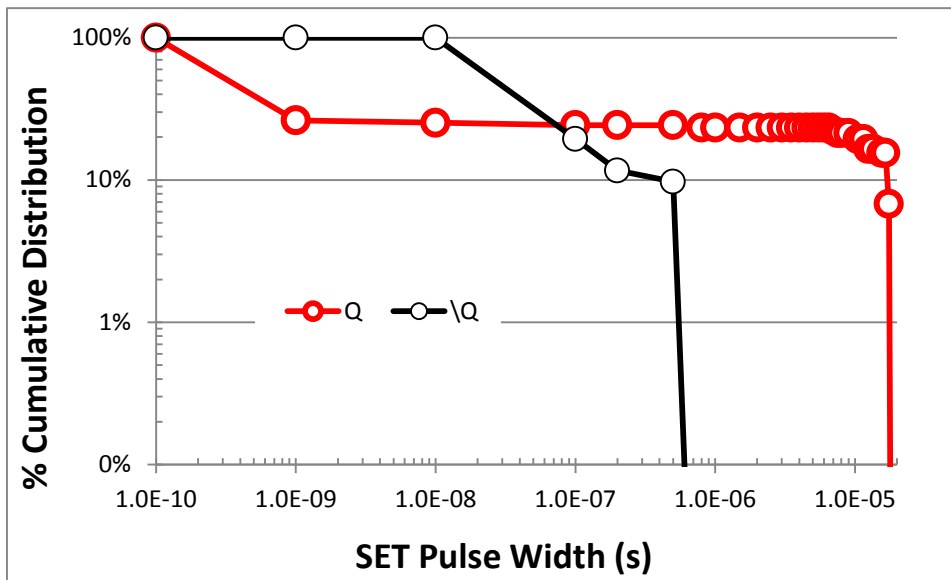
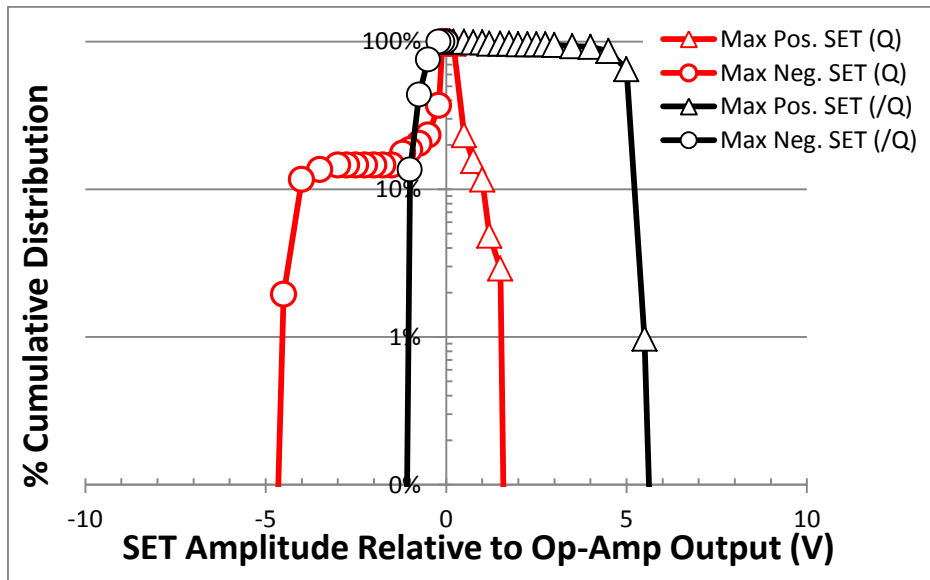


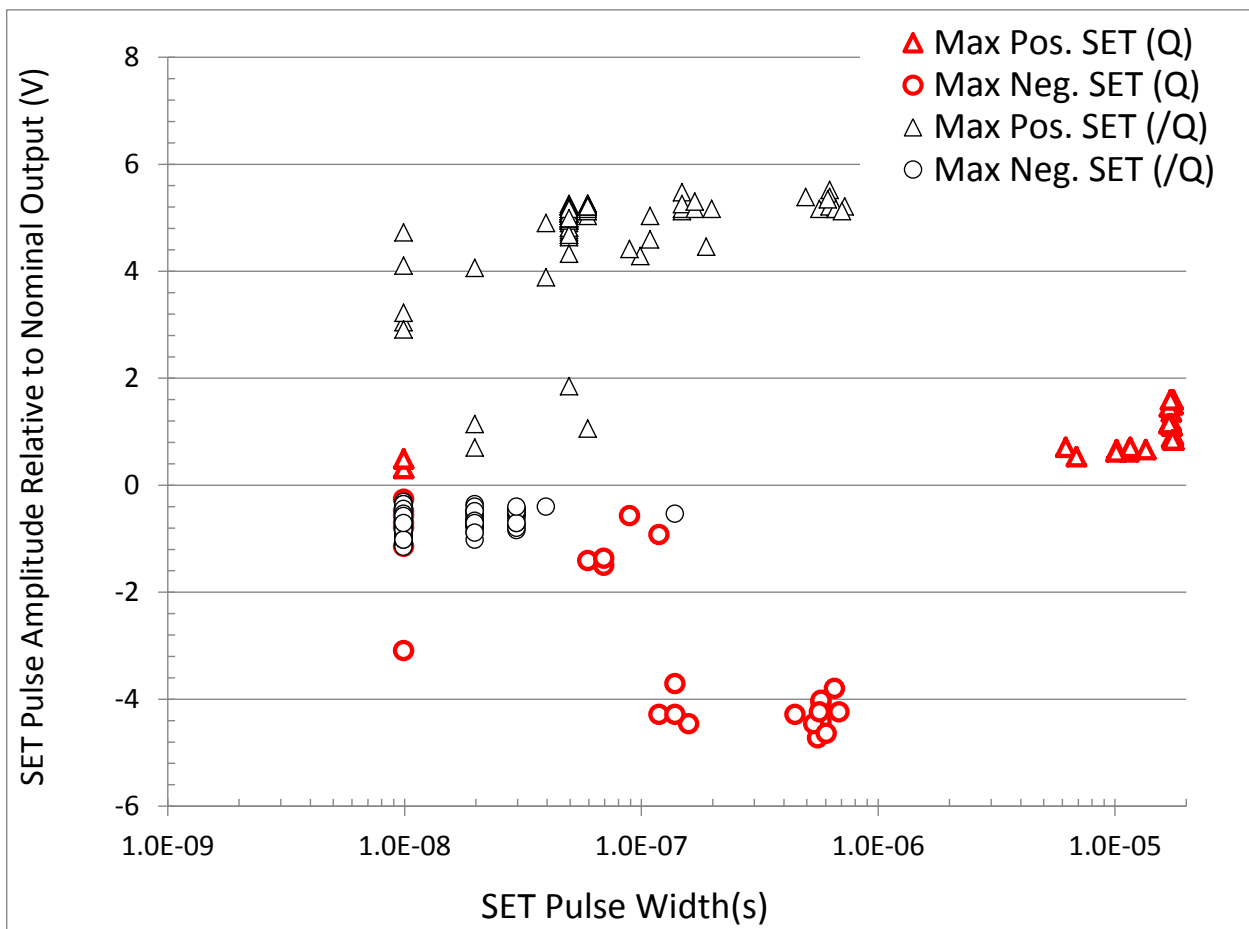
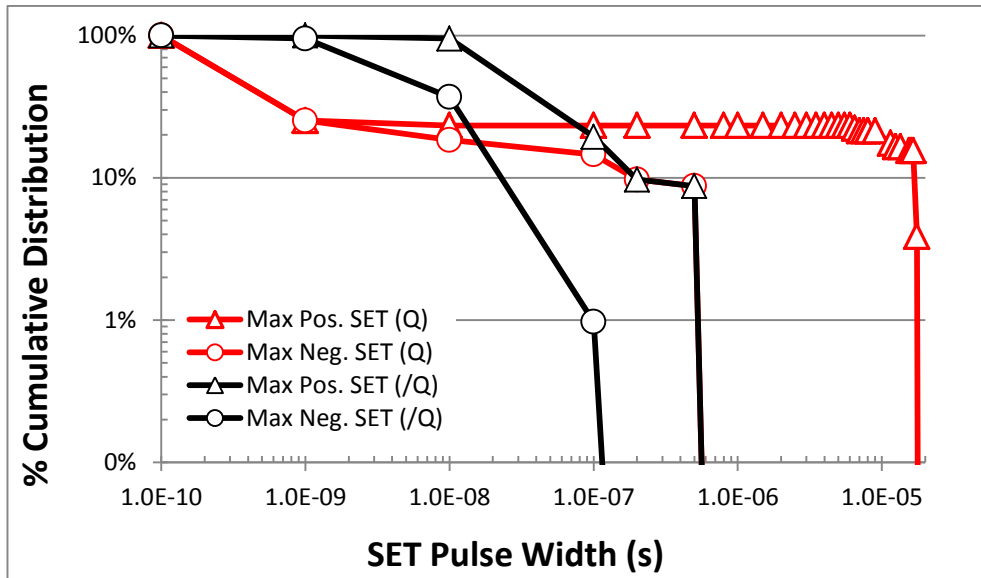
9. V supply= $\pm 5V$; V input=(0.05 to 0.4V); Silver Ions; LET=48.15 MeV.cm²/mg (Runs 206-210)



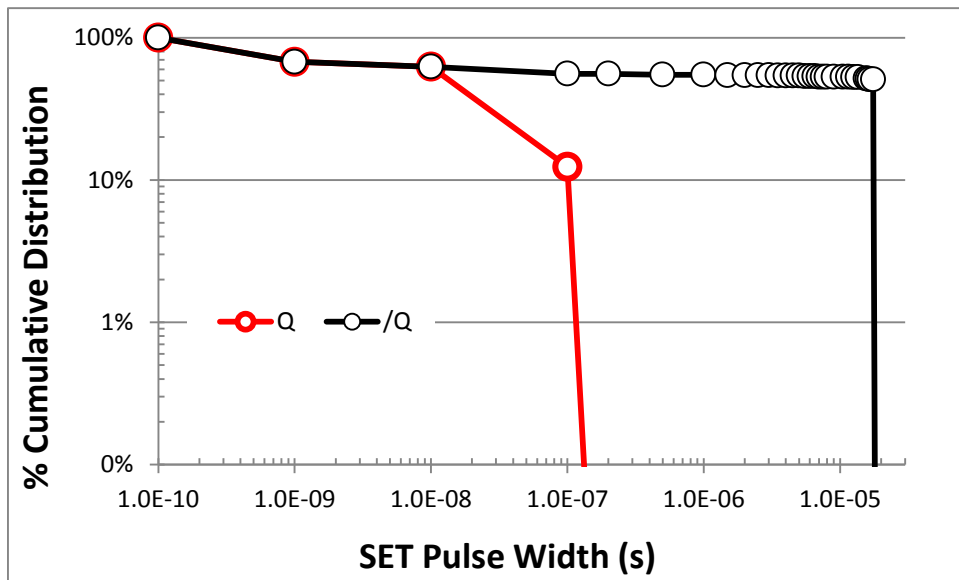
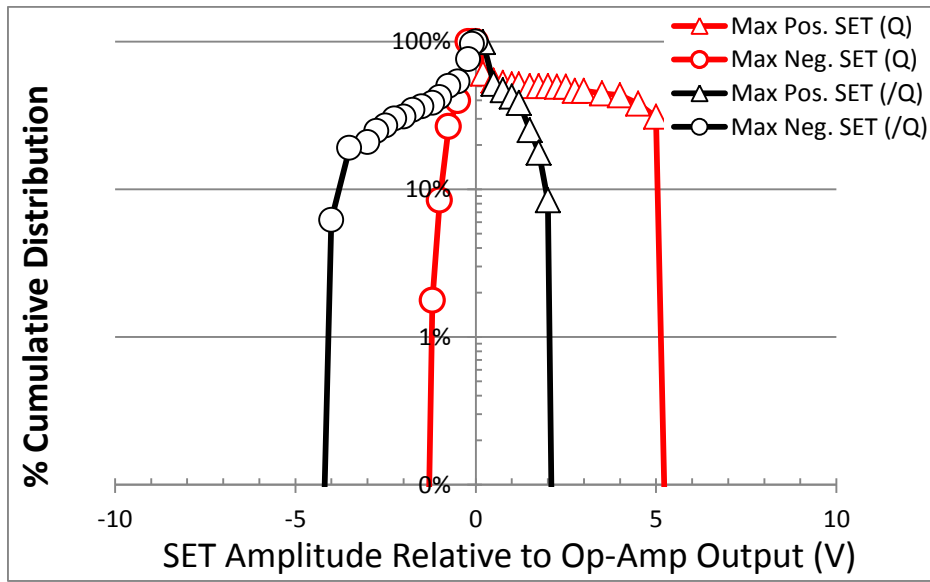


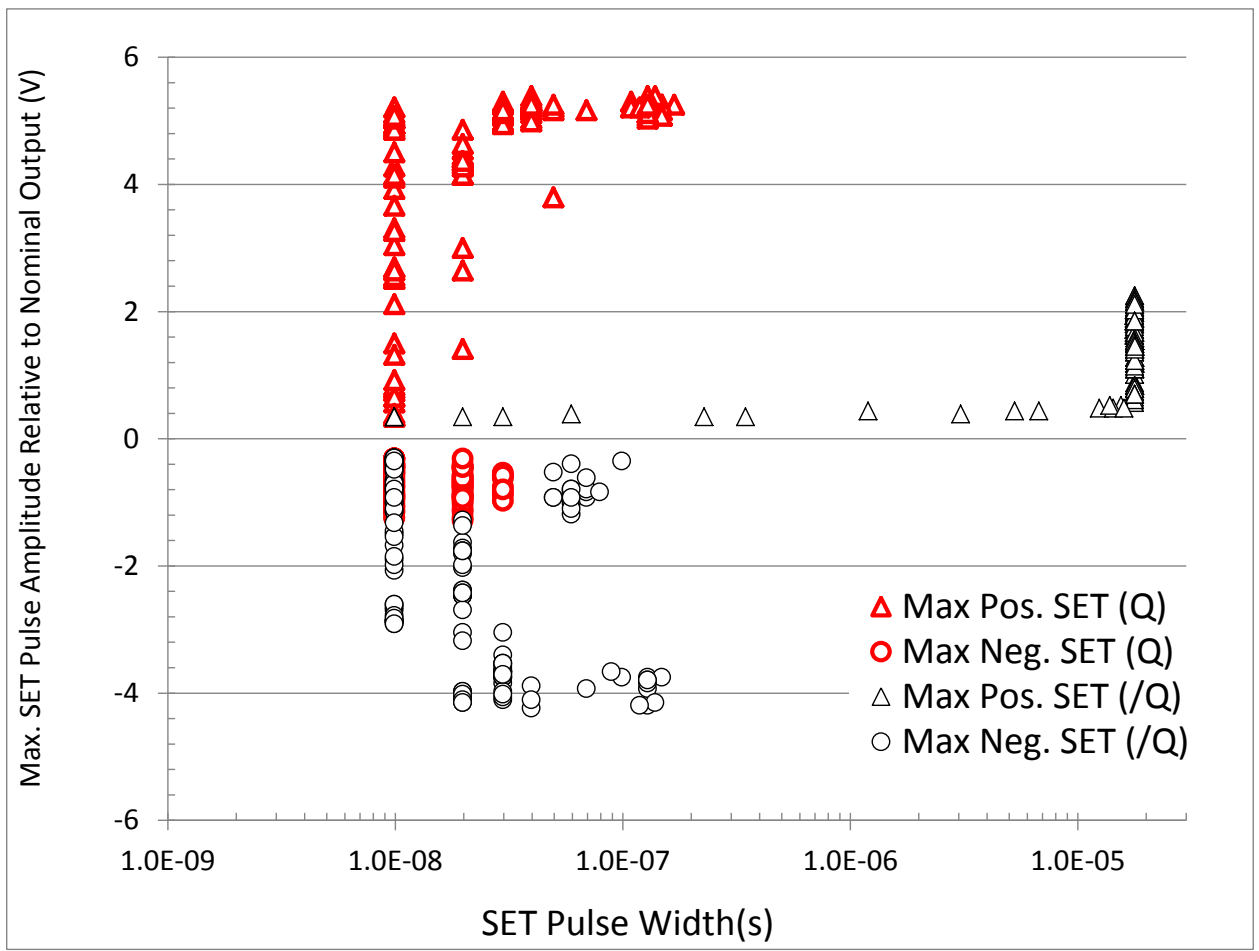
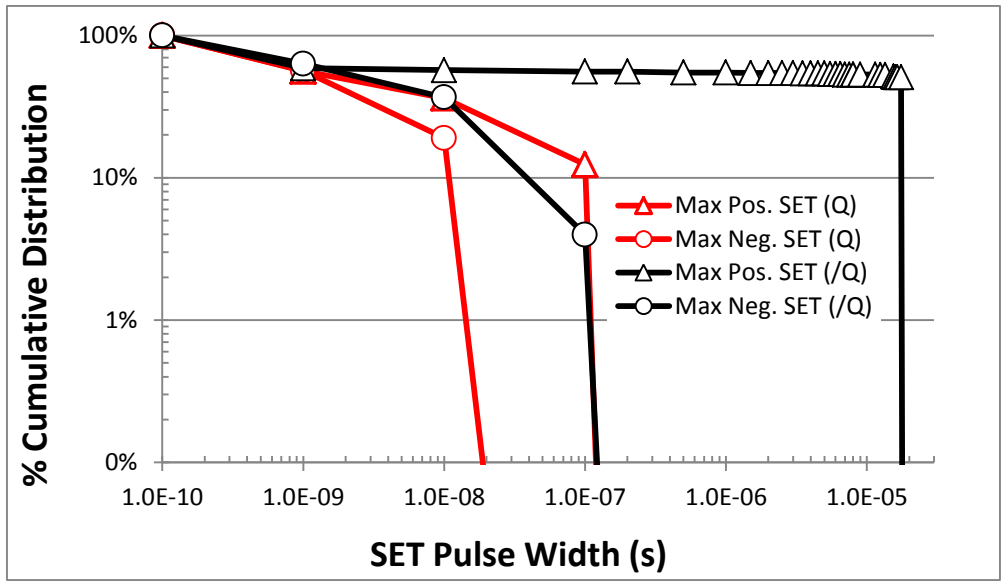
10. V supply= $\pm 5V$; V input=(0.45 to 0.5V); Silver Ions; LET=48.15 MeV.cm²/mg (Runs 211-212) 211



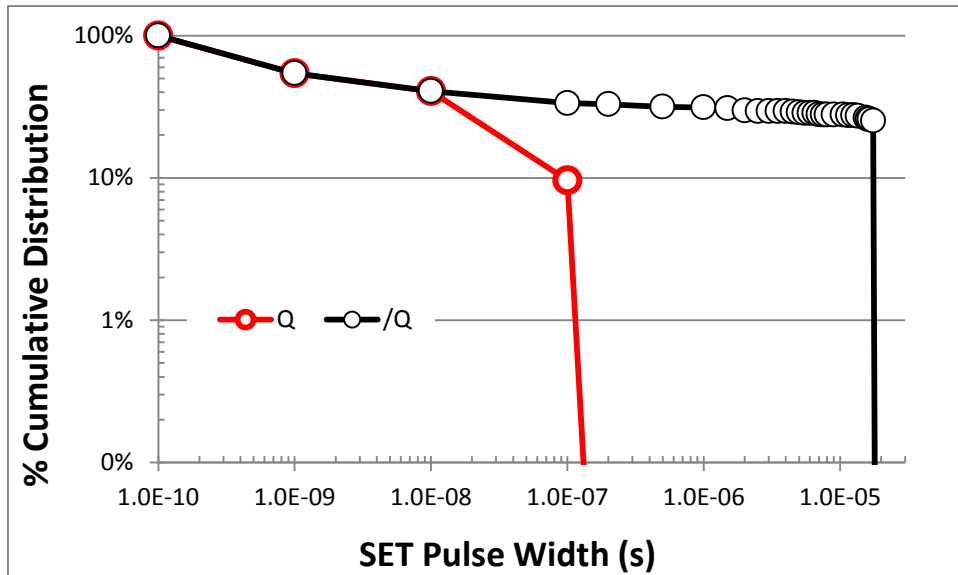
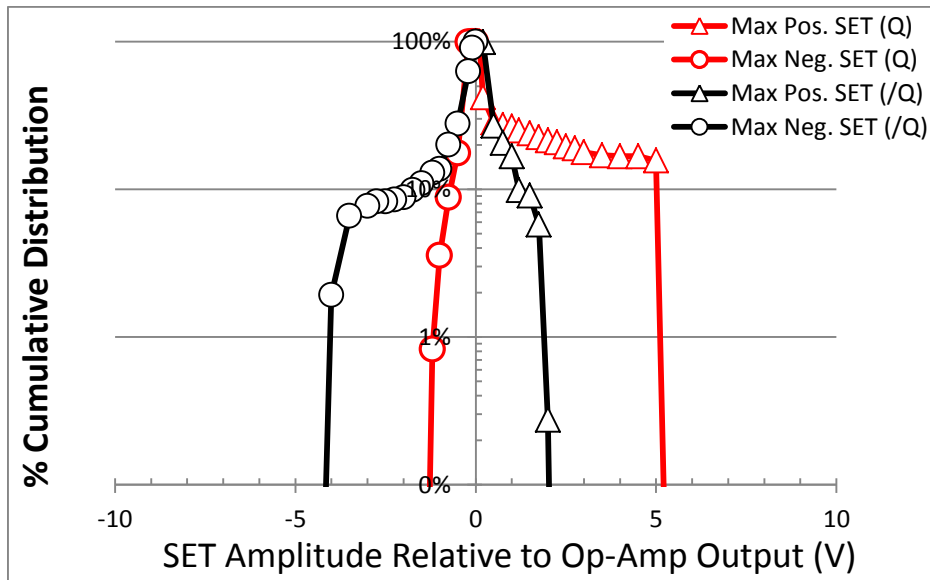


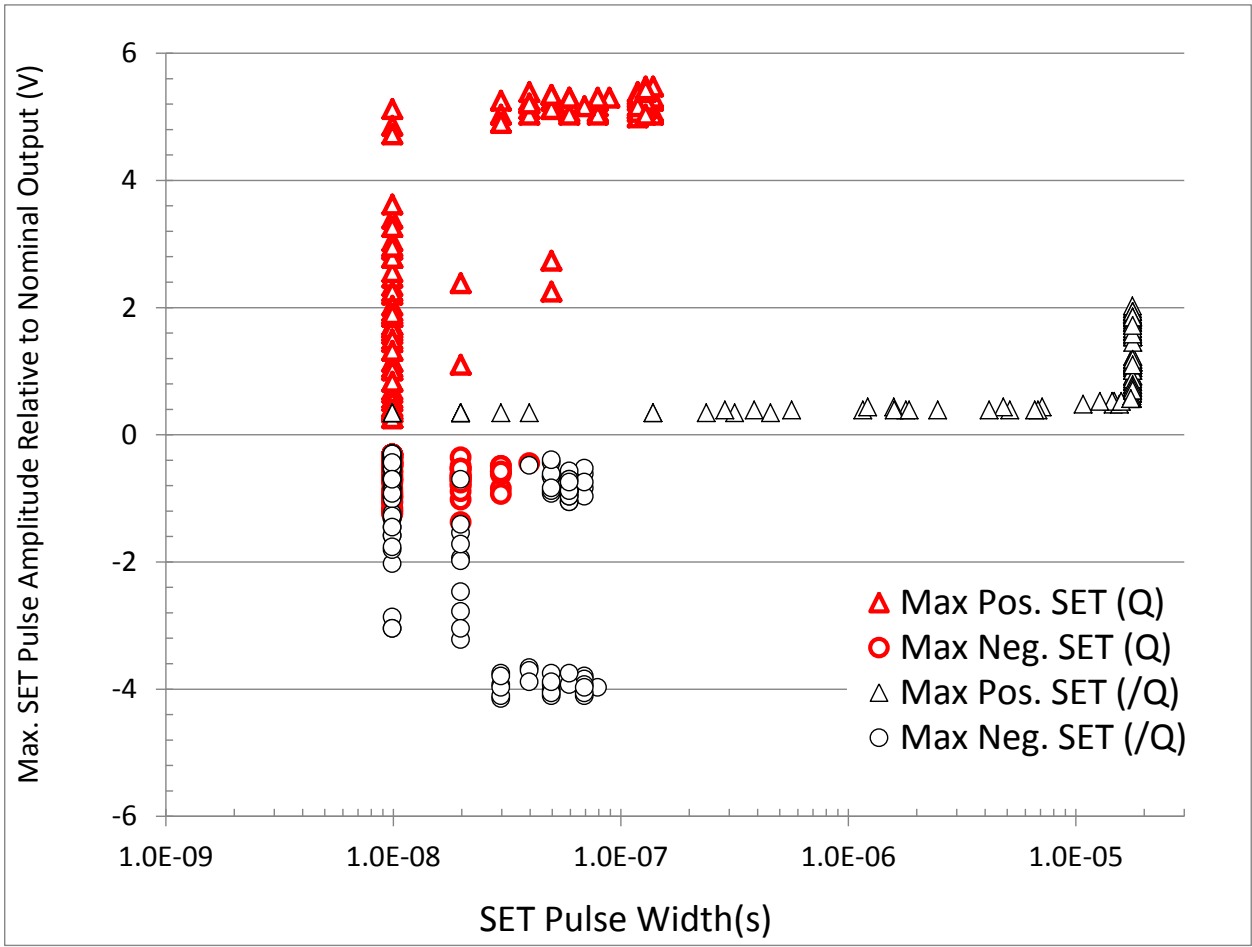
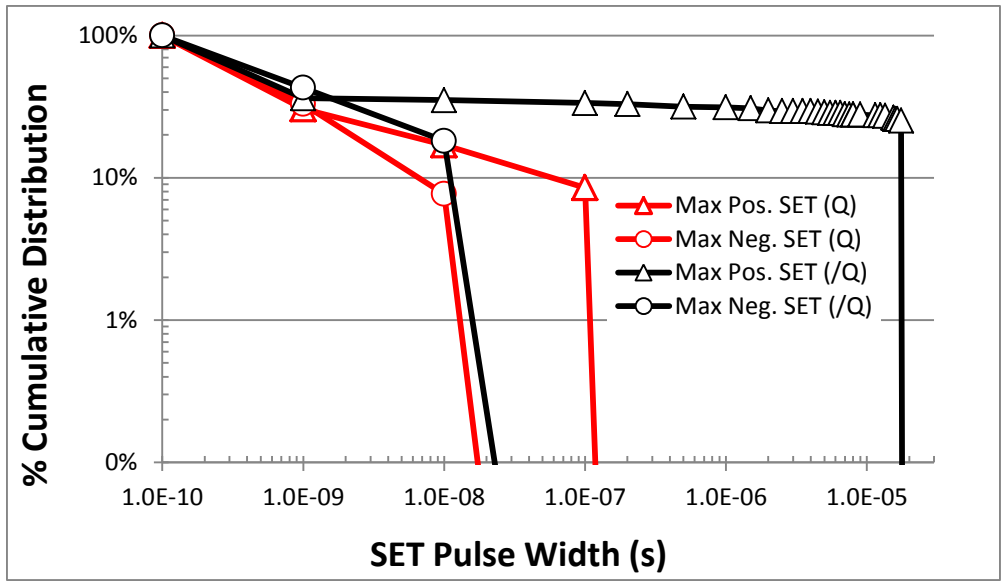
11. V supply= $\pm 5V$; V input=(0.6 to 0.65V); Silver Ions; LET=48.15 MeV.cm²/mg (Runs 213-214)





12. V supply= $\pm 5V$; V input=(0.7 to 1V); Silver Ions; LET=48.15 MeV.cm²/mg (Runs 215-219)





13. V supply= $\pm 5V$; V input=(0.05 to 0.4V); Xenon Ions; LET=58.78 MeV.cm²/mg (Runs 220-222)

